



U.S. DEPARTMENT OF
ENERGY

PNNL-17865

Prepared for the U.S. Department of Energy
under Contract DE-AC05-76RL01830

Geochemical Characterization of Chromate Contamination in the 100 Area Vadose Zone at the Hanford Site

Part 2

NP Qafoku
PE Dresel
JP McKinley
ES Ilton

W Um
CT Resch
RK Kukkadapu
SW Petersen

January 2011



Pacific Northwest
NATIONAL LABORATORY

*Proudly Operated by **Battelle** Since 1965*

DISCLAIMER

This report was prepared as an account of work sponsored by an agency of the United States Government. Neither the United States Government nor any agency thereof, nor Battelle Memorial Institute, nor any of their employees, makes **any warranty, express or implied, or assumes any legal liability or responsibility for the accuracy, completeness, or usefulness of any information, apparatus, product, or process disclosed, or represents that its use would not infringe privately owned rights**. Reference herein to any specific commercial product, process, or service by trade name, trademark, manufacturer, or otherwise does not necessarily constitute or imply its endorsement, recommendation, or favoring by the United States Government or any agency thereof, or Battelle Memorial Institute. The views and opinions of authors expressed herein do not necessarily state or reflect those of the United States Government or any agency thereof.

PACIFIC NORTHWEST NATIONAL LABORATORY

operated by

BATTELLE

for the

UNITED STATES DEPARTMENT OF ENERGY

under Contract DE-AC05-76RL01830

Printed in the United States of America

**Available to DOE and DOE contractors from the
Office of Scientific and Technical Information,
P.O. Box 62, Oak Ridge, TN 37831-0062;
ph: (865) 576-8401
fax: (865) 576-5728
email: reports@adonis.osti.gov**

**Available to the public from the National Technical Information Service,
U.S. Department of Commerce, 5285 Port Royal Rd., Springfield, VA 22161
ph: (800) 553-6847
fax: (703) 605-6900
email: orders@ntis.fedworld.gov
online ordering: <http://www.ntis.gov/ordering.htm>**



This document was printed on recycled paper.

(9/2003)

Geochemical Characterization of Chromate Contamination in the 100 Area Vadose Zone at the Hanford Site

Part 2

NP Qafoku
PE Dresel
JP McKinley
E Ilton

W Um
CT Resch
RK Kukkadapu
SW Petersen

January 2011

Prepared for
the U.S. Department of Energy
under Contract DE-AC05-76RL01830

Pacific Northwest National Laboratory
Richland, Washington 99352

Summary

At the Hanford Site in Richland, Washington, Cr was used throughout the 100 Areas (100-B, 100-C, 100-D/DR, 100-F, 100-H, and 100-K) as a corrosion inhibitor in reactor cooling water. Chromate (CrO_4^{2-}), a hexavalent Cr [Cr(VI)] chemical species, was delivered in rail cars, tanker trucks, barrels, and local pipelines as dichromate granular solid or stock solution. Many times Cr was inevitably discharged to the surface or near-surface ground through spills during handling, during disposal to cribs, or via pipeline leaks. Because the exact sources, time of discharges, and chemical compositions of these liquids are unfortunately unknown, and given that contaminant Cr(VI) mobility in surface and subsurface natural systems depends—among other factors—on the chemical composition and pH of the waste liquids, experimental work is needed to characterize Cr contamination, and determine sediment liquid and solid phase alterations as a result of exposure to waste liquids.

Successful groundwater protection from Cr contamination depends on an understanding of the currently unknown or not well understood coupled chemical reactions and hydrological processes that control or affect contaminant Cr(VI) interactions with the sediments during downward movement through the physically and mineralogically heterogeneous vadose zone. Contaminant Cr(VI) may sorb to mineral surfaces, precipitate in mineral phases with varying stability, and may also get reduced to Cr(III), a reaction that may lead to the formation of pure Cr(III) phases or Fe(III)/Cr(III) solid solutions. An estimation of the extent and rates of these reactions and processes is required to achieve a fundamental understanding of Cr vadose zone geochemistry. This may help in accelerating the 100 Area Columbia River Corridor cleanup by developing scientifically based remedial actions.

Current work is building on the U.S. Department of Energy Office of Environmental Management-funded findings published in a previous Pacific Northwest National Laboratory (PNNL) report (Dresel et al. 2008). The scope is to provide additional data on Cr(VI) behavior in sediments exposed to different waste fluids. Specifically, the scientific objectives are as follows:

1. Determine the leaching characteristics of Cr contaminant from the contaminated sediments of the 100-D Area using hydraulically unsaturated and saturated column experiments.
2. Characterize sediment Cr contamination and elucidate possible attenuation mechanism(s) responsible for Cr retention through the use of extraction techniques and microscale characterization studies.
3. Provide additional information to construct a conceptual model of Cr(VI) geochemistry in the Hanford Site 100 Area vadose zone that can be used for developing environmental remediation strategies based on a fundamental understanding of Cr(VI) vadose zone geochemistry. Because of budget and schedule limitations, this effort is acknowledged to be less comprehensive than we would have liked but of sufficient technical credibility to support decision making.

Over fiscal years 2008 and 2009, PNNL received from Washington Closure Hanford 3 contaminated and 1 uncontaminated sediment samples from the newly discovered area of Cr contamination in the 100-D-104 Area in early 2008 (hereafter called 2008 sediments), and 32 contaminated sediment samples from the 100-D-100 Area in 2009 (hereafter called 2009 sediments). From the set of 32 contaminated 2009 sediments, 5 surface sediments were selected based on their relatively high Cr concentration. The 2008 and selected 2009 sediment samples were used in a series of wet chemical extractions and hydraulically saturated and unsaturated column experiments to study Cr desorption patterns and determine Cr mobility. The contaminated sediments were characterized with X-ray diffraction, electron

microprobe, and X-ray photoelectron spectroscopy (XPS) to determine Cr mineral association and its valence state, and to identify possible mechanisms of chemical or physical Cr(VI) attenuation in these sediments. In addition, Mössbauer spectroscopy was used to gain insights on the Fe mineralogy of the sediments.

Results demonstrated that water-extractable Cr concentration (expressed as μg of Cr per g of sediment; $\mu\text{g/g}$ is the same as mg/kg) was low in all sediments. Conversely, acid- and microwave-extractable Cr concentrations were significantly higher. Smaller size fractions separated from the 2009 sediments had more microwave-extractable Cr associated with them. Collectively, the results from water, acid extractions, and microwave digestion showed that sediments contained substantial amounts of Cr that were not readily extracted in batch experiments (low solid to solution ratio).

Results from the column experiments (high solid to solution ratio) corroborated the results from the wet chemical extractions. With the exception of one 2009 sediment, almost all Cr contaminant mass remained in the sediments during leaching, demonstrating that Cr was strongly bounded to the sediments. The average effluent pH was acidic in 2008 contaminated sediments, and basic in 2009 sediments. This indicates that sediment geochemistry was significantly altered by the waste fluids (unaltered sediments from the same area usually have neutral or slightly alkaline pH), and that waste fluids with different pH and compositions were discarded in the 2008 and 2009 sediments. Low Ba concentrations were observed in the column effluents in the experiments conducted with 2008 and 2009 sediments. Most likely, the effluent aqueous Cr(VI) concentrations and contaminant mobility were not controlled by the solubility of Ba- and Cr-containing solids, although BaCrO_4 (hashemite) or other less-soluble solid solutions of $\text{BaCrO}_4 - \text{BaSO}_4$ may have been formed in these sediments.

The results from the electron microprobe inspections and measurements indicated that zones of high Cr concentration were not present in the randomly selected areas of sediment samples analyzed with electron microprobes. However, the XPS measurements confirmed that contaminant Cr was present in detectable amounts in all contaminated 2008 sediments and in at least one 2009 sediment, although the Cr signal was low. Both Cr(VI) and Cr(III) were present in the contaminated sediments. Fe occurred in both valence state, Fe(II) and Fe(III), with the predominance of Fe(III) but with an appreciable Fe(II) component. It was also found the Cr-containing regions were enriched in Fe. This enrichment, however, was only limited to the top ~ 8 nm of the sample (XPS is a surface exploring technique). The correlation of Fe and Cr implied a similar temporal origin. The Cr(III)2p binding energies were suggestive of a Cr(III)-oxyhydroxide, and not oxides, such as Cr_2O_3 . In addition, it was not possible to rule out the formation of a Fe(III)-Cr(III) oxyhydroxide or possible Cr incorporation into silicates. Mössbauer spectroscopy measurements indicated that the uncontaminated bulk sediment sample contained an appreciable Fe(II) component that potentially may donate the electron to acceptors, such as hexavalent Cr.

Based on these results, the most likely Cr(VI) attenuation mechanism in these sediments appears to be reduction to Cr(III), which may have subsequently formed solid phases and/or Cr(III)/Fe(III) solid solutions with limited solubility. The results suggest that Fe(II) may have served as a reductant of Cr(VI). Dissolution of Fe(II)-bearing minerals of Hanford Site sediments might have occurred at the time of sediment exposure to waste fluids, and Fe(II) may have been released into the aqueous phase. In addition, dissolution of the surface coatings covering Fe(II)-bearing minerals may have also occurred, exposing structural Fe(II) to redox sensitive contaminants of the contacting aqueous phase. Therefore, sorbed, structural and/or aqueous Fe(II) may have been involved in contaminant Cr(VI) reduction.

Conversely, other Cr(VI) attenuation mechanisms may have been operational, but further studies are needed to determine the relative importance of different attenuation pathways. For example, the decreased Cr mobility in the contaminated sediments may have also been caused by the formation of Cr(VI) sparingly soluble solids (such as Ba Cr). In addition, the solid phase Cr speciation remains unknown. Although XPS was successfully used to determine contaminant Cr valence state and its association with other chemical elements of interest—such as Fe—XPS is a surface-exploring technique (8 nm depth from mineral surface). Both bulk and higher resolution spectroscopic analyses are required to supplement and assist in the interpretation of the XPS data, determine the solid phase speciation of contaminant Cr, and provide evidence for additional attenuation mechanism(s) of the contaminant Cr(VI) that originated from the waste fluids.

Acronyms and Abbreviations

bgs	below ground surface
BTC	breakthrough curve
Cr(III)	trivalent chromium (the most common valence state in natural sediments)
Cr(VI)	hexavalent chromium (the valence state of chromate and dichromate)
DI	deionized
DOE	U.S. Department of Energy
Ecology	Washington State Department of Ecology
EDS	energy dispersive spectroscopy
EM	U.S. Department of Energy - Environmental Management
EMP	electron microprobe
EMPA	electron microprobe analysis
EPA	U.S. Environmental Protection Agency
h	hours
IC	ion chromatography
ICP-OES	inductively coupled plasma optical emission spectrometer
MCL	maximum contaminant level
PDF	powder diffraction files
PNNL	Pacific Northwest National Laboratory
ppm	parts per million
redox	reduction/oxidation
SEM	scanning electron microscopy
SGW	synthetic groundwater
WCH	Washington Closure Hanford
XPS	X-ray photoelectron spectroscopy
XRD	X-ray diffraction
XRF	X-ray fluorescence

Contents

Summary	iii
Acronyms and Abbreviations	vii
1.0 Introduction	1.1
1.1 Background	1.1
1.2 Overall Objectives.....	1.3
2.0 Sediment Sample Collection and Characterization	2.1
2.1 Sample Location and Nomenclature	2.1
2.1.1 2008 Sediment Samples	2.1
2.1.2 2009 Sediment Samples	2.1
2.2 Sediment Characterization	2.1
2.2.1 X-Ray Diffraction Analyses.....	2.1
2.2.2 Size-Fraction Separation	2.2
2.2.3 Chemical Extractions	2.2
2.3 Results.....	2.3
2.3.1 X-Ray Diffraction Analyses.....	2.3
2.3.2 Size-Fraction Separation	2.3
2.3.3 Chemical Extractions and Measurements	2.3
2.4 Summary of Sample Collection and Characterization	2.5
3.0 Transport Studies.....	3.1
3.1 Introduction.....	3.1
3.2 Materials and Method.....	3.1
3.2.1 Column Experiment Methodology.....	3.1
3.2.2 Leaching Solutions.....	3.2
3.2.3 Chemical Analyses.....	3.2
3.2.4 Transport Parameters Calculation	3.3
3.3 Results and Discussion.....	3.3
3.3.1 Cr(VI) Transport Behavior and Overall Mobility: 2008 Experiments.....	3.3
3.3.2 Cr(VI) Transport Behavior and Overall Mobility: 2009 Experiments.....	3.4
3.3.3 Modeling Results: 2008 Experiments	3.5
3.3.4 Effluent Solution Composition: 2008 Experiments	3.5
3.4 Summary of Transport Experiment Results	3.6
4.0 Microscopic Investigation of Sediments Chromium Spatial Distribution.....	4.1
4.1 Introduction.....	4.1
4.2 Materials and Methods.....	4.1

4.2.1	Electron Microprobe Measurements	4.1
4.2.2	X-Ray Photoelectron Spectroscopy Measurements	4.1
4.2.3	Mössbauer Spectroscopy Measurements.....	4.1
4.3	Results and Discussion.....	4.2
4.3.1	Electron Microprobe Measurements	4.2
4.3.2	X-Ray Photoelectron Spectroscopy Measurements	4.2
4.3.3	Mössbauer Spectroscopy Measurements: Preliminary Results.....	4.3
4.4	Summary of the Microscale Characterization Data.....	4.3
5.0	Summary of Major Findings.....	5.1
6.0	References	6.1

Figures

2.1	Sample locations in 100-D-100 and 100-D-104 waste sites, and preliminary schematic presentation of the Cr investigation in the southwest area.....	2.30
2.2	Photograph showing a broken pipe and stained sediments	2.31
2.3	XRD patterns of the <2 mm fraction of all 2008 sediments	2.32
2.4	XRD results of the BC sediment.....	2.33
2.5	XRD results of the BS sediment	2.34
2.6	XRD results of the YS sediment	2.35
2.7	XRD results of the YS2 sediment	2.36
2.8	XRD patterns of the <63 μm fraction of sediment J18NH6	2.37
2.9	XRD patterns of the <63 μm fraction of sediment J18NK0	2.38
2.10	XRD patterns of the <63 μm fraction of sediment J18NJ3.....	2.39
2.11	XRD patterns of the <63 μm fraction of sediment J18PH5	2.40
3.1	Experimental set up for transport experiments in unsaturated column; nylon membrane, filter paper, and nylon mesh; a picture of a quartz sand-packed column; and dissembled column and tensiometers.....	3.11
3.2	Cr(VI) leaching profile of sediment YS.....	3.12
3.3	Cr(VI) leaching profile of sediment BC.....	3.12
3.4	Cr(VI) leaching profile of sediment BSent.	3.13
3.5	Cr(VI) leaching profile of sediment J18NH6.....	3.13
3.6	Cr(VI) leaching profile of sediment J18NJ3	3.14
3.7	Cr(VI) leaching profile of sediment J18NK0.....	3.14
3.8	Cr(VI) leaching profile of sediment J18NF7	3.15
3.9	Cr(VI) leaching profile of sediment J18PH5	3.15
3.10	Changes in effluent pH during leaching Cr(VI) leaching in experiments conducted with sediments J18NH6, J18NJ3, J18NK0, J18NF7, and J18PH5	3.16
3.11	Cr(VI) leaching profiles in saturated and unsaturated column experiments conducted with sediment J18NF7	3.18
3.12	Cr(VI) leaching profiles in saturated and unsaturated column experiments conducted with sediment J18NH6.....	3.19
3.13	Cr(VI) leaching profiles in saturated and unsaturated column experiments conducted with sediment J18NJ3	3.19
3.14	Br breakthrough curves obtained in different experiments conducted with sediments YS, BC, and BS.....	3.20
3.15	Br breakthrough curves obtained in different experiments conducted with sediments J18NH6, J18NJ3, J18NK0, J18NF7, and J18PH5	3.22
4.1	Results of the EMP measurements performed in sediment BC	4.5
4.2	Results of the EMP measurements performed in sediment YS	4.6
4.3	Results of the EMP measurements performed in sediment BS.....	4.7
4.4	Results of the EMPA measurements performed in sediment J18NH6	4.8

4.5	Results of the EMPA measurements performed in sediment J18NJ3	4.9
4.6	Results of the EMP measurements performed in sediment J18NK0	4.10
4.7	Results of the EMP measurements performed in sediment J18NF7	4.11
4.8	Results of the EMP measurements performed in sediment J18PH5	4.12
4.9	XPS survey spectra	4.13
4.10	XPS of Cr2p region: Comparison of sediments BS and BC	4.14
4.11	XPS of Cr2p3/2 region for sediment YS.....	4.14
4.12	XPS of Fe2p region for sediment BS.....	4.15
4.13	XPS survey spectra of sediment J18NH6	4.15
4.14	Results from the Mössbauer spectroscopy measurements performed in sediment BC at room temperature and 77 K.....	4.16
4.15	Preliminary results of the Mössbauer spectroscopy measurements performed in sediment YS at 77 K	4.17

Tables

2.1	Sample locations, coordinates, depths, sample identifications, and analyses of the aqueous phase of acid digestion extractions conducted with all 2009 sediments	2.8
2.2	Results from particle-size analyses conducted in 2008 sediments.....	2.11
2.3	Results from particle-size distribution analysis in 2009 sediments	2.12
2.4	Results from the water extractions conducted in 2008 sediments	2.17
2.5	Results from the 0.5 M HNO ₃ extractions conducted in 2008 sediments.....	2.18
2.6	Results from the microwave digestion conducted in 2008 sediments	2.19
2.7	Results from cation analyses conducted in the aqueous phase of acid digestion extractions in all 2009 sediments	2.20
2.8	Results from anion analyses conducted in the aqueous phase of acid digestion extractions in all 2009 sediments	2.25
2.9	pH measurements in the representative 2009 sediment samples	2.27
2.10	Results from DI-water and acid extractions 2009 sediment samples.....	2.28
2.11	Results from microwave digestion conducted in 2009 sediment samples	2.29
3.1	Composition of the synthetic groundwater used in the chromium and bromine leaching experiments.....	3.7
3.2	Selected measured and calculated physical properties in each column	3.8
3.3	Results from the elemental analyses performed in effluent samples collected at different times during leaching in columns 1, 2, and 3	3.9
3.4	Results from the elemental analyses performed in effluent samples collected at different times during leaching in column experiments.....	3.10
4.1	Elemental analyses and valence states of transition metals	4.4

1.0 Introduction

1.1 Background

The Hanford Site was the location of the U.S. government's primary plutonium production during the World War II Manhattan Project and the cold war. Hexavalent chromium—mainly sodium dichromate ($\text{Na}_2\text{Cr}_2\text{O}_7 \cdot 2\text{H}_2\text{O}$)—was used extensively as a corrosion inhibitor in the nuclear reactor cooling water and for equipment decontamination (Thornton 1992; Peterson et al. 1996a). After passing through the reactor, cooling water was transported through large-diameter underground pipes to retention basins for thermal and radioactive cooling before release to the Columbia River. Sodium dichromate concentrations of 2.0 mg/L (0.7 mg/L as Cr) were added to the cooling water (Foster 1957).

Until approximately 1953, the sodium dichromate solutions were made in a batch system using 100-lb bags of granular dichromate manually hopped into large (~3600 gal) tanks to obtain final solution concentration of 15% $\text{Na}_2\text{Cr}_2\text{O}_7$ by weight (wt) (Whipple 1953). After 1953, 70% by weight (wt) $\text{Na}_2\text{Cr}_2\text{O}_7$ solutions were delivered to the Hanford Site, stored in large tanks, and diluted as required (Schroeder 1966). These concentrated solutions were delivered to various water treatment plants in rail cars, tanker trucks, barrels, and local pipelines as stock solutions. A summary of 100-D Area operations and waste sites is presented in the *100-D Area Technical Baseline Report* (Carpenter 1993).

Concentrated dichromate solutions were inevitably discharged to surface or near-surface ground through spills during handling, pipeline leaks, or when discarded to cribs. Additional Cr was discharged to the environment from decontamination operations, likely after mixing with sulfuric acid to form chromic acid (Peterson et al. 1996). The pH of these solutions, buffering capacity, and counter-ion concentration is critical to $\text{Na}_2\text{Cr}_2\text{O}_7$ solution vadose zone geochemistry. While the exact acidity of Hanford Site Cr stock solutions is not known, a 10% $\text{Na}_2\text{Cr}_2\text{O}_7$ ($0.82 \text{ mol L}^{-1} \text{ Cr}$) has a pH of 3.5, and a 70% $\text{Na}_2\text{Cr}_2\text{O}_7$ ($8.96 \text{ mol L}^{-1} \text{ Cr}$) may be lower (~1.5 to 2) (Dresel et al. 2008).

In the 1990s, after the end of the production mission, increasing attention was focused on the chemical impacts of chromium contamination, particularly in the 100 Areas (100-B, 100-C, 100-D/DR, 100-F, 100-H, and 100-K) where the nuclear reactors were located along the Columbia River. Potential sources of vadose zone and groundwater contamination include leaks from cooling water pipelines and retention basins, disposal of contaminated water to liquid waste cribs and trenches, and spills of sodium dichromate solids or solutions (Thornton 1992).

Hexavalent chromium [Cr(VI)] is a groundwater contaminant at numerous U.S. Department of Energy (DOE) sites across the nation. Chromate (CrO_4^{2-}) is one of the major contaminants of concern near the Columbia River in the 100 Areas at the Hanford Site (*Hanford Site Groundwater Monitoring and Performance Report for 2009, Volumes 1 & 2* [DOE/RL 2010]). Cr(VI), which has higher toxicity than reduced Cr(III), is highly mobile under neutral and slightly alkaline conditions that are commonly present in the Hanford Site vadose zone. For this contaminant, aquatic water quality criterion of $11 \mu\text{g L}^{-1}$ is lower than drinking water standards (0.1 mg L^{-1}).

The known extent of Cr contamination in Hanford Site groundwater is described in annual site groundwater reports (e.g., Hartman et al. 2009). The highest concentrations and greatest extent of Cr contamination are in the 100-D/DR Area groundwater. Discharge of chromium-contaminated

groundwater to the Columbia River has been documented through porewater sampling in the river bed, and small diameter sampling points (called aquifer tubes) along the shoreline (Hope and Peterson 1996). Dissolved chromium in the groundwater is dominated by hexavalent Cr(VI), as anionic chromate, CrO_4^{2-} (Thornton et al. 1995). The highest groundwater Cr concentrations are in the 100-D Area, within the 100-HR-3 CERCLA Groundwater Operable Unit. Understanding the nature of the vadose zone contamination is important to evaluating options for remediation and protection of groundwater and environmental receptors.

Activities to define the sources of groundwater Cr contamination in the 100 Areas have had limited success. Reports of characterization efforts in the 100-D Area include Lerch (1998), Thornton et al. (2000, 2001), Anselem and Kreuger (2004), and Petersen et al. (2009). Characterization activities completed in 2008 also detected only small amounts of Cr in the vadose zone although the new groundwater wells detected chromium concentrations up to 60,000 $\mu\text{g/L}$ (Petersen and Hall 2008; Mahood 2009).

Successful groundwater remediation and protection depends on the ability to understand and limit the flux of Cr(VI) to the water table from the vadose zone. The recent groundwater plume characterization has further emphasized the presence of an ongoing chromium source near the 100-D Area dichromate transfer station (Petersen and Hall 2008). Characterization of limited samples from near-surface Cr(VI)-contaminated soils in the 100-B/C and 100-D Areas has shown that although a large portion of the vadose zone chromium may be mobile as dissolved Cr, some fraction is less leachable, leading to long tailing in the release curves. At some waste sites, a considerable fraction of the Cr is immobile—likely as Cr(III) associated with the presence of an increased amount of ferric oxyhydroxide. The variability in leaching behavior indicates the importance of additional characterization of vadose zone chromium mobility for the development of realistic conceptual models and predictions of future contaminant fate and transport. A summary of previous studies is in the following paragraphs. The unknowns in Cr sources and geochemical properties lead to the characterization of additional samples, as reported here.

The vadose zone Cr geochemistry investigations are focused on defining the controls on Cr(VI) flux to the groundwater and providing a basis for predicting the attenuation of the contaminant sources. The studies are centered on available Cr(VI)-bearing sediments from field characterization or remediation activities. The studies address the following:

- Advective transport of dissolved Cr(VI): The proportion of the Cr(VI) that is readily transported is a fundamental parameter for assessing the current Cr(VI) flux to the water table. Longitudinal dispersivity and any possible retardation of the chemical transport versus the aqueous flow are considered.
- Physical sequestration in finer-grained particles (e.g., weathered clays) or dead-end pores that can contribute to tailing of the Cr(VI) movement and contribution to persistent source flux.
- Chromate minerals—e.g., $\text{Ba}(\text{SO}_4, \text{CrO}_4)$ —and incorporation of trace levels of Cr(VI) into other mineral phases.
- Oxidation-reduction reactions that naturally sequester the Cr as Cr(III) and may form the basis for in-situ remediation. The role of Fe-bearing minerals is particularly important.

- The role of codisposed chemicals on subsurface reactions between the waste and minerals. As discussed below, the codisposal of acidic or other waste is emerging as an important control on Cr(VI) mobility at some waste sites.

Previous DOE-Environmental Management (EM)-20 funded work characterized Cr contamination from 100-B/C Area samples. Those samples were collected at a shallower depth in most cases or apparently had lower levels of contamination. The degree of Cr interaction with the sediments during downward transport through the vadose zone is unknown and this remains an unresolved issue. Aqueous Cr(VI) may be involved in a number of geochemical reactions and/or processes that may affect its mobility in the vadose zone. These include reduction of Cr(VI) to Cr(III), followed by precipitation of Cr(III) phases or coprecipitation of Fe(III)/Cr(III) solid solutions, sorption of Cr(VI) to soil mineral surfaces, and precipitation of Cr(VI) mineral phases with varying stabilities. However, the EM-20 work found that most of the Cr (over 95% of total Cr) was highly mobile and only a small leaching resistant fraction was present in the sediments, producing a long tail of mobilization in saturated column experiments. Microscopic characterization indicated that Cr was found on grain coatings but some Cr was associated with individual “hot-spots” and in altered minerals. Dresel et al. (2008) recently published a report on the EM-funded work.

Recent groundwater plume characterization indicates the presence of an ongoing chromium source near the 100-D Area dichromate transfer station (Petersen and Hall 2008). The variability in leaching behavior observed in past studies indicates the importance of additional characterization of vadose zone chromium mobility for the development of realistic conceptual models and predictions of future contaminant fate and transport. The current work is building on EM-funded findings by characterizing the additional contaminated sediment samples available from the 100-D Area. The scope is to provide supplemental data from the new samples for comparison of the microscopic-scale Cr distribution and the Cr mobility to the previous samples. A series of column experiments were conducted during this study using contaminated sediments from the 100-D Area. Several extraction and microscopic-scale techniques were also used to characterize sediment contamination and identify possible mechanisms of chemical or physical Cr(VI) attenuation in these sediments. A fundamental understanding of Cr vadose zone geochemistry may help accelerate the 100 Area Columbia River Corridor cleanup by developing scientifically based remedial actions.

1.2 Overall Objectives

The research in this report addresses the following primary objectives:

1. Determine leaching characteristics of Cr(VI) from contaminated sediments collected in the 100-D Area of the Hanford Site
2. Characterize sediment contamination and elucidate possible mechanisms of Cr(VI) attenuation through the use of extraction techniques and microscale characterization
3. Provide additional information to construct a conceptual model of Cr(VI) geochemistry in the Hanford Site 100 Area vadose zone as a basis for selecting potential remedial measures.

2.0 Sediment Sample Collection and Characterization

2.1 Sample Location and Nomenclature

2.1.1 2008 Sediment Samples

Washington Closure Hanford (WCH) investigated a newly discovered area of Cr contamination from the 100-D-104 waste site in early 2008. WCH excavated at the location of a former French drain east of the 183-D Water Treatment Facility. This site is believed to have received neutralized sulfuric acid waste and dichromate. An above ground Na-dichromate storage tank was located nearby. The soil contamination was excavated down approximately 20 ft below ground surface (bgs), following discolored soil. Four samples were collected from this location. One sample was from a **yellow-stained** zone at the bottom of the track-hoe excavation (hereafter called sediment YS). The second sediment sample was from a rusty **brown-stained** zone at the excavation bottom (hereafter called sediment BS). The third sediment sample was from a shovel excavation that extended approximately 2 ft below the track-hoe pit (hereafter called sediment YS2). A small volume (~100 g) was collected from the third sample. The fourth sample was an unstained sample believed to represent the background **black “clean”** soil (hereafter called sediment BC).

2.1.2 2009 Sediment Samples

The contaminated sediments were collected in southwest of the 100-D-100 Area in early 2009 (Table 2.1 and Figures 2.1 and 2.2). Pacific Northwest National Laboratory (PNNL) received 32 samples from this location. Five of these sediment samples were selected for this study, based on the relatively high total Cr concentration in them. These sediment samples were as follows: J18NH6, J18NJ3, J18NK0, J18NF7, and J18PH5.

2.2 Sediment Characterization

2.2.1 X-Ray Diffraction Analyses

The 2008 sediment samples were particle-size separated into > and <2 mm size-fractions, and the powder of the <2 mm fractions of all sediments were characterized by X-ray diffraction (XRD).

The 2009 samples were particle-size separated into size-fractions, and the powders of the <63 μm fraction of four sediments (J18NH6, J18NJ3, J18NK0, and J18PH5) were characterized by XRD.

Each sample was analyzed using a Scintag Pad V XRD equipped with a Peltier thermoelectrically-cooled detector and a copper X-ray tube. The diffractometer was operated at 45 kV and 40 mA. Diffractograms were obtained from 2 to 75⁰ 2 θ using a step-scan increment of 0.2 degrees and a dwell time of 2 seconds. Scans were collected electronically and processed using JADE® XRD pattern-processing software.¹ Minerals identification was based on comparison of the measured XRD patterns to

¹ JADE is a trademark of Jade Software Corporation Limited.

those of mineral powder diffraction files published by the Joint Committee on Powder Diffraction Standards International Center for Diffraction Data.

2.2.2 Size-Fraction Separation

The 2009 sediment samples were sieved through a set of sieves to separate size fractions and determine the particle size distribution (in percentage) in each sediment.

2.2.3 Chemical Extractions

The <2 mm fractions of each 2008 sediment were exposed to 2 extracting solutions for 48 h: distilled (DI) water and a 0.5 M double-distilled HNO₃ solution. At the end of the extraction period, the solids were separated from the liquid phase and a full set of chemical elemental analyses was performed in the extracted liquids.

The microwave digestion technique was used to determine total Cr in the sediments. This technique consisted of the following steps:

1. Weigh out 0.50 g <2.00 mm soil in triplicate into 2 mL cryogenic vials (Corning #430488).
2. Transfer to Teflon® microwave digestion bombs. Calibrate pipets using water and three-place balance.
3. Add 9 mL concentrated HNO₃, 3 mL concentrated HF, and 2 mL concentrated HCl. Replace top. Ensure rupture seal is in place and tight. HNO₃, Fisher Optima lot 1207120; HF, Fisher Optima 7664-39-3; HCl, Fisher Optima lot 4207110.
4. Start machine using method XP1500. Microwave ramps up to 180°C and holds for 9 minutes.
5. Let cool and repeat heat cycle. Transfer to 20 mL polypropylene plastic scintillation vials containing 0.3 g boric acid (to neutralize HF).
6. Use Alfa Aesar boric acid, 99.99% (lot K07R056), 0.8 g total for two extractions.
7. Repeat acid extraction a second time with new acid. Combine the two acid extracts into a single sample.
8. Filter acid extract with 0.20-micron Teflon syringe filter (Millipore cat#SLLGC25NS).
9. Analyze filterates using an inductively coupled plasma optical emission spectrometer (ICP-OES) for Cr, Si, Mg, Al, Fe, K, Na, Ca, Ba, S, P, and Mn.

All 2009 sediments underwent acid extraction (U.S. Environmental Protection Agency [EPA] Method 3050B [EPA 1996a]) and the concentrations of 26 elements in the aqueous phase were determined with ICP at the end of the extraction period. EPA Method 3060A (EPA 1996b) was used to determine Cr(VI). The EPA Method 300 was used to determine the anion concentrations of inorganic anions using ion chromatography.¹ These analyses were performed in a Colorado laboratory.

¹ The EPA acid digestion methods are located at <http://www.cem.de/documents/pdf/publikation/digestion/Rd125.pdf>.

In addition, the <2 mm fractions of five sediments (J18NH6, J18NJ3, J18NK0, J18NF7, and J18PH5) were exposed in a PNNL laboratory to four extracting solutions; namely, DI-water, 0.5 M double-distilled HNO₃ solution, and 8 M nitric acid. Finally, the microwave digestion procedure was used to determine total Cr concentration in size fractions separated from the <2 mm fraction of each of the five sediments. At the end of the extraction period, the solids were separated from the liquid phase and a full set of chemical elemental analyses was performed in the extracted liquids.

2.3 Results

2.3.1 X-Ray Diffraction Analyses

Results from the XRD analyses of the <2 mm fraction conducted in 2008 indicated the sediments had similar mineralogy (quartz, anorthite, albite) (Figures 2.3, 2.4, 2.5, 2.6, and 2.7). Hematite was detected in sediment BC and BS.

Results from the XRD analyses of the <63 μm fraction conducted in 2009 indicated that the four Cr-contaminated sediments analyzed with this technique (i.e., J18NH6, J18NK0, J18NJ3, and J18PH5) had similar mineralogy of the silt and clay fractions. The predominant minerals are quartz, anorthite, albite, muscovite, halloysite, biotite, calcite, rutile, and clinocllore (Figures 2.8, 2.9, 2.10, and 2.11).

2.3.2 Size-Fraction Separation

Results from the fraction-size separation analyses conducted in 2008 are in Table 2.2. Sediments YS and BS had similar amounts of the <2000 μm fractions (73.5% and 77.6%, respectively), while sediment BC had only 59.5% of this fraction. Additional work is required to separate all size fractions from the sediments. Surface area and other measurements should be performed in future studies involving all size fractions to gather information on contaminant Cr and soil mineral interactions.

Results from the size-fraction separation conducted in 2009 are in Table 2.3. The particle-size fraction analyses showed that sediment J18NH6 contained 6.44 and 15.73 g of <63 μm and <125> 63 size fractions, off a total of 77.91 μm g of <2 mm size-fraction sample. Other sediments had significantly smaller amounts of these small fractions that are the most reactive fractions in the sediments. These fractions were used during the microwave Cr extractions.

2.3.3 Chemical Extractions and Measurements

2.3.3.1 Extractions and Measurements Performed in 2008 Sediment Samples

Results from the water and acid extractions of the sediments conducted in 2008 are in Tables 2.4 and 2.5. All extractions were conducted in three replicates. The results are expressed as μg of Cr per gram of sediment (the unit μg/g is the same as mg/kg).

Small and insignificant amounts of Cr were extracted from the sediments exposed to DI-water for 48 h. This indicated that contaminant Cr was immobile and not easily removable from the sediments. The greatest water extractable concentration was found in sediment YS2 ($C_{\text{WATER EXTRACTABLE YS2}} = 0.36 \pm 0.04 \mu\text{g g}^{-1}$).

Water extractable Ca and S concentrations were more than one order of magnitude greater in sediment YS than in the other sediments ($C_{\text{WATER EXTRACTABLE YS}} = 521.45 \pm 24.43 \mu\text{g g}^{-1}$, and $S_{\text{WATER EXTRACTABLE YS}} = 456.95 \pm 20.17 \mu\text{g g}^{-1}$). Similar S and Ca water extractable molar concentrations ($S = 14.25 \mu\text{mol g}^{-1}$ and $\text{Ca} = 13.01 \mu\text{mol g}^{-1}$) were present in this sediment. Appreciable or detectable amounts of Mg and Si were also released from all sediments during the 48-h water extraction.

Results from 48-h acid extraction were drastically different. Significant amounts of Cr were extracted from sediments YS, BS, and YS2. The acid extractable Cr concentration was low in sediment BC that was practically uncontaminated ($C_{\text{ACID EXTRACTABLE BC}} = 0.84 \pm 0.05 \mu\text{g g}^{-1}$), but it was much higher in the other sediments ($C_{\text{ACID EXTRACTABLE YS}} = 84.36 \pm 0.24 \mu\text{g g}^{-1}$; $C_{\text{ACID EXTRACTABLE BS}} = 114.90 \pm 0.216 \mu\text{g g}^{-1}$; and $C_{\text{ACID EXTRACTABLE YS2}} = 64.44 \pm 0.99 \mu\text{g g}^{-1}$).

In addition to Cr, substantial amounts of other elements such as S, P, Ba, Mn, Fe, Si, Mg, Ca, Al, Na, and K were also released from the sediments during the 48-h acid extraction. It would be expected that all adsorbed and surface-precipitated Cr may be dissolved during the acid extraction. However, the extent of the acid attack on the sediment matrix and dissolution/desorption of Cr that might be present in the crystalline phases of the sediment matrix is unknown. In addition, oxidative dissolution might have also occurred during nitric acid extraction, although its extent is expected to be low.

Even greater amounts of Cr were extracted from the sediments using the microwave digestion technique (Table 2.6). The microwave extractable Cr concentration was again low in sediment BC ($C_{\text{MICROWAVE EXTRACTABLE BC}} = 22.34 \pm 6.43 \mu\text{g g}^{-1}$), but it was much greater in the other sediments ($C_{\text{MICROWAVE EXTRACTABLE YS}} = 231.72 \pm 3.49 \mu\text{g g}^{-1}$; $C_{\text{MICROWAVE EXTRACTABLE BS}} = 200.81 \pm 1.13 \mu\text{g g}^{-1}$; and $C_{\text{MICROWAVE EXTRACTABLE YS2}} = 184.14 \pm 3.29 \mu\text{g g}^{-1}$).

Similarly to water and acid extraction data, the microwave extraction data clearly showed that S was present in substantial amounts in contaminated sediments YS, BS, and YS2, confirming that these sediments were exposed to sulfuric acid waste solutions. Appreciable amounts of Ba were also released from all sediments during microwave extraction.

2.3.3.2 Extractions and Measurements Performed in 2009 Sediment Samples

Results from the extractions performed following the EPA Method 3050B (EPA 1996a) are in Table 2.7. The following 26 elements were determined in the aqueous phase at the end of the extraction period: Al, Sb, As, Ba, Be, B, Cd, Ca, Cr(total), Co, Cu, Cr(hexavalent), Fe, Pb, Li, Mg, Mn, Hg, Mo, Ni, K, Se, Si, Ag, Na, V, and Zn.

In addition, results from using EPA Method 3060A (EPA 1996b) to determine hexavalent Cr concentration are also included in Table 2.7. Finally, the concentrations of the following anions were also measured and presented in Table 2.8 using the EPA Method 300 on determination of inorganic anions by ion chromatography: bromide, chloride, fluoride, nitrate, nitrite, phosphate, and sulfate. The moisture content percentage was also measured in all sediment samples.

From these results, researchers can infer that surface sediments had the greatest total and hexavalent Cr contents. Based on this initial assessment, the following surface sediments J18NH6, J18NJ3, J18NK0, J18NF7, and J18PH5 were selected for further characterization and leaching studies.

Measurements of pH that were taken in 1:1 solid: solution suspension demonstrated the aqueous phase in contact with the sediments had a basic pH, which in sediment J18NJ3, was as high as 9.21 (Table 2.9).

Results from the water and acid extractions of the sediments are in Table 2.10. Small and insignificant amounts of Cr were extracted from the sediments exposed to DI water. The greatest water extractable concentration was found in sediment J18NH6 ($C_{\text{WATER EXTRACTABLE YS2}} = 2.16 \text{ mg kg}^{-1}$).

The results from acid extractions were drastically different. Significant amounts of Cr were extracted from all sediments. The 0.5 M acid-extractable Cr concentration varied from a minimum of $30.299 \text{ mg kg}^{-1}$ in sediment J18NK0, to a maximum of $74.823 \text{ mg kg}^{-1}$ in sediment J18NH6.

The results from 8 M acid extractions were similar to the results of the 0.5 M acid extractions. The 8 M acid-extractable Cr concentration varied from a minimum of $33.505 \text{ mg kg}^{-1}$ in sediment J18NK0, to a maximum of $82.400 \text{ mg kg}^{-1}$ in sediment J18NH6. All sediments released a greater Cr amount when exposed to the 8 M acid solution as compared to the 0.5 M acid solution.

Even greater amounts of Cr were extracted from the size fractions of the sediments using the microwave digestion technique (Table 2.11). The microwave-extractable Cr concentration varied in different size-fractions, and the greatest concentration was measured in the smallest size-fractions.

2.4 Summary of Sample Collection and Characterization

Results Summary from the 2008 Effort

1. Four sediment samples were collected in early 2008 from the newly discovered area of Cr contamination in the 100-D Area. This site received neutralized sulfuric acid waste and dichromate. The first sample was from a yellow-stained zone at the bottom of the track-hoe excavation. The second sample was from a rusty brown-stained zone at the excavation bottom. The third sample was from a shovel excavation that extended approximately 2 ft below the track-hoe pit. A small volume (~100 g) was collected from the third sample. The fourth sample was an unstained sample that may represent the background black “clean” soil.
2. The XRD results indicated the sediments had similar mineralogy.
3. The size-fraction analyses showed sediment YS and BS contained between 73% and 77% of the <2000 μm fraction. Separation of all size-fractions is recommended for future studies. XRD, scanning electron microscope (SEM), energy dispersive spectroscopy (EDS), and surface area measurements should be performed in each size-fraction to collect valid information on Cr:soil mineral interactions.
4. Water-extractable Cr concentration was small and close to zero in all contaminated sediments (it varied from 0.06 to $0.36 \mu\text{g g}^{-1}$).

5. Acid extractable and microwave-digestion Cr concentrations were significantly greater in all contaminated sediments. Acid-extractable Cr concentration varied from 64.4 to 114.9 $\mu\text{g g}^{-1}$, while microwave-digestion Cr concentration varied from 184.1 to 231.7 $\mu\text{g g}^{-1}$. Current cleanup levels for WCH surface remediation sites are 2.6 $\mu\text{g g}^{-1}$ (or 0.050 mmol kg^{-1}).
6. An important conclusion from acid extraction and microwave digestion is sediments YS, BS, and YS2 contained substantial amounts of Cr that were not readily extracted with water and exhibited limited mobility.

Results Summary from the 2009 Effort

1. PNNL received 32 total sediments samples from the 100-D Area. Based on hexavalent and total Cr contents of the sediments, five surface sediments—namely sediment J18NH6, J18NJ3, J18NK0, J18NF7, and J18PH5—were selected to conduct further characterization and leaching studies.
2. The XRD results indicated the sediments had similar mineralogy. Further work is needed (e.g., semiquantitative and quantitative XRD analyses) to determine if there are differences among sediments in terms of soil mineral types and contents.
3. The particle size-fraction analyses showed that sediment J18NH6 contained 6.44 and 15.73 g of <63 μm and <125> 63 size-fractions, off a total of 77.91 $\mu\text{m g}$ of <2 mm size-fraction samples. Other sediments had significantly smaller amounts of these small fractions that are considered the most reactive fractions in the sediments. XRD, SEM, EDS, and surface area measurements should be performed in each size-fraction separated from these sediments to collect valid information on Cr:soil mineral interactions.
4. pH measurements taken in 1:1 solid: solution suspensions demonstrated that sediment pH was basic (the highest pH = 9.21 was measured in sediment J18NJ3).
5. Water-extractable Cr concentration was small and close to zero in all contaminated sediments (it varied from 0.105 mg kg^{-1} in sediment J18NF7 to 2.16 mg kg^{-1} in sediment J18NH6).
6. Acid-extractable Cr concentrations were significantly greater in all contaminated sediments. The 0.5 M acid-extractable Cr concentration varied from a minimum of 30.299 mg kg^{-1} in sediment J18NK0, to a maximum of 74.823 mg kg^{-1} in sediment J18NH6. Although greater in magnitude, results from 8 M acid extractions were similar to the 0.5 M acid extractions. The 8 M acid-extractable Cr concentration varied from a minimum of 33.505 mg kg^{-1} in sediment J18NK0 to a maximum of 82.400 mg kg^{-1} in sediment J18NH6. The analyses to determine the elemental composition of extractable solutions will be conducted in the coming weeks.
7. Microwave digestion analyses of different size-fractions separated from five sediments demonstrated that smaller size fractions had more Cr associated with them. The smallest Cr concentration of 3.938 mg kg^{-1} was in the 500 – 1000 μm fraction of sediment J18NK0, but even this concentration is well above the current cleanup level for WCH surface remediation sites, which is 2.6 mg kg^{-1} (or 0.050 mmol kg^{-1}). The analyses to determine the elemental composition of the solutions from microwave digestion will be conducted in the coming weeks.
8. The results from water, acid extractions and microwave digestion suggest that sediments contained substantial amounts of Cr that were not readily extracted with water at the high solution to solid ratios tested in these experiments.

The reduced Cr mobility in the contaminated sediments may have been caused by either the formation of Cr(VI) sparingly soluble solids (such as Ba Cr), or the reduction of Cr(VI) to Cr(III) and subsequent precipitation of Cr(III) phases and/or Cr(III)/Fe(III) solid solutions. Dissolution of soil minerals might have occurred at the time of exposure, and chemical elements such as Ba and Fe(II) might have been released into the aqueous phase. Most likely, Ba and Fe(II) were subsequently involved in chemical and/or redox reactions with aqueous Cr(VI). Both these attenuation pathways may have contributed to contaminant Cr immobilization in these sediments. Further studies are needed to determine the relative importance of these attenuation pathways.

Table 2.1. Sample locations, coordinates, depths, sample identifications, and analyses of the aqueous phase of acid digestion extractions conducted with all 2009 sediments

Sample Location	Coordinate Locations	Depth (bgs)	Sample Number	Requested Analysis	Comments
Test pit	N 151355 E 573353 <i>(Test pit moved ~10' SE of original location, need to get new coordinates from D. Shea)</i>	Surface (0.3 m [1 ft])	J18NF9	ICP metals, mercury, IC anions, hexavalent chromium	Tan, sandy silt, very little cobbles.
		0.9 m (3 ft)	J18NH0	ICP metals, mercury, IC anions, hexavalent chromium	Black sand, medium to large cobbles.
		1.5 m (5 ft)	J18NH1	ICP metals, mercury, IC anions, hexavalent chromium	Black sand, medium to large cobbles.
		2.1 m (7 ft)	J18NH2	ICP metals, mercury, IC anions, hexavalent chromium	Black sand, medium to large cobbles.
		2.7 m (9 ft)	J18NH3	ICP metals, mercury, IC anions, hexavalent chromium	Medium brown sandy silt, cobbles.
		3.4 m (11 ft)	J18NH4	ICP metals, mercury, IC anions, hexavalent chromium	Medium brown sandy silt, cobbles. Collected XRF measurements from 3 locations in backhoe bucket; 80, 65, 53 ppm total chromium.
		4.6 m (15 ft)	J18NH5	ICP metals, mercury, IC anions, hexavalent chromium	Medium brown sandy silt, cobbles. Ecology split J18PH0.
Trench (east end)	N 151365 E 573355	Surface (0.3 m [1 ft])	J18NH6	ICP metals, mercury, IC anions, hexavalent chromium	Tan, sandy silt, very little cobbles.
		0.9 m (3 ft)	J18NH7	ICP metals, mercury, IC anions, hexavalent chromium	Coarse, medium to dark brown sand, with some cobbles.
		1.5 m (5 ft)	J18NH8	ICP metals, mercury, IC anions, hexavalent chromium	Dark coarse sand.
		2.1 m (7 ft)	J18NH9	ICP metals, mercury, IC anions, hexavalent chromium	Black, coarse (Hanford) sand, cobbles.
		2.7 m (9 ft)	J18NJ0	ICP metals, mercury, IC anions, hexavalent chromium	Black (Hanford) sand, poorly sorted cobbles.
		3.4 m (11 ft)	J18NJ1	ICP metals, mercury, IC anions, hexavalent chromium	Mixture of black (Hanford) sand, brown fine sediment, cobbles.
		4.6 m (15 ft)	J18NJ2	ICP metals, mercury, IC anions, hexavalent chromium	Sandy gravel. Collected XRF measurements from three locations in backhoe bucket, ND, 49, 43 ppm total Cr. Ecology split sample J18PH1.

Table 2.1. (contd)

Sample Location	Coordinate Locations	Depth (bgs)	Sample Number	Requested Analysis	Comments
Trench (middle)	N 151366 E 573352	Surface (0.3 m [1 ft])	J18NJ3	ICP metals, mercury, IC anions, hexavalent chromium	Tan, sandy silt, very little cobbles.
		0.9 m (3 ft)	J18NJ4	ICP metals, mercury, IC anions, hexavalent chromium	Coarse, medium to dark brown sand, with some cobbles.
		1.5 m (5 ft)	J18NJ5	ICP metals, mercury, IC anions, hexavalent chromium	Dark coarse sand.
		2.1 m (7 ft)	J18NJ6	ICP metals, mercury, IC anions, hexavalent chromium	Dark (Hanford) sand, tan fines, poorly sorted cobbles.
		2.7 m (9 ft)	J18NJ7	ICP metals, mercury, IC anions, hexavalent chromium	Black (Hanford) sand, poorly sorted cobbles.
		3.4 m (11 ft)	J18NJ8	ICP metals, mercury, IC anions, hexavalent chromium	Mixture of black (Hanford) sand, brown/tan fine sediment, cobbles. Collected XRF measurements from 3 locations in backhoe bucket, 2 locations were ND, and 1 location was 67 ppm total Cr.
		4.6 m (15 ft)	J18NJ9	ICP metals, mercury, IC anions, hexavalent chromium	Sand and gravel. Ecology split sample J18PH2.
Trench (west end)	N 151366 E 573348	Surface (0.3 m [1 ft])	J18NK0	ICP metals, mercury, IC anions, hexavalent chromium	Tan, sandy silt, very little cobbles.
		0.9 m (3 ft)	J18NK1	ICP metals, mercury, IC anions, hexavalent chromium	Mix of black and tan sand, poorly sorted cobbles.
		1.5 m (5 ft)	J18NK2	ICP metals, mercury, IC anions, hexavalent chromium	Brown sand, cobbles.
		2.1 m (7 ft)	J18NK3	ICP metals, mercury, IC anions, hexavalent chromium	Course sand, gravel.
		2.7 m (9 ft)	J18NK4	ICP metals, mercury, IC anions, hexavalent chromium	Black sand, cobbles.
		3.4 m (11 ft)	J18NK5	ICP metals, mercury, IC anions, hexavalent chromium	Black sand, cobbles. Collected XRF measurements from 3 locations in backhoe bucket, 2 locations were ND, and 1 location was 52 ppm total Cr.
		4.6 m (15 ft)	J18NK6	ICP metals, mercury, IC anions, hexavalent chromium	Ecology split sample J18PH3.
Duplicate trench (west end)	N 151366 E 573348	1.5 m (5 ft)	J18NF8	ICP metals, mercury, IC anions, hexavalent chromium	Tie to J18NK2, brown sand, cobbles.

Table 2.1. (contd)

Sample Location	Coordinate Locations	Depth (bgs)	Sample Number	Requested Analysis	Comments
Duplicate test pit	<i>Need to get coordinates from D. Shea</i>	Surface (0.3 m [1 ft])	J18NF7	ICP metals, mercury, IC anions, hexavalent chromium	Tie to sample J18NF9.
Equipment blank	N/A	N/A	J18NF6	ICP metals, mercury, IC anions, hexavalent chromium	Tie to sample J18NJ0.
8 – 10 ft north of trench	<i>Need to get coordinates from D. Shea</i>	Surface (0.3 m [1 ft])	J18PH5	ICP metals, mercury, IC anions, hexavalent chromium	Yellow staining visible after 0.3 m (1 ft) of soil was removed from surface of waste site. XRF results on stained area are 1800 ppm total chromium. Focus sample collected. After material was placed in a bag and homogenized, XRF results were 150 ppm total Cr.
Ecology = Washington State Department of Ecology; IC = ion chromatography; ppm = parts per million; XRF = X-ray fluorescence.					

Table 2.2. Results from particle-size analyses conducted in 2008 sediments

Particle Size Analysis Summary							
100-D-30	Yellow Soil, 3/26/2008, 1012 hrs						
		average	standard	rep 1	rep 2	rep 3	
Sieve size		% of total	deviation	% of total	% of total	% of total	
pan	< 2000 micron	73.57348	10.66672	61.28171	80.4	79.03872	
2000 micron	>2000 micron	26.42652	10.66672	38.71829	19.6	20.96128	
100-D-30	Brown stained Soil, 3/26/2008, 1028 hrs						
		average	standard	rep 1	rep 2	rep 3	
Sieve size		% of total	deviation	% of total	% of total	% of total	
pan	< 2000 micron	77.64898	7.67114	79.43925	84.26667	69.24101	
2000 micron	>2000 micron	22.35102	7.67114	20.56075	15.73333	30.75899	
100-D-30	Black "clean" sand 3/26/2008, 1042 hrs						
		average	standard	rep 1	rep 2	rep 3	
Sieve size		% of total	deviation	% of total	% of total	% of total	
pan	< 2000 micron	59.54551	8.274551	61.30319	50.53333	66.8	
2000 micron	>2000 micron	40.45449	8.274551	38.69681	49.46667	33.2	

Table 2.3. (contd)

PARTICLE SIZE DISTRIBUTION ANALYSIS				
Input				
Balance Used:	1118401492			
Calibration Expiration:	Aug-09			
Date:	7/14/2009			
Sample ID:	J18NJ3			
Sample + container Wt:	112.48	(moisture in bag)		
Tare Wt:	12.98			
TOTAL SOIL MATERIAL(g):	99.50	Calc		
	Input	Input	Calc	
SIEVE NUMBER (8 inch)	mm	TARE	TOTAL WEIGHT	SOIL WEIGHT
10	2	435.39	440.10	4.71
18	1	338.82	349.71	10.89
35	0.5	273.05	336.69	63.64
60	0.25	388.76	399.78	11.02
120	0.125	261.05	265.74	4.69
230	0.063	246.33	247.60	1.27
PAN	----	375.66	375.84	0.18
Calc				
TOTAL SIEVED*		99.50		
TOTAL RECOVERED		96.40		
% RECOVERED		96.88%		

Table 2.3. (contd)

PARTICLE SIZE DISTRIBUTION ANALYSIS				
Input				
Balance Used:	1118401492			
Calibration Expiration:	Aug-09			
Date:	7/14/2009			
Sample ID:	J18NF7			
Sample + container Wt:	116.95	(moisture in bag)		
Tare Wt:	12.95			
TOTAL SOIL MATERIAL(g):	104.00	Calc		
	Input	Input	Calc	
SIEVE NUMBER (8 inch)	mm	TARE	TOTAL WEIGHT	SOIL WEIGHT
10	2	435.39	449.33	13.94
18	1	338.82	373.75	34.93
35	0.5	273.05	325.94	52.89
60	0.25	388.76	389.87	1.11
120	0.125	261.05	261.23	0.18
230	0.063	246.33	246.49	0.16
PAN	----	375.66	375.77	0.11
		Calc		
	TOTAL SIEVED*	104.00		
	TOTAL RECOVERED	103.32		
	% RECOVERED	99.35%		

Table 2.3. (contd)

PARTICLE SIZE DISTRIBUTION ANALYSIS				
Input				
Balance Used:	1118401492			
Calibration Expiration:	Aug-09			
Date:	7/14/2009			
Sample ID:	J18PH5			
Sample + container Wt:	112.77			
Tare Wt:	12.79			
TOTAL SOIL MATERIAL(g):	99.98	Calc		
	Input	Input	Calc	
SIEVE NUMBER (8 inch)	mm	TARE	TOTAL WEIGHT	SOIL WEIGHT
10	2	435.39	440.19	4.80
18	1	338.82	350.89	12.07
35	0.5	273.05	305.85	32.80
60	0.25	388.76	403.79	15.03
120	0.125	261.05	273.90	12.85
230	0.063	246.33	265.06	18.73
PAN	----	375.66	378.89	3.23
Calc				
TOTAL SIEVED*		99.98		
TOTAL RECOVERED		99.51		
% RECOVERED		99.53%		

Table 2.4. Results from the water extractions conducted in 2008 sediments

Table 2										
Extract 100-D-30 Cr soils with DI H2O for 48 hours										
Soil	Extracted Cr (ug/g soil)	Extracted S (ug/g soil)	Extracted P (ug/g soil)	Extracted Ba (ug/g soil)	Extracted Mn (ug/g soil)	Extracted Fe (ug/g soil)	Extracted Si (ug/g soil)	Extracted Mg (ug/g soil)	Extracted Ca (ug/g soil)	Extracted Al (ug/g soil)
yellow soil, 3/26/2008, 1012 hrs	0.07	478.15	< 4	< 0.1	0.12	< 1	58.36	22.87	544.92	< 1
yellow soil, 3/26/2008, 1012 hrs	0.08	454.72	< 4	< 0.1	0.12	< 1	58.54	22.71	523.26	< 1
yellow soil, 3/26/2008, 1012 hrs	0.07	437.99	< 4	< 0.1	0.12	< 1	59.98	22.38	496.16	< 1
average	0.07	456.95	0.00	0.00	0.12	0.00	58.96	22.65	521.45	0.00
stdv	0.004	20.171	0.000	0.000	0.005	0.000	0.887	0.249	24.433	0.000
brown stained soil, 3/26/2008, 1028 hrs	0.07	26.60	< 4	< 0.1	0.09	< 1	30.26	1.98	29.92	< 1
brown stained soil, 3/26/2008, 1028 hrs	0.05	22.49	< 4	< 0.1	0.08	< 1	30.78	1.69	25.08	< 1
brown stained soil, 3/26/2008, 1028 hrs	0.05	22.01	< 4	< 0.1	0.08	< 1	30.54	1.66	24.94	< 1
average	0.06	23.70	0.00	0.00	0.08	0.00	30.53	1.78	26.64	0.00
stdv	0.007	2.523	0.000	0.000	0.003	0.000	0.260	0.178	2.835	0.000
black "clean" sand 3/26/2008, 1042 hrs	< 0.1	< 20	< 4	< 0.1	< 0.1	0.79	27.16	2.60	14.82	0.58
black "clean" sand 3/26/2008, 1042 hrs	< 0.1	< 20	< 4	< 0.1	< 0.1	0.68	26.97	2.68	15.59	0.51
black "clean" sand 3/26/2008, 1042 hrs	< 0.1	< 20	< 4	< 0.1	< 0.1	0.85	28.71	2.79	15.83	0.60
average	0.00	0.00	0.00	0.00	0.00	0.77	27.61	2.69	15.41	0.56
stdv	0.000	0.000	0.000	0.000	0.000	0.085	0.952	0.096	0.530	0.046
yellow soil 2' below grade, 3/26/2008	0.34	< 20	< 4	< 0.1	< 0.1	5.07	60.88	1.41	12.01	0.41
yellow soil 2' below grade, 3/26/2008	0.40	< 20	< 4	< 0.1	< 0.1	6.52	60.82	1.37	10.86	0.55
yellow soil 2' below grade, 3/26/2008	0.34	< 20	< 4	< 0.1	< 0.1	5.11	61.03	1.33	10.62	0.42
average	0.36	0.00	0.00	0.00	0.00	5.57	60.91	1.37	11.16	0.46
stdv	0.036	0.000	0.000	0.000	0.000	0.824	0.110	0.044	0.746	0.075

Table 2.5. Results from the 0.5 M HNO₃ extractions conducted in 2008 sediments

Table 3											
Extract 100-D-30 Cr soils with 0.5 M/L GFS double distilled nitric acid for 48 hours											
	Extracted										
Soil	Cr (ug/g soil)	S (ug/g soil)	P (ug/g soil)	Ba (ug/g soil)	Mn (ug/g soil)	Fe (ug/g soil)	Si (ug/g soil)	Mg (ug/g soil)	Ca (ug/g soil)	Al (ug/g soil)	Na (ug/g soil)
yellow soil, 3/26/2008, 1012 hrs	84.13	583.68	553.99	4.95	31.50	3617.86	535.66	830.27	2782.79	821.50	115.57
yellow soil, 3/26/2008, 1012 hrs	84.61	511.40	542.54	5.20	28.84	3409.74	486.22	803.49	2699.07	791.93	109.21
yellow soil, 3/26/2008, 1012 hrs	84.35	527.78	577.73	4.78	29.83	3525.01	492.48	815.86	2913.49	831.52	111.60
average	84.36	540.96	558.09	4.98	30.06	3517.54	504.79	816.54	2798.45	814.98	112.13
stdv	0.236	37.899	17.948	0.208	1.343	104.261	26.921	13.400	108.063	20.584	3.211
brown stained soil, 3/26/2008, 1028	114.82	109.74	1379.49	11.08	72.71	6759.42	790.03	1718.02	3581.83	1215.59	40.80
brown stained soil, 3/26/2008, 1028	115.15	108.66	1356.27	11.72	77.27	6660.13	785.51	1702.28	3499.75	1189.45	41.29
brown stained soil, 3/26/2008, 1028	114.75	108.06	1348.36	11.41	86.03	6512.88	755.27	1665.89	3366.87	1186.04	41.26
average	114.90	108.82	1361.38	11.40	78.67	6644.14	776.93	1695.39	3482.81	1197.03	41.11
stdv	0.216	0.848	16.182	0.320	6.768	124.047	18.900	26.737	108.476	16.164	0.274
black "clean" sand 3/26/2008, 1042	0.89	< 20	1222.35	25.82	120.81	5627.13	776.15	2033.44	4112.30	1223.60	70.52
black "clean" sand 3/26/2008, 1042	0.83	< 20	1265.46	27.60	144.95	5899.73	802.15	2090.90	4112.38	1191.13	64.53
black "clean" sand 3/26/2008, 1042	0.79	< 20	1262.00	25.00	128.33	5918.28	806.80	2045.51	4094.26	1177.38	68.42
average	0.84	#DIV/0!	1249.94	26.14	131.36	5815.05	795.03	2056.61	4106.31	1197.37	67.83
stdv	0.052	#DIV/0!	23.954	1.331	12.356	163.007	16.518	30.297	10.439	23.735	3.038
yellow soil 2' below grade, 3/26/200	64.75	180.09	577.93	9.44	27.05	3716.70	521.67	835.15	2387.55	844.61	96.83
yellow soil 2' below grade, 3/26/200	63.32	163.28	605.42	9.50	26.25	3798.28	512.17	871.81	2418.54	840.02	97.48
yellow soil 2' below grade, 3/26/200	65.21	171.09	622.38	9.76	27.28	3821.36	524.60	890.82	2534.61	872.91	102.49
average	64.43	171.48	601.91	9.57	26.86	3778.78	519.48	865.93	2446.90	852.51	98.93
stdv	0.990	8.413	22.433	0.170	0.538	54.989	6.498	28.296	77.523	17.811	3.096

Table 2.6. Results from the microwave digestion conducted in 2008 sediments

Table 4											
Microwave digestion of the sediments											
	Extracted		Extracted	Extracted	Extracted	Extracted	Extracted	Extracted	Extracted	Extracted	Extracted
Soil	Cr (ug/g soil)	Cr mmol/kg	S (ug/g soil)	P (ug/g soil)	Ba (ug/g soil)	Mn (ug/g soil)	Fe (ug/g soil)	Si (ug/g soil)	Mg (ug/g soil)	Ca (ug/g soil)	Al (ug/g soil)
yellow soil, 3/26/2008, 1012 hrs	234.30	4.51	2239.93	817.97	247.03	1135.22	56932.44	795873.58	48.65	131.11	3949.86
yellow soil, 3/26/2008, 1012 hrs	233.12	4.48	2246.54	976.24	124.40	1089.56	72256.67	357326.19	70.35	166.99	10026.14
yellow soil, 3/26/2008, 1012 hrs	227.74	4.38	2966.15	832.97	212.76	1178.46	59831.40	294173.83	53.64	126.78	3599.30
average	231.72	4.46	2484.21	875.73	194.73	1134.41	63006.84	482457.87	57.54	141.63	5858.43
stdv	3.494	0.067	417.385	87.367	63.269	44.457	8140.670	273256.498	11.367	22.072	3613.590
brown stained soil, 3/26/2008, 1028	199.64	3.84	3102.95	1640.37	129.40	1170.90	70620.39	211564.52	93.58	228.08	10633.82
brown stained soil, 3/26/2008, 1028	201.90	3.88	591.55	1476.11	220.04	1246.41	55794.64	301807.27	62.90	145.63	3264.87
brown stained soil, 3/26/2008, 1028	200.89	3.86	544.10	1684.54	155.06	1210.97	71472.15	296607.34	110.73	241.92	10157.76
average	200.81	3.86	1412.87	1600.34	168.17	1209.42	65962.39	269993.04	89.07	205.21	8018.82
stdv	1.130	0.022	1463.850	109.829	46.719	37.780	8815.824	50667.336	24.234	52.060	4123.911
black "clean" sand 3/26/2008, 1042	23.28	0.45	243.97	1351.03	213.73	1375.40	55797.77	280415.69	102.62	169.13	2992.49
black "clean" sand 3/26/2008, 1042	28.25	0.54	294.08	1507.18	131.51	1206.42	71514.96	291711.19	106.60	234.15	11043.09
black "clean" sand 3/26/2008, 1042	15.49	0.30	175.30	1352.41	228.38	1316.55	48198.92	297136.62	75.94	165.00	3217.10
average	22.34	0.43	237.78	1403.54	191.21	1299.46	58503.88	289754.50	95.05	189.43	5750.89
stdv	6.433	0.124	59.631	89.760	52.216	85.780	11891.246	8530.463	16.673	38.786	4584.551
yellow soil 2' below grade, 3/26/200	187.89	3.61	1879.95	921.90	119.25	1092.43	58894.02	308978.08	81.14	126.81	8098.84
yellow soil 2' below grade, 3/26/200	181.76	3.50	1695.65	858.98	209.81	1210.31	51360.50	288336.31	55.06	124.90	3591.14
yellow soil 2' below grade, 3/26/200	182.76	3.51	1809.54	792.88	251.49	1114.71	54511.41	284533.74	71.68	120.95	5052.63
average	184.14	3.54	1795.05	857.92	193.52	1139.15	54921.98	293949.38	69.29	124.22	5580.87
stdv	3.290	0.063	93.001	64.519	67.611	62.627	3783.506	13153.379	13.201	2.990	2299.809

Table 2.7. Results from cation analyses conducted in the aqueous phase of acid digestion extractions in all 2009 sediments

100-D-100 Sample Summary																					
HEIS Number	Location	Depth	Sample Date	Aluminum			Antimony			Arsenic			Barium			Beryllium			Boron		
				mg/kg	Q	PQL	mg/kg	Q	PQL	mg/kg	Q	PQL	mg/kg	Q	PQL	mg/kg	Q	PQL	mg/kg	Q	PQL
J18NF9	Test Pit	-1		5400	L	1.6	0.4	UM	0.4	3.4		0.7	53	L	0.08	0.19	B	0.04	1	UM	1
J18NH0	Test Pit	-3		5100	L	1.6	0.4	U	0.4	2.7		0.69	41	L	0.08	0.12	B	0.04	1	U	1
J18NH1	Test Pit	-5		4200	L	1.6	0.4	U	0.4	1.6	B	0.7	57	L	0.08	0.13	B	0.04	2.1		1
J18NH2	Test Pit	-7		3800	L	1.6	0.39	U	0.39	2	B	0.68	52	L	0.08	0.1	B	0.03	1	U	1
J18NH3	Test Pit	-9		5800	L	1.7	0.41	U	0.41	2.4		0.71	56	L	0.08	0.19	B	0.04	1.1	U	1.1
J18NH4	Test Pit	-11		5400	L	1.7	0.41	U	0.41	2.7		0.71	61	L	0.08	0.2	B	0.04	1.1	U	1.1
J18NH5	Test Pit	-15		5000	L	1.7	0.41	U	0.41	2.8		0.7	62	L	0.08	0.19	B	0.04	1	U	1
J18NH6	Trench East End	-1		5900		1.6	1.1	BM	0.4	3.5		0.69	74		0.08	0.81		0.03	1	U	1
J18NH7	Trench East End	-3		5100		1.6	0.4	U	0.4	2.3		0.69	60		0.08	0.69		0.04	1	U	1
J18NH8	Trench East End	-5		6000		1.7	0.41	U	0.41	2.6		0.71	81		0.08	1		0.04	1.1	U	1.1
J18NH9	Trench East End	-7		4000		1.6	0.39	U	0.39	1.6	B	0.68	55		0.08	0.93		0.03	1	U	1
J18NJ0	Trench East End	-9		4500		1.6	0.39	U	0.39	1.7	B	0.69	66		0.08	0.93		0.03	1	U	1
J18NJ1	Trench East End	-11		5000		1.6	0.4	U	0.4	1.9	B	0.69	62		0.08	0.79		0.04	2.5		1
J18NJ2	Trench East End	-15		5600		1.7	0.4	U	0.4	2	B	0.7	76		0.08	0.81		0.04	1	U	1
J18NJ3	Trench Middle	-1		6300	L	1.6	0.43	B	0.39	3.6		0.68	75	L	0.08	0.69		0.03	1	U	1
J18NJ4	Trench Middle	-3		5900	L	1.6	0.4	U	0.4	3.4		0.7	57	L	0.08	0.78		0.04	1	U	1
J18NJ5	Trench Middle	-5		4400	L	1.6	0.4	U	0.4	2.1		0.7	56	L	0.08	0.77		0.04	1	U	1
J18NJ6	Trench Middle	-7		4600	L	1.6	0.4	U	0.4	1.6	B	0.69	53	L	0.08	0.99		0.03	1	U	1
J18NJ7	Trench Middle	-9		4800	L	1.6	0.4	U	0.4	1.8	B	0.69	68	L	0.08	1		0.03	1	U	1
J18NJ8	Trench Middle	-11		4500	L	1.7	0.4	U	0.4	2	B	0.7	68	L	0.08	0.72		0.04	1	U	1
J18NJ9	Trench Middle	-15		6600	L	1.7	0.41	U	0.41	2.7		0.72	72	L	0.08	0.84		0.04	1.1	U	1.1
J18NK0	Trench West End	-1		5400		1.6	0.38	U	0.38	3.2		0.67	46		0.08	0.18	B	0.03	3.3	M	0.99
J18NK1	Trench West End	-3		4600		1.6	0.76	B	0.39	1.9	B	0.69	50		0.08	0.77		0.03	1	U	1
J18NK2	Trench West End	-5		5400		1.7	0.52	B	0.4	2.7		0.7	96		0.08	1		0.04	1	U	1
J18NK3	Trench West End	-7		4900		1.6	0.52	B	0.4	2	B	0.69	54		0.08	1		0.04	1	U	1
J18NK4	Trench West End	-9		4100		1.6	0.55	B	0.39	1.8	B	0.68	65		0.08	0.96		0.03	1	U	1
J18NK5	Trench West End	-11		5400		1.7	0.44	B	0.4	2.1		0.7	77		0.08	0.94		0.04	1	U	1
J18NK6	Trench West End	-15		5100		1.7	0.51	B	0.41	2	B	0.71	68		0.08	0.89		0.04	1	U	1
J18NF8	Trench West End	-5		5700		1.6	0.4	U	0.4	2.3		0.7	62		0.08	0.9		0.04	1	U	1
J18NF7	Test Pit	-1		6000		1.6	0.4	U	0.4	3.5		0.7	57		0.08	0.7		0.04	1.3	B	1
J18NF6	Equipment Blank	NA		180	N	1.6	0.38	U	0.38	0.66	U	0.66	3.2	M	0.08	0.033	U	0.03	0.98	U	0.98
J18PH5	North of trench	-1		5900		1.6	0.7	B	0.4	3.6		0.69	67		0.08	0.76		0.03	2.1	C	1

Table 2.7. (contd)

100-D-100 Sample Summary

HEIS Number	Location	Depth	Sample Date	Cadmium			Calcium			Total Chromium			Cobalt			Copper			Hexavalent Chromium		
				mg/kg	Q	PQL	mg/kg	Q	PQL	mg/kg	Q	PQL	mg/kg	Q	PQL	mg/kg	Q	PQL	mg/kg	Q	PQL
J18NF9	Test Pit	-1		0.092	B	0.04	11000	L	15	79	L	0.06	6.9	L	0.11	13	L	0.23	30		0.155
J18NH0	Test Pit	-3		0.062	B	0.04	4600	L	15	11	L	0.06	8.5	L	0.11	17	L	0.23	1.49		0.155
J18NH1	Test Pit	-5		0.06	B	0.04	4500	L	15	6.3	L	0.06	8.2	L	0.11	12	L	0.23	1.73		0.155
J18NH2	Test Pit	-7		0.044	B	0.04	4900	L	15	8.1	L	0.06	8.8	L	0.1	13	L	0.22	0.796		0.155
J18NH3	Test Pit	-9		0.049	B	0.04	5100	L	15	11	L	0.06	8.3	L	0.11	15	L	0.23	3.06		0.155
J18NH4	Test Pit	-11		0.044	U	0.04	6400	L	15	13	L	0.06	7.9	L	0.11	15	L	0.23	4.91		0.155
J18NH5	Test Pit	-15		0.044	U	0.04	5200	L	15	12	L	0.06	8.2	L	0.11	15	L	0.23	4.14		0.155
J18NH6	Trench East End	-1		0.071	BM	0.04	11000		15	150	L	0.06	8.7	L	0.1	15		0.23	87		1.54
J18NH7	Trench East End	-3		0.043	U	0.04	6300		15	30	L	0.06	7.4	L	0.1	14		0.23	3.27		0.155
J18NH8	Trench East End	-5		0.044	U	0.04	5700		15	28	L	0.06	9.1	L	0.11	14		0.23	2.23		0.155
J18NH9	Trench East End	-7		0.042	U	0.04	4700		15	14	L	0.06	9.4	L	0.1	12		0.22	0.155	U	0.155
J18NJ0	Trench East End	-9		0.043	U	0.04	4700		15	15	L	0.06	9.1	L	0.1	12		0.23	4.72		0.155
J18NJ1	Trench East End	-11		0.043	U	0.04	6800		15	17	L	0.06	7.4	L	0.1	13		0.23	1.73		0.155
J18NJ2	Trench East End	-15		0.044	U	0.04	5000		15	31	L	0.06	8.1	L	0.11	12		0.23	17.6		0.155
J18NJ3	Trench Middle	-1		0.043	U	0.04	15000	L	15	46	L	0.06	6.9	L	0.1	12	L	0.22	1.93		0.155
J18NJ4	Trench Middle	-3		0.043	U	0.04	8800	L	15	25	L	0.06	7.8	L	0.11	15	L	0.23	1.03		0.155
J18NJ5	Trench Middle	-5		0.043	U	0.04	3900	L	15	10	L	0.06	7.9	L	0.11	11	L	0.23	1.15		0.155
J18NJ6	Trench Middle	-7		0.043	U	0.04	4500	L	15	11	L	0.06	9.3	L	0.1	12	L	0.23	0.94		0.155
J18NJ7	Trench Middle	-9		0.043	U	0.04	4600	L	15	13	L	0.06	9.1	L	0.1	11	L	0.23	1.46		0.155
J18NJ8	Trench Middle	-11		0.044	U	0.04	4100	L	15	13	L	0.06	8.4	L	0.11	16	L	0.23	2.75		0.155
J18NJ9	Trench Middle	-15		0.044	U	0.04	5900	L	15	29	L	0.06	8.3	L	0.11	14	L	0.24	12.1		0.155
J18NK0	Trench West End	-1		0.074	B	0.04	8100		14	41		0.06	6.4	L	0.1	13		0.22	1.77		0.155
J18NK1	Trench West End	-3		0.043	U	0.04	5900		15	9.1	L	0.06	9.4	L	0.1	15		0.23	0.175		0.155
J18NK2	Trench West End	-5		0.044	U	0.04	5000		15	8.4	L	0.06	13	L	0.11	17		0.23	0.527		0.155
J18NK3	Trench West End	-7		0.043	U	0.04	5300		15	9.4	L	0.06	11	L	0.1	16		0.23	1.02		0.155
J18NK4	Trench West End	-9		0.042	U	0.04	4700		15	9.2	L	0.06	11	L	0.1	15		0.22	1.28		0.155
J18NK5	Trench West End	-11		0.044	U	0.04	5500		15	15	L	0.06	11	L	0.11	16		0.23	3.16		0.155
J18NK6	Trench West End	-15		0.044	U	0.04	5100		15	13	L	0.06	10	L	0.11	15		0.23	2.51		0.155
J18NF8	Trench West End	-5		0.044	U	0.04	4800		15	7.4		0.06	8.7		0.11	13		0.23	0.57		0.155
J18NF7	Test Pit	-1		0.043	U	0.04	11000		15	86		0.06	7.4		0.11	13		0.23	29.3		0.155
J18NF6	Equipment Blank	NA		0.041	U	0.04	53	C	14	0.16	B	0.06	0.1	U	0.1	0.43	BC	0.22	0.155	U	0.155
J18PH5	North of trench	-1		0.043	U	0.04	11000		15	86		0.06	8	L	0.1	13	L	0.23	33.7		0.155

Table 2.7. (contd)

100-D-100 Sample Summary

HEIS Number	Location	Depth	Sample Date	Iron			Lead			Lithium			Magnesium			Manganese			Mercury		
				mg/kg	Q	PQL	mg/kg	Q	PQL	mg/kg	Q	PQL	mg/kg	Q	PQL	mg/kg	Q	PQL	mg/kg	Q	PQL
J18NF9	Test Pit	-1		19000	L	4	2.5		0.29	5.5	N	0.32	4600	L	3.9	270	L	0.11	0.0059	U	0.006
J18NH0	Test Pit	-3		23000	L	4	3.1		0.28	5.1		0.32	4300	L	3.9	300	L	0.11	0.0058	U	0.006
J18NH1	Test Pit	-5		22000	L	4	3.3		0.28	4.6		0.32	3800	L	3.9	290	L	0.11	0.0058	U	0.006
J18NH2	Test Pit	-7		24000	L	3.9	2.1		0.28	3.6		0.31	4200	L	3.8	280	L	0.1	0.0057	U	0.006
J18NH3	Test Pit	-9		21000	L	4.1	3.6		0.29	5.6		0.32	4300	L	4	280	L	0.11	0.006	U	0.006
J18NH4	Test Pit	-11		21000	L	4.1	3.7		0.29	5.8		0.32	4200	L	4	290	L	0.11	0.0059	U	0.006
J18NH5	Test Pit	-15		21000	L	4.1	3.2		0.29	5.6		0.32	4200	L	3.9	300	L	0.11	0.0059	U	0.006
J18NH6	Trench East End	-1		20000		4	3		0.28	5.7		0.31	4500		3.9	270	L	0.1	0.0058	U	0.006
J18NH7	Trench East End	-3		21000		4	2.4		0.28	5.1		0.31	4300		3.9	280	L	0.1	0.0058	U	0.006
J18NH8	Trench East End	-5		26000		4.1	3.5		0.29	5.8		0.32	4800		4	310	L	0.11	0.0059	U	0.006
J18NH9	Trench East End	-7		25000		3.9	2		0.28	3.6		0.31	4100		3.8	290	L	0.1	0.0057	U	0.006
J18NJ0	Trench East End	-9		25000		3.9	2.1		0.28	3.8		0.31	4100		3.8	340	L	0.1	0.0057	U	0.006
J18NJ1	Trench East End	-11		22000		4	2.7		0.28	3.9		0.31	3700		3.9	230	L	0.1	0.0058	U	0.006
J18NJ2	Trench East End	-15		21000		4	3		0.29	5.9		0.32	4200		3.9	270	L	0.11	0.0059	U	0.006
J18NJ3	Trench Middle	-1		19000	L	3.9	3		0.28	6.1	N	0.31	4300	L	3.8	260	L	0.1	0.0057	U	0.006
J18NJ4	Trench Middle	-3		22000	L	4	3		0.28	5.8		0.32	4700	L	3.9	280	L	0.11	0.0058	U	0.006
J18NJ5	Trench Middle	-5		22000	L	4	2.4		0.29	4.1		0.32	4000	L	3.9	270	L	0.11	0.0059	U	0.006
J18NJ6	Trench Middle	-7		26000	L	4	2		0.28	3.5		0.31	3900	L	3.8	290	L	0.1	0.0058	U	0.006
J18NJ7	Trench Middle	-9		26000	L	4	2.1		0.28	3.9		0.31	4000	L	3.9	330	L	0.1	0.0058	U	0.006
J18NJ8	Trench Middle	-11		20000	L	4	2.7		0.29	4.5		0.32	3500	L	3.9	250	L	0.11	0.0059	U	0.006
J18NJ9	Trench Middle	-15		22000	L	4.1	3.7		0.29	5.9		0.33	4400	L	4	290	L	0.11	0.006	U	0.006
J18NK0	Trench West End	-1		18000	L	3.8	2.7		0.27	6	N	0.3	4400	L	3.7	250	L	0.1	0.0056	U	0.006
J18NK1	Trench West End	-3		21000	L	3.9	2.3		0.28	4.3		0.31	4100		3.8	260	L	0.1	0.0071	BM	0.006
J18NK2	Trench West End	-5		25000	L	4	3.5		0.29	5.9		0.32	5000		3.9	480	L	0.11	0.0059	U	0.006
J18NK3	Trench West End	-7		25000	L	4	2.7		0.28	4.7		0.31	4100		3.9	310	L	0.1	0.0058	U	0.006
J18NK4	Trench West End	-9		24000	L	3.9	2.2		0.28	3.5		0.31	4000		3.8	280	L	0.1	0.0057	U	0.006
J18NK5	Trench West End	-11		22000	L	4	3.2		0.29	5.6		0.32	4300		3.9	290	L	0.11	0.0059	U	0.006
J18NK6	Trench West End	-15		22000	L	4.1	3		0.29	5.2		0.32	4200		4	290	L	0.11	0.0059	U	0.006
J18NF8	Trench West End	-5		24000		4	3.1		0.29	5.4		0.32	4600		3.9	300		0.11	0.0059	U	0.006
J18NF7	Test Pit	-1		20000		4	2.9		0.29	5.5		0.32	4700		3.9	270		0.11	0.0059	U	0.006
J18NF6	Equipment Blank	NA		240	N	3.8	0.47	BM	0.27	0.3	U	0.3	27		3.7	4		0.1	0.0055	U	0.006
J18PH5	North of trench	-1		21000		4	3.2		0.28	5.8		0.31	4700		3.8	290		0.1	0.0057	U	0.006

Table 2.7. (contd)

100-D-100 Sample Summary

HEIS Number	Location	Depth	Sample Date	Molybdenum			Nickel			Potassium			Selenium			Silicon			Silver		
				mg/kg	Q	PQL	mg/kg	Q	PQL	mg/kg	Q	PQL	mg/kg	Q	PQL	mg/kg	Q	PQL	mg/kg	Q	PQL
J18NF9	Test Pit	-1		0.28	U	0.28	9.4	L	0.13	700		43	0.91	U	0.91	340	L	2.2	0.17	U	0.17
J18NH0	Test Pit	-3		0.27	U	0.27	8.1	L	0.13	710		43	0.9	U	0.9	240	L	2.2	0.17	UN	0.17
J18NH1	Test Pit	-5		0.27	U	0.27	6.5	L	0.13	820		43	0.91	U	0.91	320	L	2.2	0.17	U	0.17
J18NH2	Test Pit	-7		0.27	U	0.27	12	L	0.13	500		42	0.89	U	0.89	210	L	2.2	0.17	U	0.17
J18NH3	Test Pit	-9		0.28	U	0.28	10	L	0.13	890		44	0.93	U	0.93	250	L	2.3	0.17	U	0.17
J18NH4	Test Pit	-11		0.28	U	0.28	8	L	0.13	820		44	0.92	U	0.92	340	L	2.3	0.17	U	0.17
J18NH5	Test Pit	-15		0.28	U	0.28	11	L	0.13	720		44	0.92	U	0.92	260	L	2.2	0.17	U	0.17
J18NH6	Trench East End	-1		0.45	BM	0.27	10	L	0.13	790		43	0.9	U	0.9	220	LM	2.2	0.17	U	0.17
J18NH7	Trench East End	-3		0.27	U	0.27	8.2	L	0.13	680		43	0.9	U	0.9	360	L	2.2	0.17	U	0.17
J18NH8	Trench East End	-5		0.28	U	0.28	10	L	0.13	970		44	0.92	U	0.92	910	L	2.3	0.17	U	0.17
J18NH9	Trench East End	-7		0.28	B	0.27	8.1	L	0.13	550		42	0.89	U	0.89	410	L	2.2	0.17	U	0.17
J18NJ0	Trench East End	-9		0.27	B	0.27	9.5	L	0.13	640		43	0.89	U	0.89	400	L	2.2	0.17	U	0.17
J18NJ1	Trench East End	-11		0.27	U	0.27	7.3	L	0.13	630		43	0.9	U	0.9	460	L	2.2	0.17	U	0.17
J18NJ2	Trench East End	-15		0.28	U	0.28	9.2	L	0.13	810		44	0.92	U	0.92	550	L	2.2	0.17	U	0.17
J18NJ3	Trench Middle	-1		0.31	B	0.27	10	L	0.13	790		43	0.89	U	0.89	340	L	2.2	0.17	UN	0.17
J18NJ4	Trench Middle	-3		0.27	U	0.27	13	L	0.13	740		43	0.91	U	0.91	260	L	2.2	0.17	U	0.17
J18NJ5	Trench Middle	-5		0.28	U	0.28	8	L	0.13	680		43	0.91	U	0.91	460	L	2.2	0.17	U	0.17
J18NJ6	Trench Middle	-7		0.27	U	0.27	8.2	L	0.13	540		43	0.89	U	0.89	270	L	2.2	0.17	U	0.17
J18NJ7	Trench Middle	-9		0.31	B	0.27	8.5	L	0.13	630		43	0.9	U	0.9	420	L	2.2	0.17	U	0.17
J18NJ8	Trench Middle	-11		0.28	U	0.28	7.3	L	0.13	710		44	0.92	U	0.92	510	L	2.2	0.17	U	0.17
J18NJ9	Trench Middle	-15		0.28	U	0.28	11	L	0.13	950		44	0.93	U	0.93	470	L	2.3	0.17	U	0.17
J18NK0	Trench West End	-1		0.26	U	0.26	9.8	L	0.12	760		41	0.87	U	0.87	370	LN	2.1	0.16	U	0.16
J18NK1	Trench West End	-3		0.38	B	0.27	10	L	0.13	550		43	0.89	U	0.89	200	L	2.2	0.17	U	0.17
J18NK2	Trench West End	-5		0.3	B	0.28	13	L	0.13	890		44	0.92	U	0.92	300	L	2.2	0.17	U	0.17
J18NK3	Trench West End	-7		0.32	B	0.27	8	L	0.13	750		43	0.9	U	0.9	260	L	2.2	0.17	U	0.17
J18NK4	Trench West End	-9		0.28	B	0.27	9.6	L	0.13	590		42	0.89	U	0.89	190	L	2.2	0.17	U	0.17
J18NK5	Trench West End	-11		0.28	U	0.28	10	L	0.13	840		44	0.92	U	0.92	280	L	2.2	0.17	U	0.17
J18NK6	Trench West End	-15		0.28	U	0.28	10	L	0.13	780		44	0.92	U	0.92	240	L	2.2	0.17	U	0.17
J18NF8	Trench West End	-5		0.28	U	0.28	8.2		0.13	850		44	0.91	U	0.91	570		2.2	0.17	U	0.17
J18NF7	Test Pit	-1		0.28	U	0.28	9.8		0.13	750		43	0.91	U	0.91	460		2.2	0.17	U	0.17
J18NF6	Equipment Blank	NA		0.26	U	0.26	0.12	U	0.12	44	BM	41	0.86	U	0.86	160		2.1	0.16	U	0.16
J18PH5	North of trench	-1		0.35	B	0.27	10		0.13	740		43	0.89	U	0.89	390	N	2.2	0.17	U	0.17

Table 2.7. (contd)

100-D-100 Sample Summary

HEIS Number	Location	Depth	Sample Date	Sodium			Vanadium			Zinc		
				mg/kg	Q	PQL	mg/kg	Q	PQL	mg/kg	Q	PQL
J18NF9	Test Pit	-1		600		63	54	L	0.1	36	L	0.42
J18NH0	Test Pit	-3		520		62	69	L	0.1	42	L	0.42
J18NH1	Test Pit	-5		360		62	57	L	0.1	39	L	0.42
J18NH2	Test Pit	-7		400		61	69	L	0.1	43	L	0.41
J18NH3	Test Pit	-9		540		64	58	L	0.1	42	L	0.43
J18NH4	Test Pit	-11		510		63	58	L	0.1	40	L	0.43
J18NH5	Test Pit	-15		560		63	54	L	0.1	40	L	0.42
J18NH6	Trench East End	-1		1200		61	60		0.1	40	L	0.41
J18NH7	Trench East End	-3		610		62	53		0.1	34	L	0.42
J18NH8	Trench East End	-5		660		63	68		0.1	45	L	0.43
J18NH9	Trench East End	-7		620		61	71		0.1	42	L	0.41
J18NJ0	Trench East End	-9		560		61	71		0.1	42	L	0.41
J18NJ1	Trench East End	-11		630		62	57		0.1	38	L	0.42
J18NJ2	Trench East End	-15		480		63	56		0.1	40	L	0.42
J18NJ3	Trench Middle	-1		920		61	51	L	0.1	34	L	0.41
J18NJ4	Trench Middle	-3		820		62	61	L	0.1	40	L	0.42
J18NJ5	Trench Middle	-5		570		62	58	L	0.1	37	L	0.42
J18NJ6	Trench Middle	-7		680		61	75	L	0.1	42	L	0.41
J18NJ7	Trench Middle	-9		690		62	73	L	0.1	43	L	0.42
J18NJ8	Trench Middle	-11		530		63	53	L	0.1	35	L	0.42
J18NJ9	Trench Middle	-15		680		64	58	L	0.1	39	L	0.43
J18NK0	Trench West End	-1		490		60	50		0.1	35	L	0.4
J18NK1	Trench West End	-3		660		61	61	L	0.1	38	L	0.41
J18NK2	Trench West End	-5		600		63	70	L	0.1	46	L	0.42
J18NK3	Trench West End	-7		650		62	75	L	0.1	46	L	0.42
J18NK4	Trench West End	-9		560		61	71	L	0.1	42	L	0.41
J18NK5	Trench West End	-11		730		63	65	L	0.1	43	L	0.42
J18NK6	Trench West End	-15		510		63	63	L	0.1	40	L	0.43
J18NF8	Trench West End	-5		590		63	66		0.1	42		0.42
J18NF7	Test Pit	-1		640		62	55		0.1	35		0.42
J18NF6	Equipment Blank	NA		59	U	59	0.32	B	0.09	0.73	B	0.4
J18PH5	North of trench	-1		1600		61	56		0.1	36		0.41

Table 2.8. Results from anion analyses conducted in the aqueous phase of acid digestion extractions in all 2009 sediments

100-D-100 Sample Summary

HEIS Number	Location	Depth	Sample Date	Bromide			Chloride			Fluoride			Nitrogen in Nitrate		
				mg/kg	Q	PQL	mg/kg	Q	PQL	mg/kg	Q	PQL	mg/kg	Q	PQL
J18NF9	Test Pit	-1		1.6	B	0.41	11		2.1	3	B	0.87	57	N	0.33
J18NH0	Test Pit	-3		0.41	U	0.41	4	BM	2.1	3.8	BMN	0.86	3.2		0.33
J18NH1	Test Pit	-5		0.41	U	0.41	6.7		2.1	2.1	B	0.87	3.3		0.33
J18NH2	Test Pit	-7		0.4	U	0.4	6.4		2	1.1	B	0.85	2	B	0.32
J18NH3	Test Pit	-9		0.45	B	0.42	8.8		2.1	1.3	B	0.89	8.3		0.34
J18NH4	Test Pit	-11		0.49	B	0.42	7.9		2.1	0.88	U	0.88	9.5		0.34
J18NH5	Test Pit	-15		0.41	U	0.41	7.5		2.1	1.2	B	0.88	5.4		0.34
J18NH6	Trench East End	-1		1.9	B	0.4	15		2.1	3.6	B	0.86	110	DN	0.65
J18NH7	Trench East End	-3		0.41	U	0.41	4.7	B	2.1	2.3	B	0.86	3.4		0.33
J18NH8	Trench East End	-5		0.42	U	0.42	5.6		2.1	1	B	0.88	7.1		0.34
J18NH9	Trench East End	-7		0.4	U	0.4	4.3	B	2	1.1	B	0.85	2.3	B	0.33
J18NJ0	Trench East End	-9		0.4	U	0.4	3.9	B	2	1.1	B	0.85	2	B	0.33
J18NJ1	Trench East End	-11		0.41	U	0.41	5	B	2.1	1.3	B	0.86	2.2	B	0.33
J18NJ2	Trench East End	-15		0.41	U	0.41	4.7	B	2.1	1.1	B	0.88	2.3	B	0.33
J18NJ3	Trench Middle	-1		0.4	U	0.4	4.5	B	2	10		0.85	3.8		0.33
J18NJ4	Trench Middle	-3		0.41	U	0.41	4.8	B	2.1	3.5	B	0.87	6.6		0.33
J18NJ5	Trench Middle	-5		0.41	U	0.41	4.9	B	2.1	3.1	B	0.87	4.4		0.33
J18NJ6	Trench Middle	-7		0.4	U	0.4	4.2	B	2	2	B	0.85	2	B	0.33
J18NJ7	Trench Middle	-9		0.4	U	0.4	4.8	B	2.1	0.97	B	0.86	2.4	B	0.33
J18NJ8	Trench Middle	-11		0.41	U	0.41	5.1	B	2.1	1.7	B	0.88	3.1		0.33
J18NJ9	Trench Middle	-15		0.42	U	0.42	5.6		2.1	1.1	B	0.89	3		0.34
J18NK0	Trench West End	-1		0.39	U	0.39	3.2	B	2	1.4	B	0.83	2.3	B	0.32
J18NK1	Trench West End	-3		0.4	U	0.4	5	BM	2	1.2	B	0.85	0.52	B	0.33
J18NK2	Trench West End	-5		0.41	U	0.41	7.1		2.1	1.4	B	0.88	0.86	B	0.33
J18NK3	Trench West End	-7		0.41	U	0.41	6.7		2.1	1.6	B	0.86	0.87	B	0.33
J18NK4	Trench West End	-9		0.4	U	0.4	6.3		2	0.85	U	0.85	0.51	B	0.32
J18NK5	Trench West End	-11		0.41	U	0.41	7.4		2.1	1.2	B	0.88	0.78	B	0.33
J18NK6	Trench West End	-15		0.42	U	0.42	7		2.1	1.1	B	0.88	0.88	B	0.34
J18NF8	Trench West End	-5		0.41	U	0.41	4.5	B	2.1	1.6	B	0.87	1.1	B	0.33
J18NF7	Test Pit	-1		1.5	B	0.41	17		2.1	2.7	B	0.87	53		0.33
J18NF6	Equipment Blank	NA		0.39	U	0.39	5.3		2	0.82	U	0.82	0.31	U	0.31
J18PH5	North of trench	-1		4.2	M	2	36		2	4	B	0.85	170	D	1.6

Table 2.8. (contd)

100-D-100 Sample Summary

HEIS Number	Location	Depth	Sample Date	Nitrogen in Nitrite			Phosphorous in Phosphate			Sulfate			% moisture (wet sample)
				mg/kg	Q	PQL	mg/kg	Q	PQL	mg/kg	Q	PQL	mg/kg
J18NF9	Test Pit	-1		0.36	U	0.36	1.3	U	1.3	98		1.8	5.6
J18NH0	Test Pit	-3		0.35	U	0.35	1.3	U	1.3	24	M	1.8	4.8
J18NH1	Test Pit	-5		0.43	B	0.35	1.3	U	1.3	240		1.8	5.1
J18NH2	Test Pit	-7		0.42	B	0.35	1.3	U	1.3	28		1.8	3.1
J18NH3	Test Pit	-9		0.46	B	0.36	1.3	U	1.3	93		1.9	7.2
J18NH4	Test Pit	-11		0.43	B	0.36	1.3	U	1.3	92		1.9	7
J18NH5	Test Pit	-15		0.41	B	0.36	1.3	U	1.3	72		1.8	6.3
J18NH6	Trench East End	-1		0.35	U	0.35	1.3	U	1.3	430		1.8	3.9
J18NH7	Trench East End	-3		0.43	B	0.35	1.3	U	1.3	44		1.8	4.6
J18NH8	Trench East End	-5		0.4	B	0.36	1.3	U	1.3	480		1.9	6.7
J18NH9	Trench East End	-7		0.35	U	0.35	1.3	U	1.3	110		1.8	3.4
J18NJ0	Trench East End	-9		0.35	U	0.35	1.3	U	1.3	170		1.8	3.8
J18NJ1	Trench East End	-11		0.46	B	0.35	1.3	U	1.3	360		1.8	4.7
J18NJ2	Trench East End	-15		0.43	B	0.36	1.3	U	1.3	93		1.8	6.1
J18NJ3	Trench Middle	-1		0.35	U	0.35	1.3	U	1.3	5.3		1.8	3.5
J18NJ4	Trench Middle	-3		0.46	B	0.35	1.3	U	1.3	15		1.8	5.1
J18NJ5	Trench Middle	-5		0.44	B	0.36	1.3	U	1.3	26		1.8	5.6
J18NJ6	Trench Middle	-7		0.37	B	0.35	1.3	U	1.3	25		1.8	3.8
J18NJ7	Trench Middle	-9		0.37	B	0.35	1.3	U	1.3	35		1.8	4.1
J18NJ8	Trench Middle	-11		0.41	B	0.36	1.3	U	1.3	49		1.8	6.1
J18NJ9	Trench Middle	-15		0.41	B	0.36	1.3	U	1.3	79		1.9	7.8
J18NK0	Trench West End	-1		0.34	U	0.34	1.3	U	1.3	5		1.7	0.98
J18NK1	Trench West End	-3		0.38	B	0.35	1.3	U	1.3	2.7	B	1.8	3.7
J18NK2	Trench West End	-5		0.4	B	0.36	1.3	U	1.3	18		1.8	6.1
J18NK3	Trench West End	-7		0.43	B	0.35	1.3	U	1.3	150		1.8	4.6
J18NK4	Trench West End	-9		0.4	B	0.35	1.3	U	1.3	120		1.8	3.2
J18NK5	Trench West End	-11		0.39	B	0.36	1.3	U	1.3	310		1.8	6.2
J18NK6	Trench West End	-15		0.4	B	0.36	1.3	U	1.3	51		1.9	6.6
J18NF8	Trench West End	-5		0.36	U	0.36	1.3	U	1.3	25		1.8	5.9
J18NF7	Test Pit	-1		0.36	U	0.36	1.3	U	1.3	88		1.8	5.6
J18NF6	Equipment Blank	NA		0.34	U	0.34	1.2	U	1.2	1.9	B	1.7	0.12
J18PH5	North of trench	-1		0.35	U	0.35	1.3	U	1.3	920	D	9	3.8

Table 2.9. pH measurements in the representative 2009 sediment samples

Steven's pH measurements: 7/23/09 in lab 325					Michelle's pH measurements: 7/24/09 in lab 305				
buffer 7 check:		6.98			buffer 7 check:		7.07		
1st measurement					2nd measurement				
Sample ID	pH value				Sample ID	pH value		average	stdv
PB	7.50				PB	6.39			
J18NK0	8.95		J18PH5 n=4		J18NK0	8.96		8.96	0.0071
J18NJ3	9.21		average	stdv	J18NJ3	9.19		9.20	0.0141
J18PH5	8.22		8.17	0.0804	J18PH5	8.21		8.22	0.0071
J18PH5 DUP	8.05				J18PH5 DUP	8.20		8.13	0.1061
J18NH6	8.44				J18NH6	8.54		8.49	0.0707
J18NF7	8.56				J18NF7	8.62		8.59	0.0424
buffer 7 check:		7.08			buffer 4 check:		3.93		
					buffer 7 check:		7.06		
					buffer 10 check:		10.03		

Table 2.10. Results from DI-water and acid extractions 2009 sediment samples

Water Extraction						
Sample	Tube Tare (g)	Soil Wt (g)	H2O (mL)	Cr ug/L	Cr ug	Cr mg/kg
J18NK0	14.52	10.95	10.98	120.231	1.320136	0.12056
J18NJ3	14.40	10.53	10.55	111.092	1.172015	0.111303
J18PH5	14.40	10.75	10.76	115.670	1.244609	0.115778
J18PH5 Dup	14.48	10.74	10.73	115.240	1.236527	0.115133
J18NH6	14.42	10.81	10.80	2162.000	23.3496	2.16
J18NF7	14.38	10.29	10.29	105.884	1.089547	0.105884
Acid Extraction (0.5M HNO3, No HCl)						
Sample	Tube Tare (g)	Soil Wt (g)	HNO3 (mL)	Cr ug/L	Cr ug	Cr mg/kg
J18NK0	13.33	5.12	18	8618.5227	155.1334	30.29949
J18NJ3	13.45	5.08	18	9188.73697	165.3973	32.55852
J18PH5	13.33	5.23	18	13668.8003	246.0384	47.04367
J18PH5 Dup	13.45	5.05	18	13422.6233	241.6072	47.84301
J18NH6	13.39	5.09	18	21158.285	380.8491	74.82301
J18NF7	13.37	5.15	18	14626.4853	263.2767	51.1217
Acid Extraction (8M HNO3, No HCl)						
Sample	Tube Tare (g)	Soil Wt (g)	HNO3 (mL)	Cr ug/L	Cr ug	Cr mg/kg
J18NK0	13.43	5.13	18	9549.087	171.8836	33.50557
J18NJ3	13.36	5.06	18	12199.029	219.5825	43.39576
J18PH5	13.36	5.13	18	16643.600	299.5848	58.3986
J18PH5 Dup	13.30	5.09	18	16661.648	299.9097	58.92135
J18NH6	13.32	5.09	18	23300.986	419.4177	82.40034
J18NF7	13.28	5.10	18	18803.670	338.4661	66.3659

Table 2.11. Results from microwave digestion conducted in 2009 sediment samples

Microwave Digestion: Different Sediment Fractions										
Sample	Soil Fraction	Boric Acid (g)	Sample Wt (g)	HNO3 (mL)	HF (mL)	HCl (mL)	Solution (ml)	Cr ug/L	Cr ug	Cr mg/kg
J18NK0	1.0 mm	0.43	0.1783	9.0	3.0	2.0	14.4	760.3436	10.97176	5.485879
	0.5 mm	0.45	0.1770	9.0	3.0	2.0	14.5	545.1451	7.877347	3.938673
	0.25 mm	0.43	0.1935	9.0	3.0	2.0	14.4	724.743	10.45804	5.229021
	0.125 mm	0.43	0.1906	9.0	3.0	2.0	14.4	768.0258	11.08261	5.541306
	0.063 mm	0.44	0.2002	9.0	3.0	2.0	14.4	1495.93	21.60124	10.80062
	<0.063 mm	0.45	0.1730	9.0	3.0	2.0	14.5	2702.411	39.04984	19.52492
J18NJ3	1.0 mm	0.41	0.1887	9.0	3.0	2.0	14.4	806.1862	11.61714	5.808571
	0.5 mm	0.43	0.1928	9.0	3.0	2.0	14.4	1168.973	16.86828	8.43414
	0.25 mm	0.42	0.1762	9.0	3.0	2.0	14.4	1097.648	15.82808	7.914039
	0.125 mm	0.42	0.1882	9.0	3.0	2.0	14.4	1472.303	21.23061	10.6153
	0.063 mm	0.45	0.1853	9.0	3.0	2.0	14.5	1192.018	17.22466	8.612331
	<0.063 mm	0.42	0.2239	9.0	3.0	2.0	14.4	1405.949	20.27379	10.13689
J18PH5	1.0 mm	0.45	0.1995	9.0	3.0	2.0	14.5	970.7303	14.02705	7.013526
	0.5 mm	0.43	0.2198	9.0	3.0	2.0	14.4	1161.106	16.75476	8.377378
	0.25 mm	0.42	0.2439	9.0	3.0	2.0	14.4	1357.572	19.57618	9.788091
	0.125 mm	0.43	0.1977	9.0	3.0	2.0	14.4	2044.997	29.50931	14.75465
	0.063 mm	0.42	0.2055	9.0	3.0	2.0	14.4	2566.856	37.01406	18.50703
	<0.063 mm	0.42	0.2192	9.0	3.0	2.0	14.4	3461.098	49.90904	24.95452
J18NH6	1.0 mm	0.43	0.2000	9.0	3.0	2.0	14.4	1532.661	22.1163	11.05815
	0.5 mm	0.44	0.2371	9.0	3.0	2.0	14.4	2053.837	29.6574	14.8287
	0.25 mm	0.44	0.1909	9.0	3.0	2.0	14.4	1717.923	24.80681	12.4034
	0.125 mm	0.43	0.2143	9.0	3.0	2.0	14.4	2661.36	38.40342	19.20171
	0.063 mm	0.44	0.2224	9.0	3.0	2.0	14.4	5175.483	74.73398	37.36699
	<0.063 mm	0.42	0.2001	9.0	3.0	2.0	14.4	4530.212	65.32565	32.66283
J18NF7	1.0 mm	0.41	0.2416	9.0	3.0	2.0	14.4	1461.896	21.06591	10.53296
	0.5 mm	0.43	0.2345	9.0	3.0	2.0	14.4	1839.046	26.53743	13.26871
	0.25 mm	0.45	0.1947	9.0	3.0	2.0	14.5	1793.445	25.91528	12.95764



Figure 2.2. Photograph showing a broken pipe and stained sediments

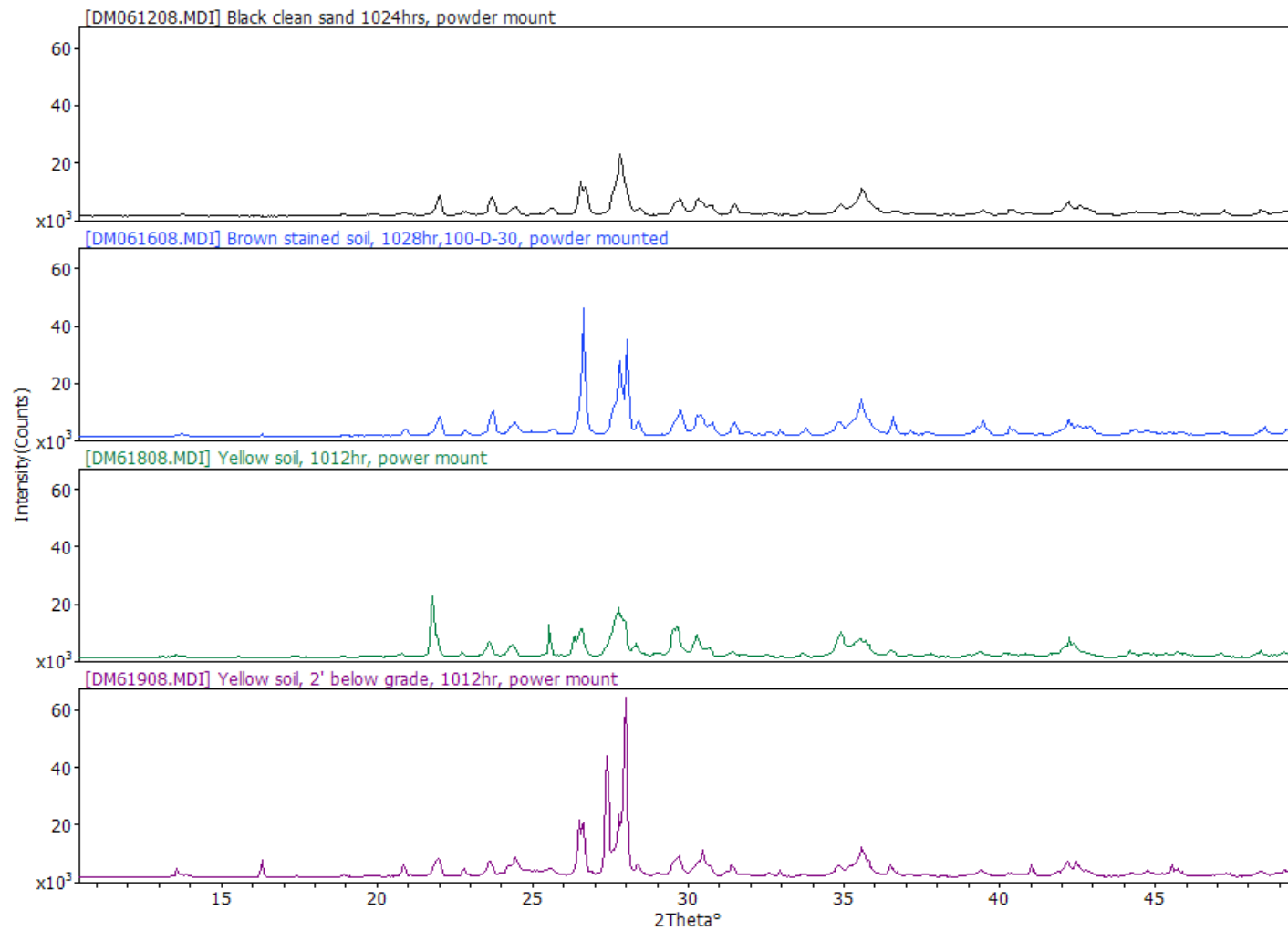


Figure 2.3. XRD patterns of the <2 mm fraction of all 2008 sediments

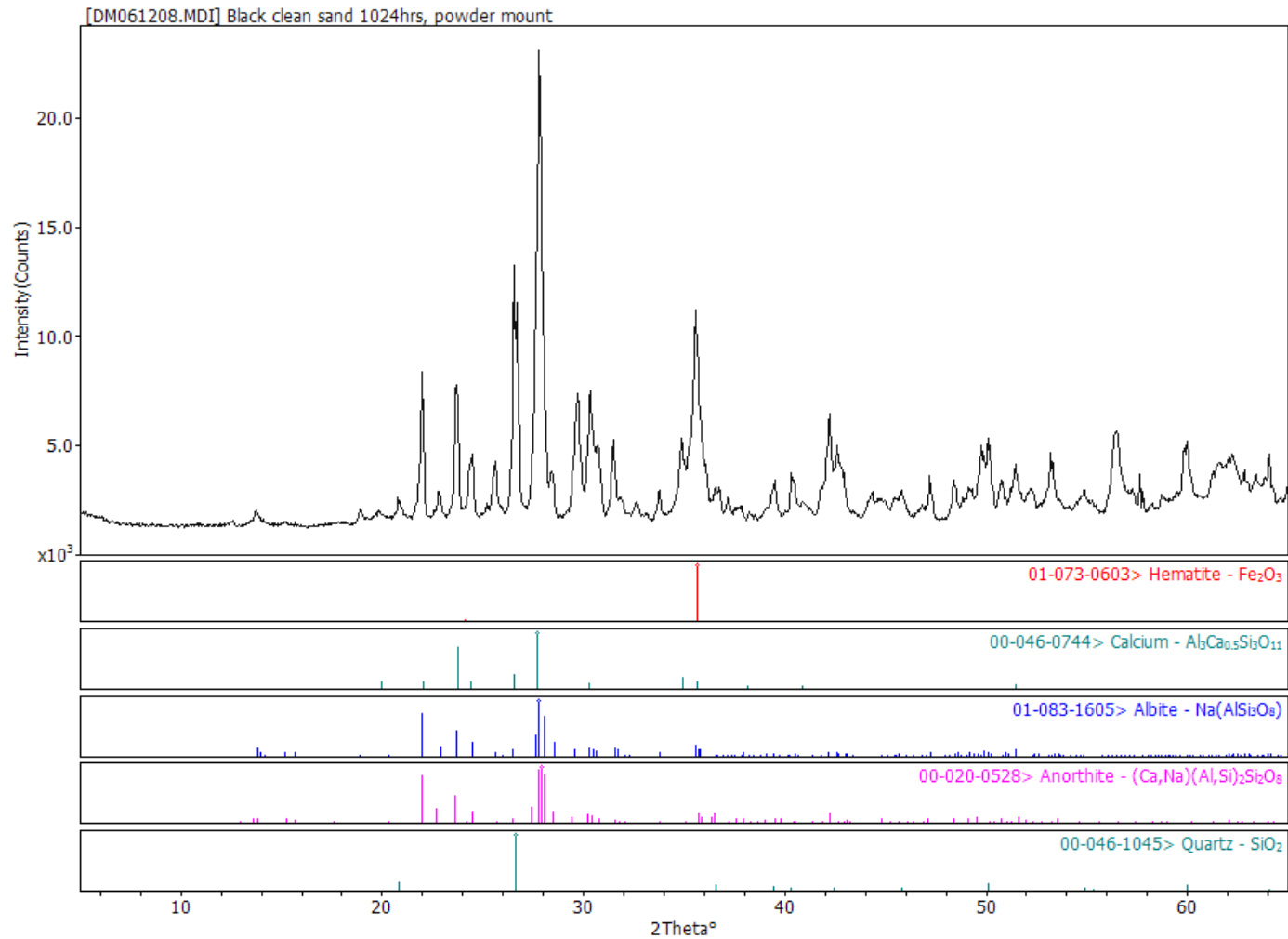


Figure 2.4. XRD results of the BC sediment (2009). Minerals identification was based on comparison of the measured XRD patterns to those of mineral powder diffraction files (PDFTM) published by the Joint Committee on Powder Diffraction Standards International Center for Diffraction Data.

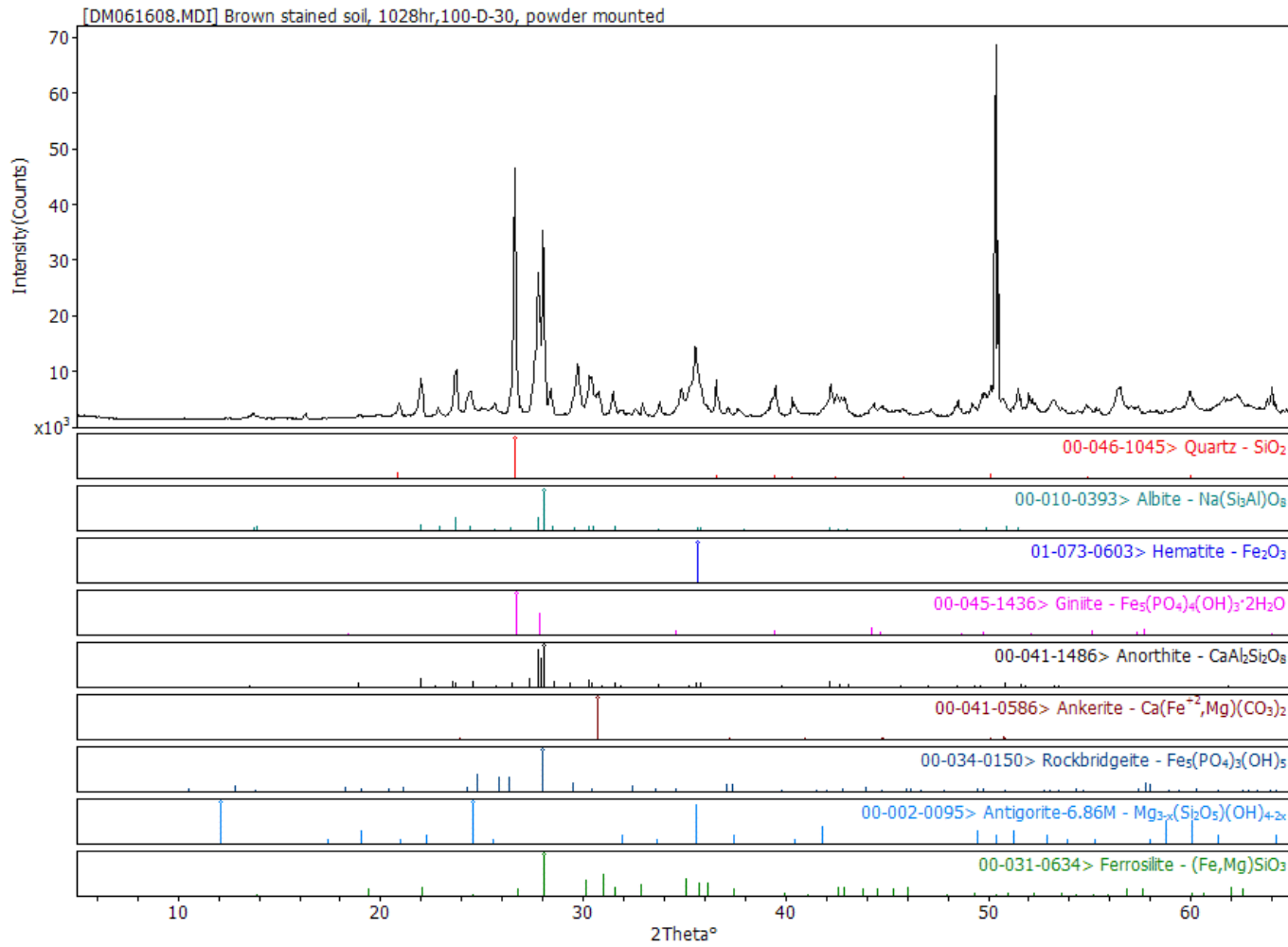


Figure 2.5. XRD results of the BS sediment (2008)

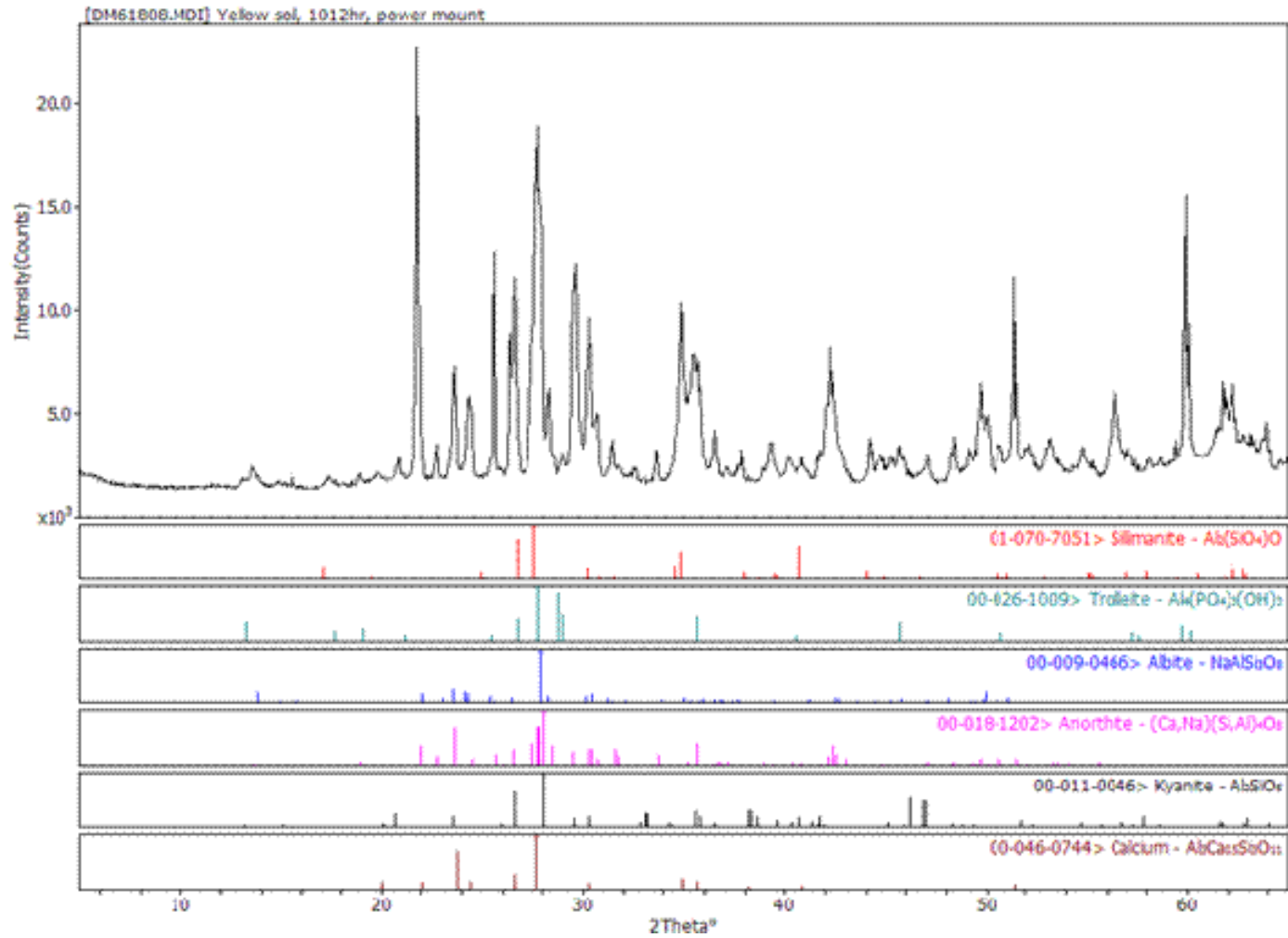


Figure 2.6. XRD results of the YS sediment (2008)

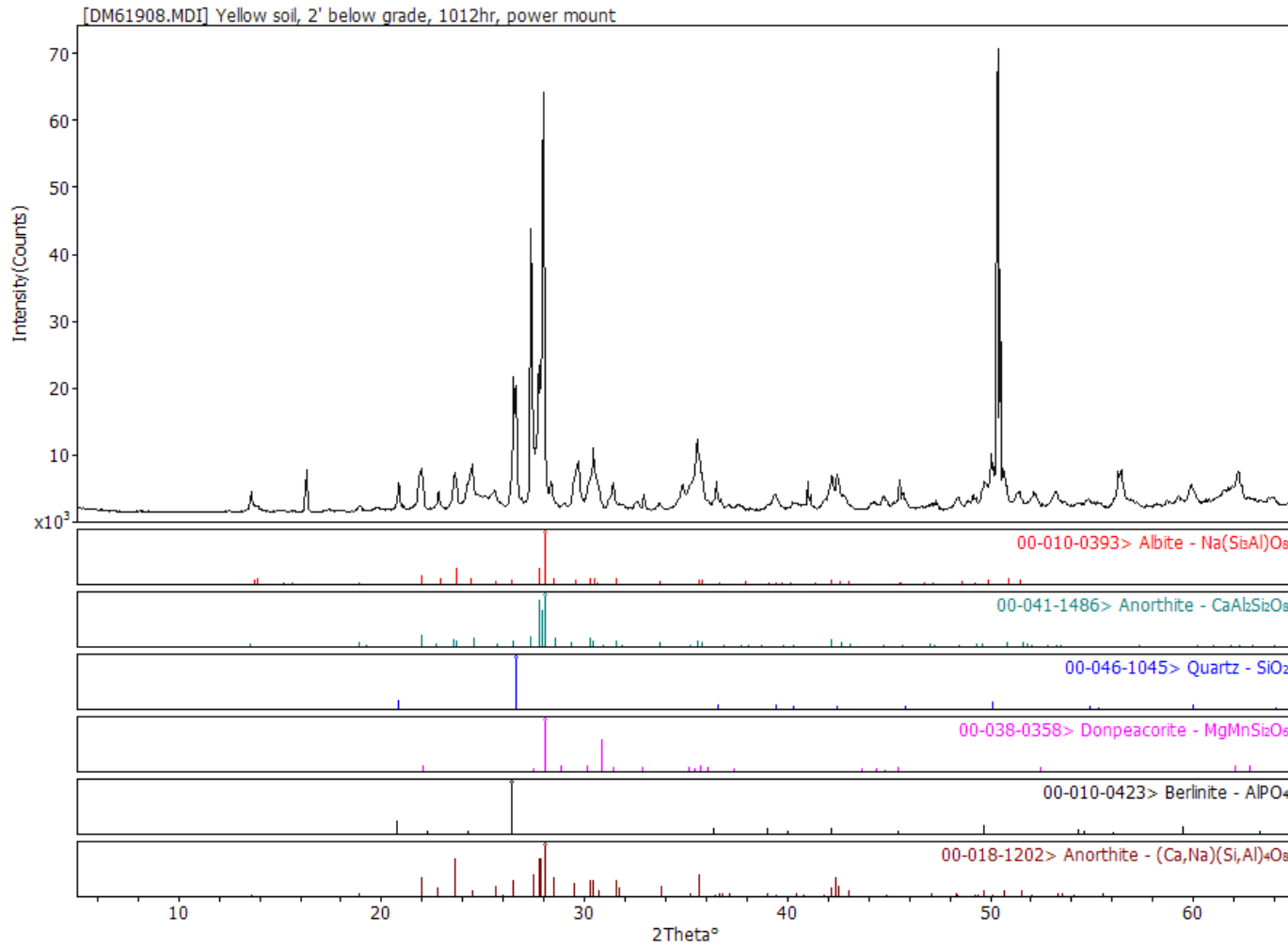


Figure 2.7. XRD results of the YS2 sediment (2008)

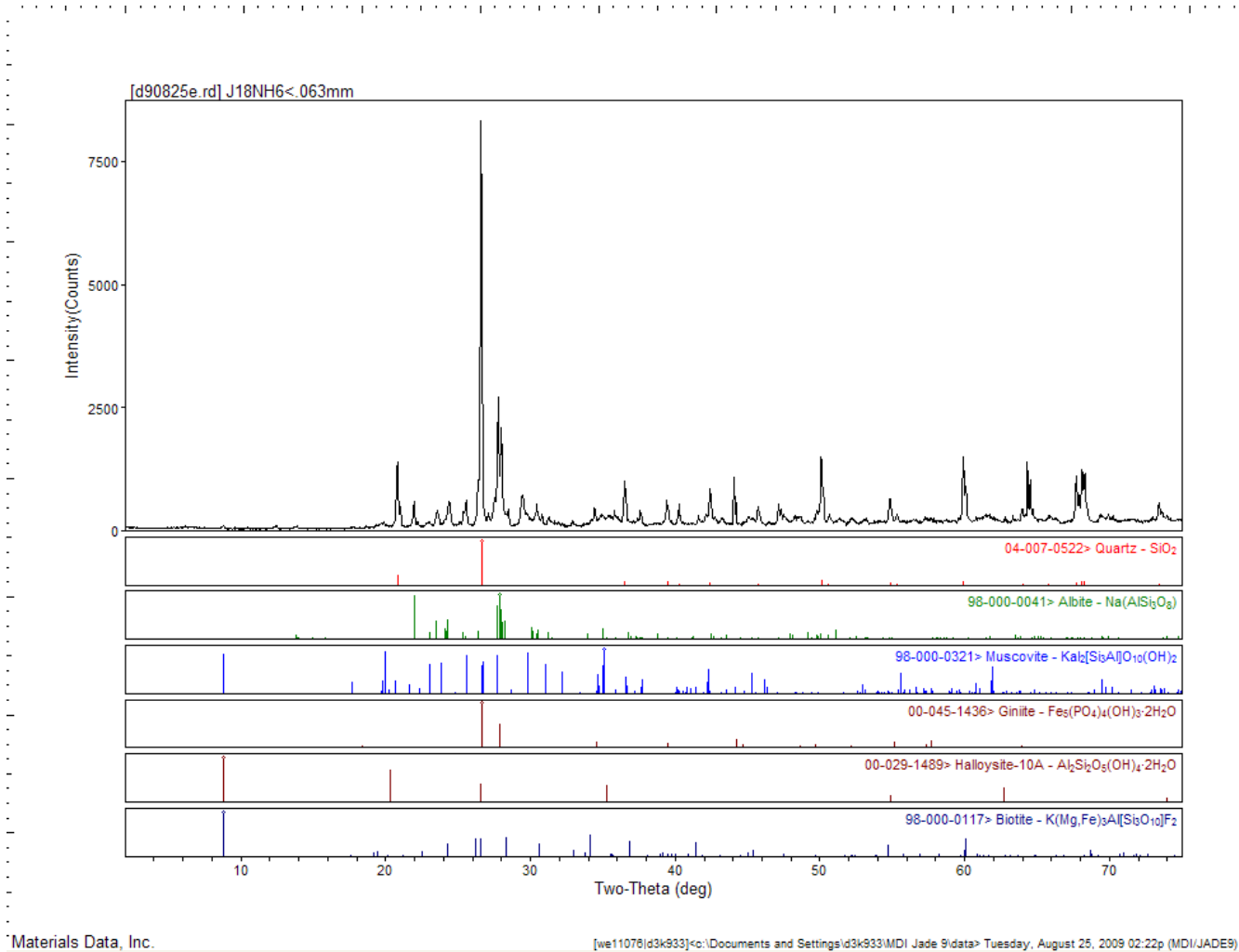


Figure 2.8. XRD patterns of the <63 μm fraction of sediment J18NH6 (2009). Minerals identification was based on comparison of the measured XRD patterns to those of mineral powder diffraction files (PDFTM) published by the Joint Committee on Powder Diffraction Standards International Center for Diffraction Data.

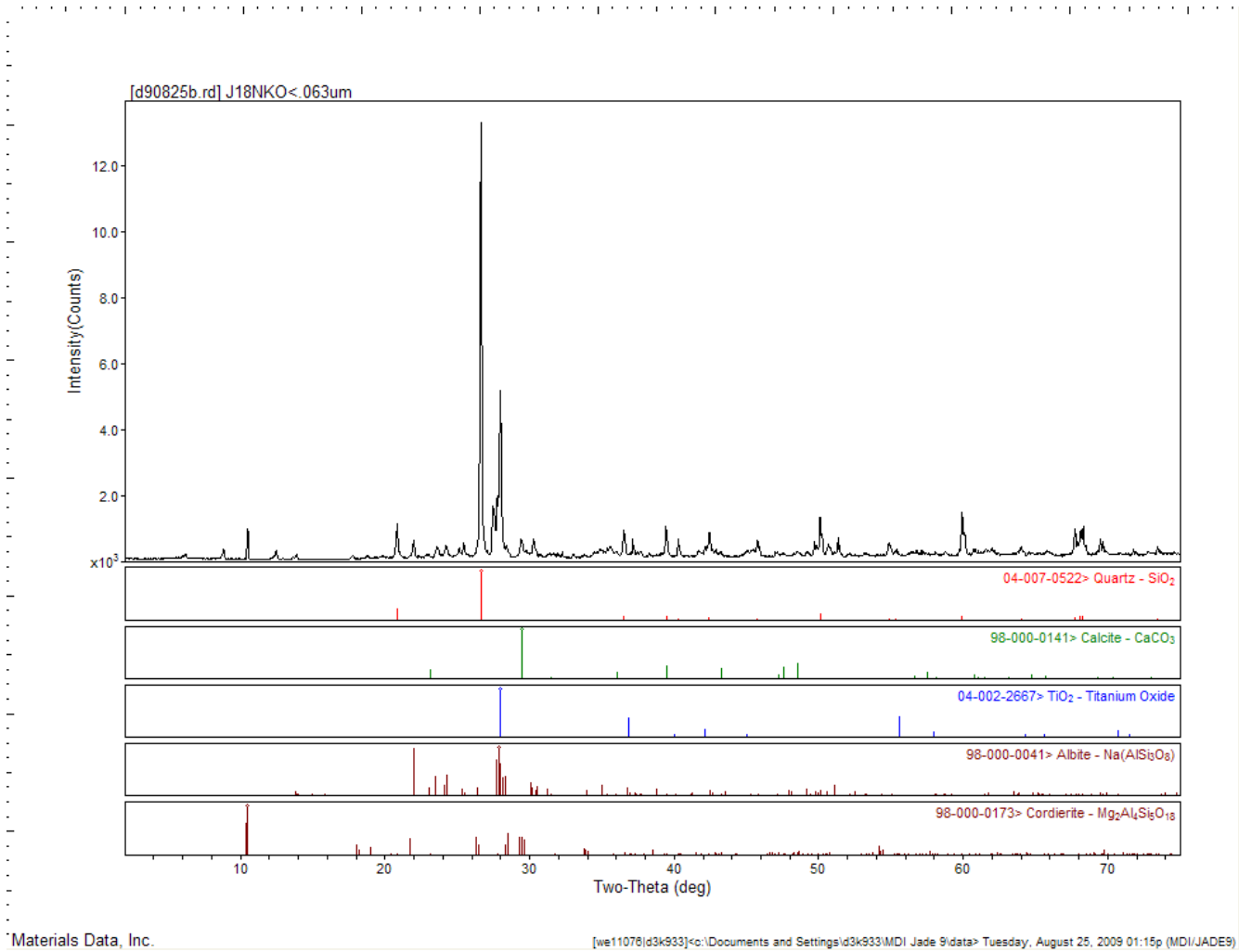


Figure 2.9. XRD patterns of the <63 μm fraction of sediment J18NKO (2009)

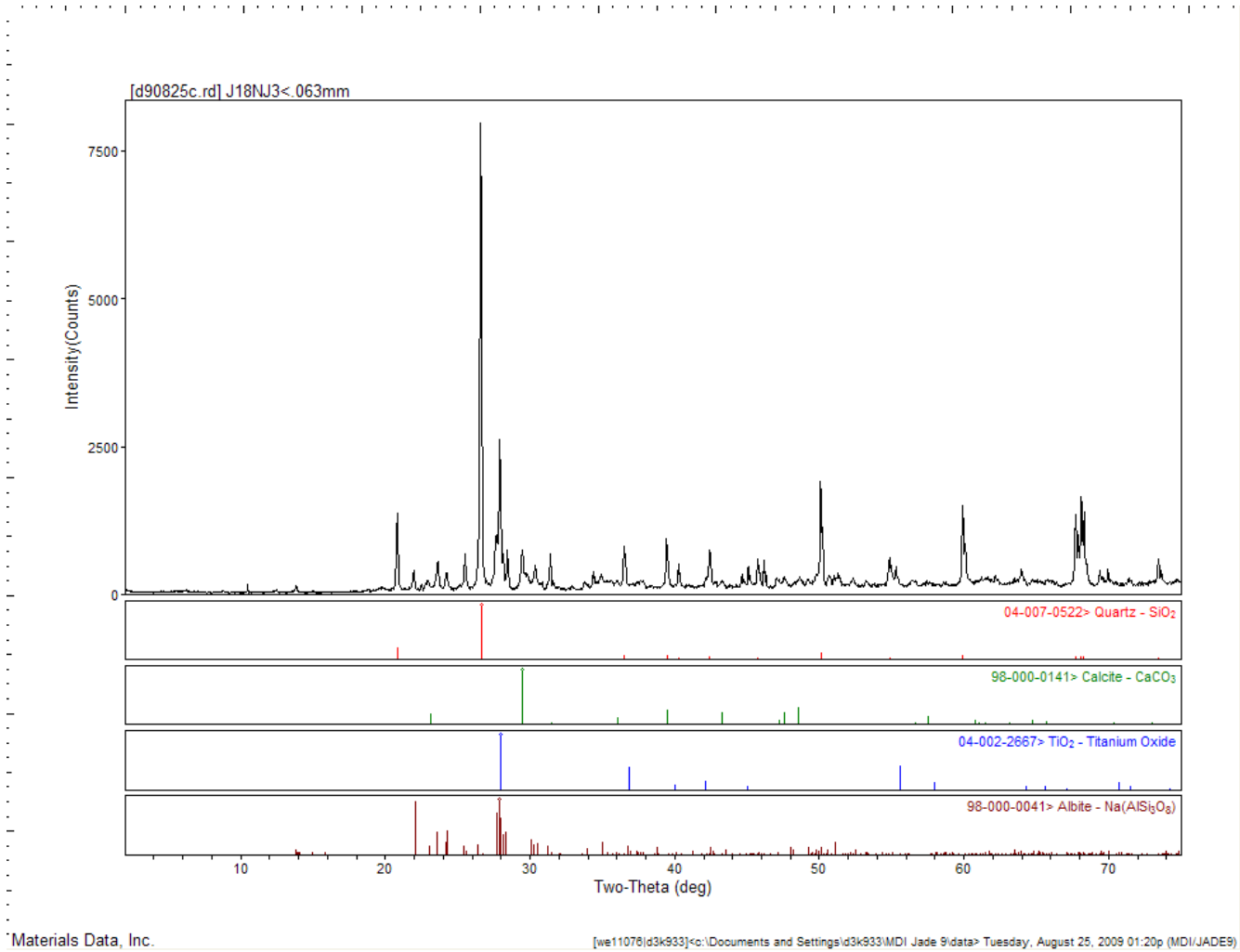


Figure 2.10. XRD patterns of the <63 μm fraction of sediment J18NJ3 (2009)

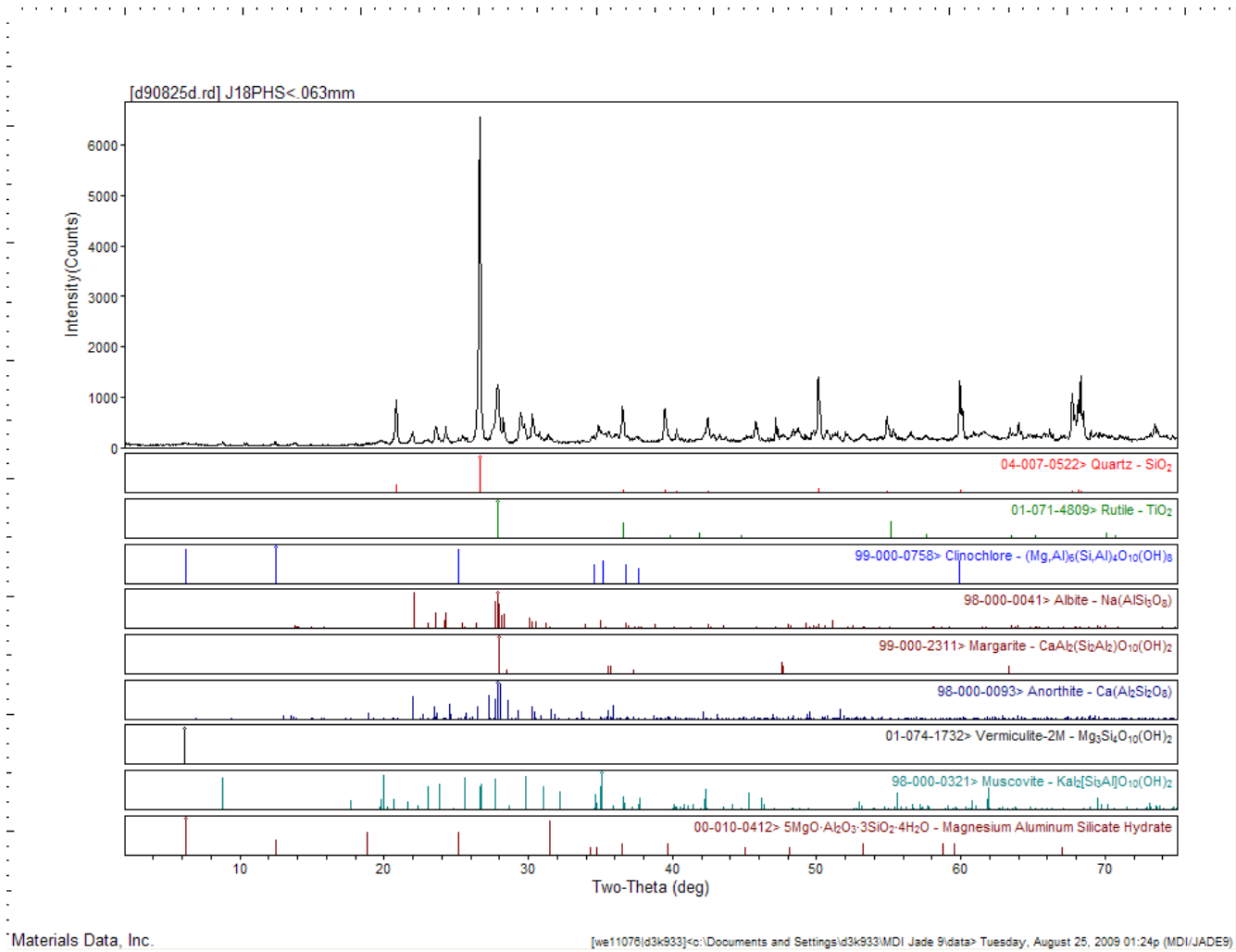


Figure 2.11. XRD patterns of the <63 μm fraction of sediment J18PH5 (2009)

3.0 Transport Studies

3.1 Introduction

The transport of chromate [Cr(VI)O_4^{2-}] through uncontaminated sediments is not expected to exhibit retardation due to adsorption (sediments may exhibit minimum adsorption capacity under the given conditions of neutral or slightly basic pH because all variable charge sorbents may be slightly negatively charged) (Qafoku et al. 2003, 2007, 2009, 2010; Ginder-Vogel et al. 2005; Dresel et al. 2008). However, as clearly shown in some of these references (e.g., Qafoku et al. 2003, 2009, 2010; Dresel et al. 2008), waste fluids may have altered the natural background geochemical conditions in the Hanford Site sediments of the Cr-contaminated locations of the 100-D Area. Although the pH and the chemical composition of the mixed waste fluids is unknown, it is possible these waste fluids have interacted with the sediments and altered the solid phase speciation over time via 1) dissolution of the existing soil minerals [releasing into the aqueous phase Cr(VI) reductants such Fe(II) or other chemical elements such as Ba]; and 2) precipitation of new stable Cr(VI), Cr(III) or other solid phases that might incorporate contaminant Cr in their structures.

The following attenuation pathways are possible:

1. Cr(VI) immobilization via precipitation (as Ba Cr)
2. Cr(VI) incorporation into the newly formed solid phases
3. Aqueous Cr(VI) reduction to Cr(III) by aqueous Fe(II) released from dissolved Fe(II)-bearing minerals that are present in Hanford Site sediments
4. Cr(III) precipitation or coprecipitation with aqueous Fe(III) and formation of [Cr(III) – Fe(III)] solid solutions of different elemental ratios and solubilities.

A series of column experiments were conducted to investigate Cr(VI) mobility during advective transport under saturated and unsaturated conditions to test the following hypotheses:

1. Only a small portion of the total amount of Cr present in the sediments may be released from the sediments exposed to Cr and waste solutions, although the actual pH conditions may be neutral.
2. Cr(VI) release from remote sorption and/or precipitation sites may be kinetically controlled and the release rate should be a function of the pore-water velocity; i.e., fluid residence time.
3. During late phases of leaching, Cr(VI) release—if observed—may be controlled by the solubility of the Cr(VI) solid phases and/or solid solutions.

3.2 Materials and Method

3.2.1 Column Experiment Methodology

The column apparatus and methodology is described in Qafoku et al. (2003, 2004). For this study, polyvinyl-chloride columns were packed uniformly with the unsorted and not sieved contaminated sediments from the 100 Area. Column packing was performed in about 10-g increments that were then tamped by hand with a plastic dowel to as high a density as possible. The tamped portion surface was

lightly scratched before adding the next increment to minimize layering inside the columns. Porous plates (0.25-cm thick and 10- μ m pore diameter) were used at the top and bottom of each column to distribute the leaching solution and to collect fines (that were found to be minimal) at the column exit. High performance liquid chromatography or medical pumps were used to control advective flow and yield preselected fluid residence times. Column effluent was collected in a fraction collector. The stop-flow technique (Brusseau et al. 1997) was frequently used to test whether nonequilibrium conditions were affecting Cr(VI)_{aq} transport at different times during breakthrough, and to measure rates of Cr(VI)_{aq} release from the contaminated sediment.

For the unsaturated column experiments, an acrylic column with internal diameter (3.81 cm) and length (20.3 cm) was used in a hanging water-column system packed with Cr-contaminated 100-D Area Hanford Site sediment. A porous ceramic tensiometer is made of 1.37-cm outside diameter (OD) plastic pipe with a 0.67-cm OD ceramic porous cup (2.54-cm long) at the lower end, and a 6-cm section of clear plastic pipe at the upper end (Soil Measurement Systems, Tucson, Arizona). Two tensiometers are mounted on opposite sides of each column at 5 cm from each column end, thus yielding a 10-cm length between the two tensiometers (Figure 3.1). Each tensiometer is connected to a model 130 pressure transducer, with a pressure range up to 1 bar and operating temperature range of -30 to 70°C (purchased through Soil Measurement Systems). The transducers are connected to a datalogger (CR1000, Campbell Scientific Inc., California) to monitor water potential. Care was taken to ensure a continuous column of water between the saturated porous cup and the transducer. A low-flow peristaltic pump (Fisherbrand* Variable-Flow Peristaltic Pump, Fisher Scientific) was used to inject solution to the packed-column inlet, which was covered by nylon membrane. A constant water potential (suction) was controlled by a hanging water column attached to the outlet at the bottom of the column. The weight of the column was measured using a balance to monitor the water content change before, during, and after the experiment. Changes in the water content can also be indirectly measured by continuous water potential records in the datalogger from the two tensiometers installed in the column.

3.2.2 Leaching Solutions

A synthetic groundwater (SGW) with a pH = 8.05 (\pm 0.04) and a total inorganic carbon ($[\text{CO}_3]_{\text{TOT}}$) concentration of $1.05 \times 10^{-3} \text{ mol L}^{-1}$ was used in all experiments. The SGW simulated vadose zone pore-water composition. The chemical composition of the SGW is presented in Table 3.1. Thermodynamic aqueous speciation and saturation index calculations were performed for this electrolyte using the computer program MINTEQA2 (Allison et al. 1991, 1998). The solution was undersaturated with respect to all possible secondary phases that might form during these experiments.

3.2.3 Chemical Analyses

Cr(VI) (as CrO_4^{2-}) effluent concentrations in columns 1, 2, and 3 conducted with the 2008 sediment samples were determined spectrophotometrically by the 1,5-diphenylcarbazide method (Bartlett and James 1996). Cuvettes (1-cm long) were used to measure the absorbance of samples at 540 nm with a spectrophotometer. Total effluent Cr concentrations in the 2009 column experiments were determined with ICP-OES.

Ion chromatography was used to measure aqueous Br effluent concentrations. Br was injected with the SGW (Br was added as CaBr_2 in SGW) at the end of the Cr desorption experiments.

Frequent pH measurements were taken in all column effluents with a combined pH microelectrode. Some representative effluent samples collected in different column experiments and at selected times during leaching were analyzed for different elements using a Perkin Elmer model 3300 DV ICP-OES and ion chromatography.

3.2.4 Transport Parameters Calculation

The CXTFIT code (Parker and van Genuchten 1984; Toride et al. 1999) was used to calculate transport parameters based on the bromide breakthrough curve (BTC) of each column. Mean pore-water velocity V was calculated as the experimental water flux divided by the volumetric water content (θ). CXTFIT was then used to calculate the values of D (dispersion coefficient) and R (retardation coefficient) (Table 3.2). The experimental water flux was calculated using the average of several flow rate measurements made during experiments, divided by the column surface area.

3.3 Results and Discussion

3.3.1 Cr(VI) Transport Behavior and Overall Mobility: 2008 Experiments

Three saturated packed-column experiments were conducted as part of this study with sediments YS (column 1), BC (column 2), and BS (column 3) (Figures 3.2, 3.3, and 3.4). Stop-flow events with different durations were applied in all column experiments to test for the presence of chemical and/or physical nonequilibrium during leaching, and to create dynamic/variable fluid-residence time conditions to reveal the importance of time-dependent reactions and processes. Selected measured and calculated physical properties in each column are summarized in Table 3.2.

These experiments were run for relatively short periods of time (~14, 8, and 10 PV, respectively) because the concentration of Cr in the effluents was 0 or close to 0 after the first peak observed in the first PV. Effluent Cr(VI) concentration remained low during these experiments and desorption profiles did not show prolonged tailings.

The average effluent pH in column 2 (sediment BC) was $\text{pH}_{\text{AVERAGE BC}} = 8.15 \pm 0.10$. This was similar to the pH value of the input solution. The pH value of the first effluent volume was slightly smaller than the average value, but pH did not change during or after the 94-h stop-flow event applied in this column.

The average effluent pH in columns 1 and 3 (sediment YS and BS) was acidic ($\text{pH}_{\text{AVERAGE YS}} = 6.91 \pm 0.61$ and $\text{pH}_{\text{AVERAGE BS}} = 6.20 \pm 0.70$, respectively). Even more acidic was the pH of the effluent collected after the last stop-flow event of more than 450 h applied in both columns. This indicated that the sediments were altered by the acidic waste fluids.

Stop-flow events with different durations were applied during leaching in all experiments, after the pseudo steady-state was achieved. The aqueous Cr(VI) concentration was not perturbed during the stop flow as indicated by the data presented in Figures 3.2, 3.3, and 3.4. This indicated that contaminant Cr was immobile in these sediment under the tested experimental conditions.

Total mass of desorbed and subsequently released Cr(VI) in the effluents calculated by integration was extremely low: 0.0132, 0.00015, and 0.000041 mmol kg⁻¹ in column 1 (sediment YS), column 2 (sediment BC), and column 3 (sediment BS), respectively. While results of the experiment conducted with sediment BC were expected (this sediment was considered “clean”), results from the experiments conducted with the other two contaminated sediments were unexpected.

Unsorted and not sieved sediment materials were used in these column experiments. However, the <2-mm size fraction was used in the extraction experiments described in Section 2.0, which were used to determine water, acid, and microwave-digestion Cr concentrations in these sediments.

The <2-mm size fraction is considered the most reactive fraction and most Cr contamination is believed to be associated with this fraction. Sediment YS and BS contained more than 73% of the <2-mm size fraction, and sediment BC contained more than 59% of the same fraction. However, even in this case, the total amount of Cr released from the sediments during the column experiments would have been expressed in terms of the mass of the <2-mm fraction. Additionally, the desorbed Cr mass may have been insignificant compared to the total Cr mass associated with these sediments and measured by microwave digestion. Therefore, only a small portion of the total amount of Cr present in the contaminated sediments YS, YS2, and BS was removed from them during these leaching experiments.

Lastly, these sediments were not able to sustain an aqueous concentration greater than the EPA maximum contaminant level (MCL) of 0.1 ppm or 0.00192 mmol L⁻¹, but close to zero effluent Cr concentrations were measured after the second PV in all column experiments.

Note the amount of Cr released from sediment BS was even smaller than that released from the clean sediment BC, indicating that contaminant Cr was immobile in this sample and the other contaminated sediment samples.

3.3.2 Cr(VI) Transport Behavior and Overall Mobility: 2009 Experiments

Five saturated column experiments were conducted as part of this study with sediments J18NH6, J18NJ3, J18NK0, J18NF7, and J18PH5. Results are presented in Figures 3.5, 3.6, 3.7, 3.8, and 3.9.

These experiments had different durations depending on the effluent Cr concentration. However, they were all run for a sufficient period of time, and at least 30 pore volumes of effluent were collected at the column outlet in each of these column experiments.

Cr(VI) leaching patterns observed in these experiments were similar: a peak of high concentration was observed in the first pore volume, followed by a shoulder of exponentially decreasing Cr concentrations. A considerable amount of Cr released in the column effluent was observed only in the experiment conducted with sediment J18NH6. In all other tested sediments, the total Cr amount that appeared in the column effluents was substantially lower than the amount of Cr measured by the microwave digestion technique.

Stop-flow events with different durations were applied during leaching in all experiments. The aqueous Cr(VI) concentration was perturbed during the stop flow in all experiments as indicated by the peaks of Cr concentrations after the flow was reestablished. This indicated contaminant Cr release was time dependent under the experimental conditions tested during this study.

The average effluent pH varied between 8.05-8.79 in these experiments (Figure 3.10). The effluent pH was greater than the input solution pH (~8.10) in the first 10 to 15 pore volumes (values close to 10 were observed in some cases). Surprisingly, the pH decreased during the stop-flow events, down to values close to or smaller than the input solution pH.

The Cr desorption patterns observed in the unsaturated column experiments were different from the ones observed in the saturated column experiments, although the total amounts of Cr released in the saturated and unsaturated column experiments were not significantly different (Figures 3.11, 3.12, and 3.13).

3.3.3 Modeling Results: 2008 Experiments

The CXTFIT code (Parker and van Genuchten 1984; Toride et al. 1999) was used to calculate transport parameters based on the BTC from each column experiment (Figure 3.14 and 3.15).

The dispersion coefficient (D) values were used with the pore-water velocities (V) values to calculate dispersivity, λ ($\lambda = D/V$) (Jury et al. 1991) (Table 3.2), which is the characteristic mixing length, or the average travel distance in one pore before entering another. The calculated values of dispersivity were within the range of typical values observed in packed laboratory columns (dispersivity <2 cm) (Jury et al. 1991). The values of the Péclet number ($PN = L/\lambda$, where L is the column length) for the column experiments conducted during 2008, varied between 55.6 to 206.6 (Table 3.2).

3.3.4 Effluent Solution Composition: 2008 Experiments

Effluent samples from all column experiments (2008 sediments YS, BC, and BS) were subjected to a full elemental analysis (Table 3.3). Effluent chemical composition was determined in samples collected at different times during leaching, as well as in effluent samples collected before and after the stop-flow events.

Results indicated that in addition to Cr, appreciable amounts of Ca, Mg, S, and Si were released in the effluents of these columns, demonstrating that the contaminated sediments YS and BS were exposed to waste fluids that contained these chemical elements. Low Ba concentrations were observed in the effluent collected at the beginning of the experiments, but apparently Ba Cr was not contributing significantly to Cr(VI) release from these sediments.

Significant increases in effluent elemental composition before and after the stop-flow events applied in columns 1 and 3 were observed for S and Si, but little or no changes (increase or decrease) were observed for Ca and Mg. The dramatic change in effluent pH after the 450+ h stop-flow events applied in columns 1 and 3 is another indication of the waste fluid: sediment interactions.

Effluent samples from four 2009 column experiments were subjected to analyses to determine chemical element concentrations at different times during leaching, and to estimate changes in these concentrations before and after the stop-flow events (Table 3.4).

Results indicated that in addition to Cr, a large amount of alkali (such as Na and K) and alkaline earth metals (such as Ca and Mg) were released in the first volume of effluents collected at the outlet of all

columns. In addition, their concentrations increased significantly during the stop-flow events. The presence of high Na concentrations in these sediments may explain the high pH values observed in these sediments.

Si concentration also changed significantly during leaching with the highest concentrations observed in the first pore volume and after the stop-flow events. Low Ba concentrations were observed in the effluent, and apparently Ba Cr was not contributing in a significant way to Cr(VI) release from these sediments.

3.4 Summary of Transport Experiment Results

Results from the 2008 Column Experiments

1. The objective of the 2008 column experiments was to study Cr(VI) desorption from three sediments of the 100-D Area at the Hanford Site, which were exposed to mixed or different Cr and neutralized acid waste fluids.
2. Experimental data indicated that Cr was strongly bounded to the sediments and it was not removed from them during the saturated column experiments conducted with a slightly alkaline artificial groundwater.
3. The average effluent pH in column 2 (relatively clean sediment BC) was $\text{pH}_{\text{AVERAGE BC}} = 8.15 \pm 0.10$, which was similar to the pH value of the input solution. The average effluent pH in columns 1 and 3 (packed with contaminated sediment YS and BS, respectively) was significantly lower ($\text{pH}_{\text{AVERAGE YS}} = 6.91 \pm 0.61$ and $\text{pH}_{\text{AVERAGE BS}} = 6.20 \pm 0.70$, respectively).
4. The aqueous phase pH decreased dramatically during the 450+ h stop-flow events applied in columns 1 and 3 as a result of a time-dependent desorption reaction. This indicated the sediments' geochemistry was significantly altered as a result of waste fluid: sediment interactions.
5. Analyses of effluent samples indicated that in addition to Cr, appreciable amounts of Ca, Mg, S, and Si were released from sediments YS and BS. Low Ba concentrations were observed in the effluent collected at the beginning of the experiments, but apparently BaCrO_4 (hashemite) or other less-soluble solid solutions of $\text{BaCrO}_4 - \text{BaSO}_4$, which usually form under high Cr(VI) concentrations, were not contributing substantially to Cr(VI) solubility and mobility.
6. Significant increases in effluent elemental composition before and after the stop-flow events applied in columns 1 and 3 were observed for S and Si, but little or no changes (increase or decrease) were observed for Ca and Mg. The dramatic change observed in the effluent pH before and after the 450+ h stop-flow events applied in columns 1 and 3 is another indication that these sediments were geochemically altered by the interactions with the waste fluids.

Results from the 2009 Column Experiments

1. The objective of the 2009 column experiments was to study Cr(VI) desorption of five Cr-contaminated sediments from the 100 Area at the Hanford Site, which were exposed to Cr-containing waste fluids.
2. Experimental data clearly indicated that in at least one sediment, Cr was mobile. However, Cr was strongly bounded in other sediments and it was not removed from them during the saturated or unsaturated column experiments conducted with a slightly alkaline artificial groundwater.

3. The average effluent pH was basic and above the pH usually observed in the sediments from this site, indicating that waste fluid with high pH were discarded in the vicinity of the site where these sediments were collected.
4. The aqueous phase pH decreased significantly during all stop-flow events of different durations, applied during the saturated column experiments again indicating that the sediments' geochemistry was significantly altered as a result of waste fluid: sediment interactions.
5. Results from the effluent analyses indicated that in addition to Cr, a large amount of alkali (such as Na and K) and alkaline earth metals (such as Ca and Mg), was released during these experiments, especially in the first volume of effluents. In addition, the concentrations of these elements increased significantly during the stop-flow events.
6. The presence of high Na concentrations in these sediments may explain the high pH values observed in these sediments.
7. Si concentration also changed significantly during leaching with the highest concentrations observed in the first pore volume and after the stop-flow events. Low Ba concentrations were observed in the effluent, and apparently Ba Cr was not contributing in a significant way to Cr(VI) release from these sediments.

Table 3.1. Composition of the synthetic groundwater used in the chromium and bromine leaching experiments

Analyte	Concentration $\times 10^{-4} \text{ mol L}^{-1}$
Na	15.29
Ca	5.97
Mg	5.29
K	4.30
DIC ^a ($[\text{CO}_3]_{\text{TOT}}$)	10.45
HCO ₃ (calc.) ^b	10.33
CO ₃ (calc.) ^b	0.11
SO ₄	9.81
Br	6.23
NO ₃	5.71
Ionic Strength	59.3
P _{CO2}	10 ^{-3.5} atm
pH ^a	8.29
pH ^c	8.05

^aDIC = Dissolved inorganic carbon.
^bSpeciations or calculations performed with MINTEQA2.
^cMeasured analytically.

Table 3.2. Selected measured and calculated physical properties in each column

Column	1 Sediment YS	2 Sediment BC	3 Sediment BS
Pore volume ^b (cm ³)	44.93	39.95	41.88
Water content ^b (cm ³ cm ⁻³)	0.39	0.34	0.36
Residence time ^b (h)	7.84	7.06	7.26
Bulk density ^b (g cm ⁻³)	1.63	1.73	1.70
Flow rate ^a (cm ³ min ⁻¹)	0.095 ± 0.006	0.095 ± 0.005	0.096 ± 0.005
Water flux (cm min ⁻¹)	0.0118	0.0118	0.0119
Pore-water velocity (cm day ⁻¹)	44.27	49.42	47.84
Dispersion coefficient (cm ² day ⁻¹)	3.6	3.7	11.3
Dispersivity (cm)	0.08	0.07	0.26
Péclet number	181	207	56

^aThe average flow rate was calculated from experimental measurements.

^bPore volume, water content, residence time and bulk density were calculated based on the amount of sediments added in each column and the mass of water used to saturate the columns.

Table 3.3. Results from the elemental analyses performed in effluent samples collected at different times during leaching in columns 1, 2, and 3 (2008 sediment samples)

EFFLUENT ANALYSES															
COLUMNS 1, 2 AND 3															
ICP-OES															
		Effluent													
	Sample number	Samples	S (ug/L)	P (ug/L)	Ba (ug/L)	Fe (ug/L)	Si (ug/L)	Mn (ug/L)	Cr (ug/L)	Mg (ug/L)	Ca (ug/L)	Al (ug/L)	Na (ug/L)	K (ug/L)	
column 1	1	1,2,3	591858	< 200	19.7	< 50	44525	50	3728	37390	65910	< 50	31249	9107	
	2	14,18	623606	< 200	7.6	< 50	43131	269	322.6	44100	64310	< 50	34250	5872	
	Before 95 h SF	3	52,55	584731	< 200	6.2	< 50	35762	260	47.4	29600	65680	< 50	16969	5697
	After 95 h SF	4	57,58	592857	< 200	6.9	< 50	42018	265	76.3	25010	65850	< 50	17352	3384
	5	75,78	583641	< 200	4.5	< 50	36863	154	25.1	10160	66190	< 50	23460	3256	
	Before 96 h SF	6	107,108	330965	< 200	6.2	< 50	31934	53	10.4	1990	40080	< 50	13014	7325
	Before 96 h SF	7	111,112	401688	< 200	5.3	< 50	38984	74	25.7	2071	47010	< 50	30020	2638
	8	132,135	124219	< 200	< 5	< 50	35071	18	10.0	501	15230	< 50	15600	1368	
	Before 96 h SF	9	147,150	60348	< 200	< 5	< 50	31713	10	9.7	260	7463	< 50	17353	3035
	After 96 h SF	10	154,155	64328	< 200	< 5	< 50	35718	21	7.7	522	7217	< 50	21382	25922
	11	166,169	35087	< 200	< 5	< 50	33844	7.7	9.2	243	3050	< 50	19672	1177	
	Before 451 h SF	12	178,181	30970	< 200	< 5	< 50	29600	5.0	9.5	204	4789	< 50	22074	12274
	After 451 h SF	13	183,184	49904	< 200	< 5	< 50	37094	7.3	75.2	356	3671	< 50	22643	1197
	14	197,200	30013	< 200	< 5	< 50	34636	< 5	17.4	283	4513	< 50	24279	17328	
	15	215,228	25840	< 200	< 5	< 50	31611	< 5	16.6	227	4330	< 50	21702	6046	
column 2	16	1,2,3	52885	< 200	20.0	< 50	18225	< 5	214.5	7673	3579	< 50	36956	13126	
	17	10,12	28458	< 200	16.3	< 50	20273	< 5	20.0	6087	5309	< 50	28724	8739	
	Before 94 h SF	18	46,49	25287	< 200	17.7	< 50	14427	< 5	9.5	5653	3328	< 50	26295	11865
	After 94 h SF	19	54,55	30063	< 200	21.8	< 50	17165	< 5	22.4	7846	3034	< 50	28622	9647
	20	99,102	25398	< 200	17.8	< 50	11597	< 5	< 5	5974	4092	< 50	23752	8332	
column 3	21	1,2,3	191300	< 200	45.0	< 50	44734	95.9	59.4	15920	3110	< 50	19500	5512	
	22	10,14	56050	< 200	13.2	< 50	29778	101.8	45.1	8390	18860	< 50	10845	1866	
	Before 96 h SF	23	48,50	34800	< 200	11.4	< 50	16794	159.6	24.1	3148	6299	< 50	13311	4299
	After 96 h SF	24	52,54	42550	< 200	13.3	< 50	30289	194.6	19.9	4008	3507	< 50	15719	50925
	25	75,78	33530	< 200	7.9	< 50	22155	99.5	14.5	2220	4186	< 50	19033	1538	
	Before 455 h SF	26	90,93	30520	< 200	7.2	< 50	17089	84.0	15.2	1841	2930	< 50	20393	1868
	After 455 h SF	27	95,96	39500	< 200	9.5	< 50	33810	136.2	45.1	2381	2478	< 50	21705	1629
	28	114,120	34120	< 200	6.4	< 50	24717	88.3	11.7	1822	2918	< 50	23019	14771	
	29	135,140	30250	< 200	5.3	< 50	16092	72.2	11.8	1524	2531	< 50	23117	4317	

Table 3.4. Results from the elemental analyses performed in effluent samples collected at different times during leaching in column experiments (2009 sediment samples)

Cr Project 2009																
ICP sample number	Nik's sample #	Sample consecutive #	Comments	Cr (ug/L)	Sr (ug/L)	Ba (ug/L)	Fe (ug/L)	Si (ug/L)	Mn (ug/L)	Mg (ug/L)	Ca (ug/L)	Al (ug/L)	Na (ug/L)	K (ug/L)		pH
Column 30: J18NF7																
Nik7-16-09-65	30_1	4+5+6		50177.61	274.03	39.36	< 50	19100.00	< 5	7915.63	44088.45	< 5	304541.07	14980.80		8.30
Nik7-16-09-66	30_2	10+11+12		2325.35	24.00	7.36	< 50	18030.00	< 5	623.00	4599.44	< 5	109860.33	4483.90		9.09
Nik7-16-09-67	30_3	19+20+21		730.40	17.69	5.04	< 50	12760.00	< 5	453.31	3536.01	< 5	93591.00	912.19		8.89
Nik7-16-09-68	30_4	25+26+27		436.46	16.60	4.75	< 50	10080.00	< 5	427.71	3271.30	< 5	91745.45	861.55		
Nik7-16-09-69	30_5	36+37+38	Before 49 h SF	215.17	46.27	11.78	< 50	7438.00	< 5	1235.03	6944.89	< 5	77460.70	9708.68		8.73
Column 8: J18NH6																
Nik7-16-09-70	8_1	4+5+6		44905.00	170.04	35.96	< 50	21820.00	< 5	4576.21	24941.56	< 5	360973.07	23575.84		8.78
Nik7-16-09-71	8_2	10+11+12		4623.19	16.77	6.74	< 50	25240.00	< 5	415.85	3221.73	< 5	139408.50	2482.20		9.27
Nik7-16-09-72	8_3	19+20+21		1122.26	11.93	< 5	< 50	16890.00	< 5	288.65	2557.46	< 5	115266.15	811.76		9.40
Nik7-16-09-73	8_4	25+26+27		755.39	8.25	< 5	< 50	13470.00	< 5	176.38	1836.41	< 5	114111.14	613.59		9.50
Nik7-16-09-74	8_5	35+36+37	Before 49 h SF	490.21	8.03	< 5	< 50	9820.00	< 5	162.07	1797.55	< 5	106325.00	590.79		9.59
Column 15: J18NJ3																
Nik7-16-09-75	15_1	4+5+6		128.70	34.51	17.88	< 50	25900.00	< 5	553.08	20395.96	< 5	199607.26	3966.39		8.60
Nik7-16-09-76	15_2	10+11+12		27.86	16.94	7.47	< 50	26010.00	< 5	246.82	8115.35	< 5	155918.77	9462.33		9.58
Nik7-16-09-77	15_3	19+20+21		69.72	73.66	39.45	289.67	20160.00	15.90	1103.22	48909.20	< 5	139735.85	745.06		9.74
Nik7-16-09-78	15_4	25+26+27		49.49	55.44	24.89	195.85	16520.00	10.70	775.25	31409.16	< 5	132118.21	739.93		9.58
Nik7-16-09-79	15_5	40+41+42	Before 98.5 h SF	26.28	28.60	13.95	86.04	10530.00	4.41	388.29	17265.80	< 5	124517.45	18903.70		9.84
Nik7-16-09-80	15_6	44+45+46	After 98.5 h SF	116.57	43.99	15.79	127.02	14080.00	6.56	673.02	22928.59	< 5	139724.55	1017.23		8.36
Nik7-16-09-81	15_7	62+63+64		6.75	8.39	< 5	< 50	8951.00	< 5	114.44	2575.62	< 5	109333.15	679.56		9.44
Nik7-16-09-82	15_8	81+82+83	Before 98 h SF	3.48	83.76	8.72	< 50	5507.00	< 5	1350.26	18461.42	< 5	72466.04	1067.70		8.95
Nik7-16-09-83	15_9	86+87+88	After 98 h SF	71.57	163.81	43.59	< 50	8526.00	< 5	2068.80	29940.45	< 5	82721.68	3958.67		7.85
Nik7-16-09-84	15_10	126+127+128		1.63	204.04	32.35	< 50	4497.00	< 5	3716.26	42926.66	< 5	24706.78	18572.09		7.89
Column 22: J18NK0																
Nik7-16-09-85	22_1	4+5+6		76.78	49.51	18.65	212.86	21270.00	6.48	766.56	49433.20	< 5	130968.00	6434.98		8.19
Nik7-16-09-86	22_2	10+11+12		16.79	20.58	7.18	< 50	19910.00	< 5	270.91	9927.08	< 5	104826.82	11614.96		9.02
Nik7-16-09-87	22_3	19+20+21		10.11	19.03	< 5	< 50	14620.00	< 5	227.71	6539.17	< 5	95679.54	1273.36		9.10
Nik7-16-09-88	22_4	25+26+27		7.02	20.77	< 5	< 50	12210.00	< 5	200.55	4691.44	< 5	94399.64	1212.50		
Nik7-16-09-89	22_5	34+35+36	Before 98.5 h SF	4.92	20.97	< 5	< 50	9573.00	< 5	202.96	3743.01	< 5	90366.09	9898.55		9.27
Nik7-16-09-90	22_6	37+38+39	After 98.5 h SF	64.23	271.31	16.33	< 50	14370.00	51.47	7576.17	22737.03	< 5	112123.60	2169.81		8.11
Nik7-16-09-91	22_7	56+57+58		1.75	118.91	16.34	< 50	8382.00	< 5	2953.00	28745.02	< 5	49715.00	2395.51		8.14
Nik7-16-09-92	22_8	76+77+78	Before 98 h SF	0.84	153.80	24.05	< 50	5905.00	< 5	4441.22	39854.33	< 5	25389.76	2647.23		8.08
Nik7-16-09-93	22_9	79+80+81	After 98 h SF	30.44	229.37	47.04	< 50	11180.00	23.94	5318.53	51321.27	< 5	42452.27	6638.07		7.22
Nik7-16-09-94	22_10	120+121+122		0.41	158.09	20.14	< 50	4514.00	< 5	4611.86	39880.30	< 5	23773.83	12567.32		7.91



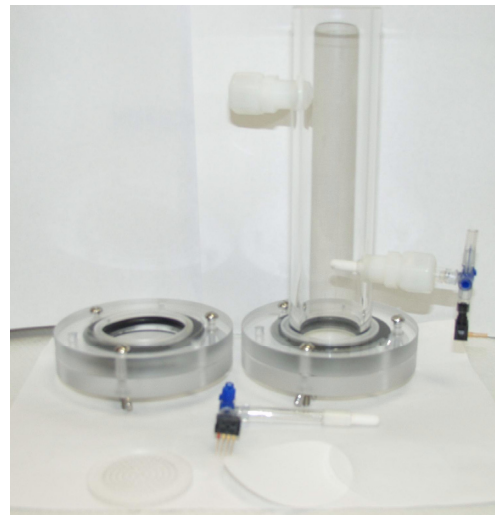
a)



c)



b)



d)

Figure 3.1. a) Experimental set up for transport experiments in unsaturated column; b) nylon membrane, filter paper, and nylon mesh; c) a picture of a quartz sand-packed column; and d) disassembled column and tensiometers

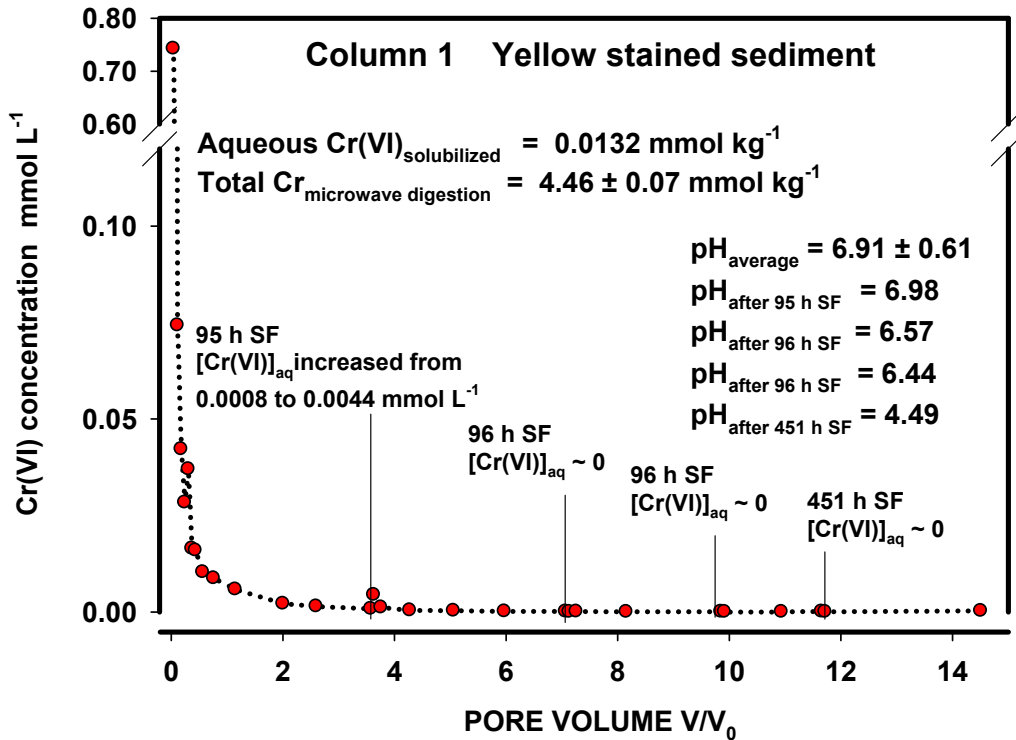


Figure 3.2. Cr(VI) leaching profile of sediment YS. Four stop-flow events with a duration of 95, 96, 96, and 451 h were applied during this experiment.

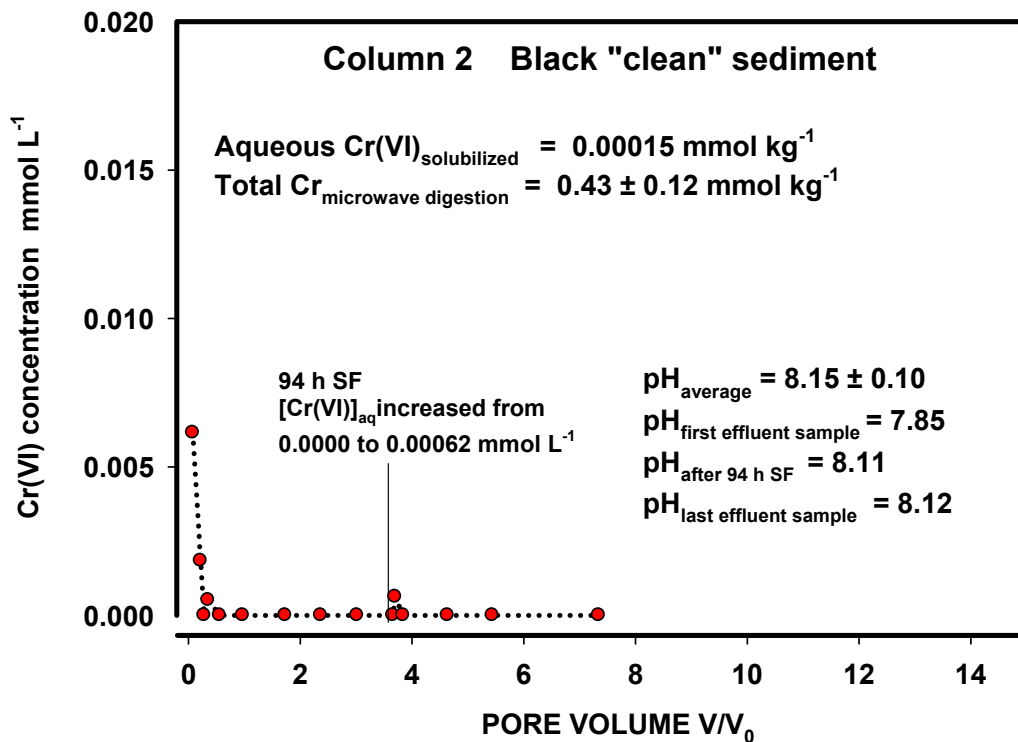


Figure 3.3. Cr(VI) leaching profile of sediment BC. One stop-flow event (94 h) was applied during this experiment.

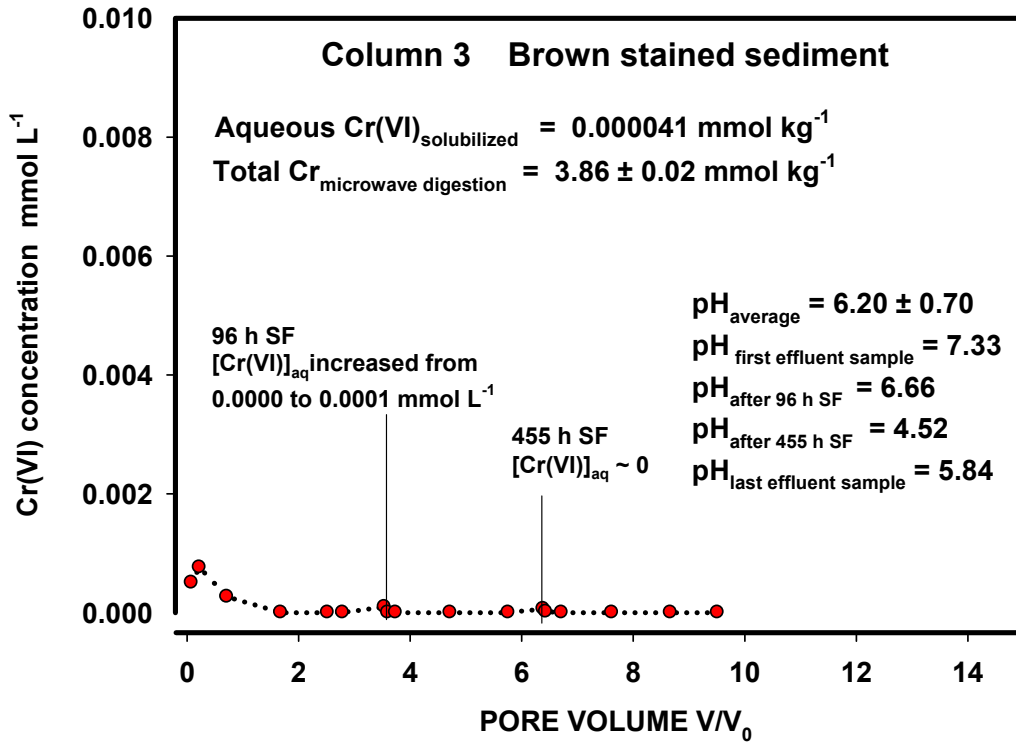


Figure 3.4. Cr(VI) leaching profile of sediment BS. Two stop-flow events with a duration of 96 and 455 h were applied during this experiment.

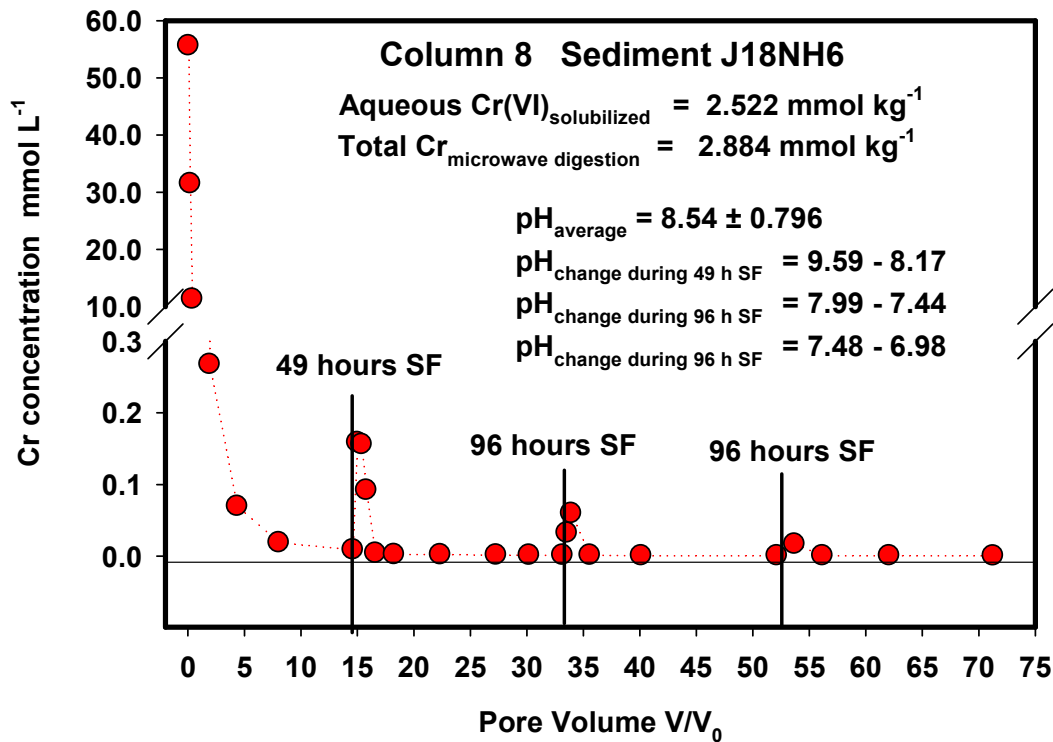


Figure 3.5. Cr(VI) leaching profile of sediment J18NH6. Three stop-flow events with durations of 49, 96, and 96 h were applied during this experiment.

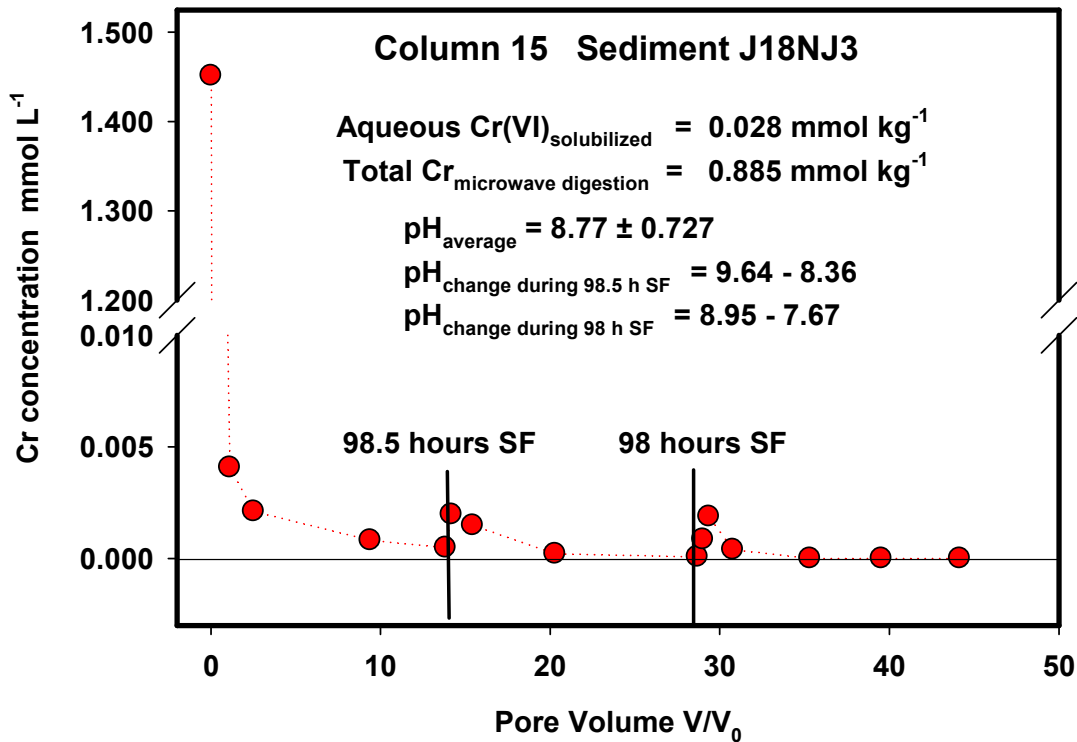


Figure 3.6. Cr(VI) leaching profile of sediment J18NJ3. Two stop-flow events of durations of 98.5 and 98 h were applied during this experiment.

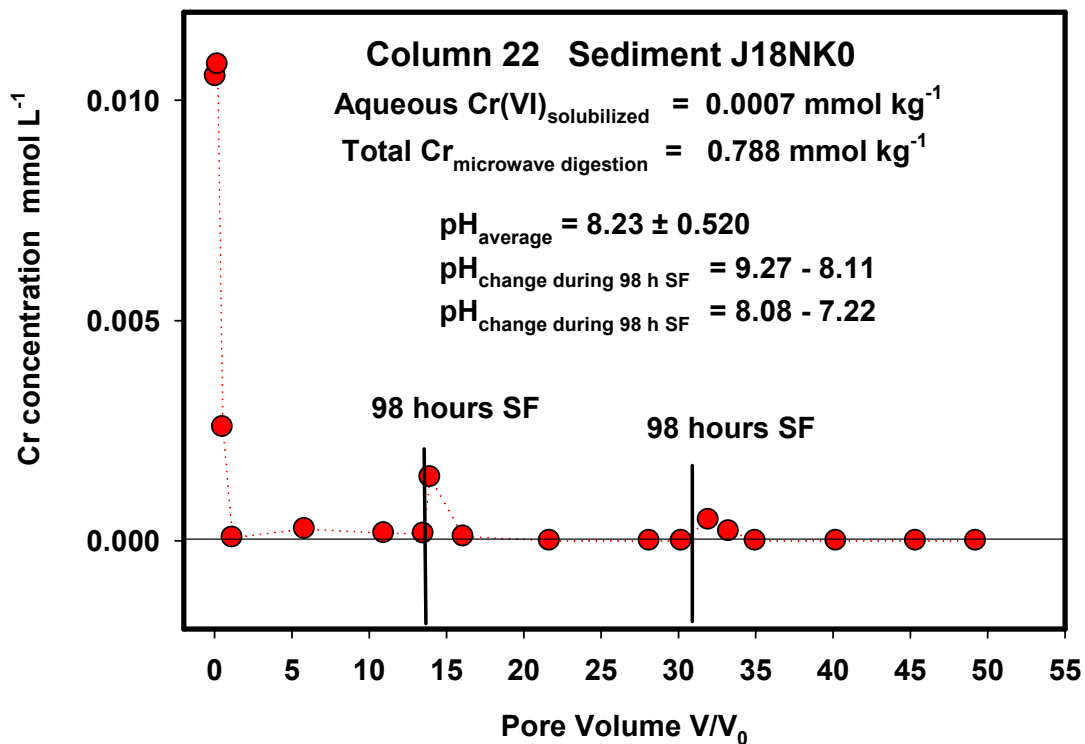


Figure 3.7. Cr(VI) leaching profile of sediment J18NK0. Two stop-flow events with durations of 98 and 98 h were applied during this experiment.

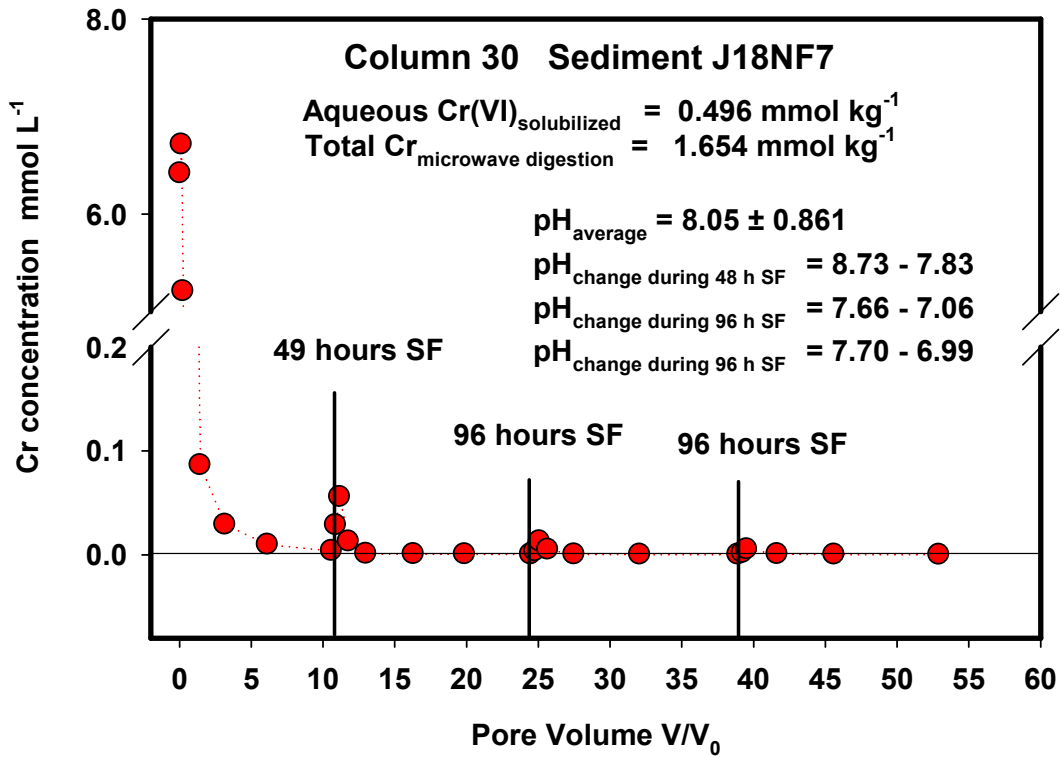


Figure 3.8. Cr(VI) leaching profile of sediment J18NF7. Three stop-flow events with durations of 49, 96, and 96 h were applied during this experiment.

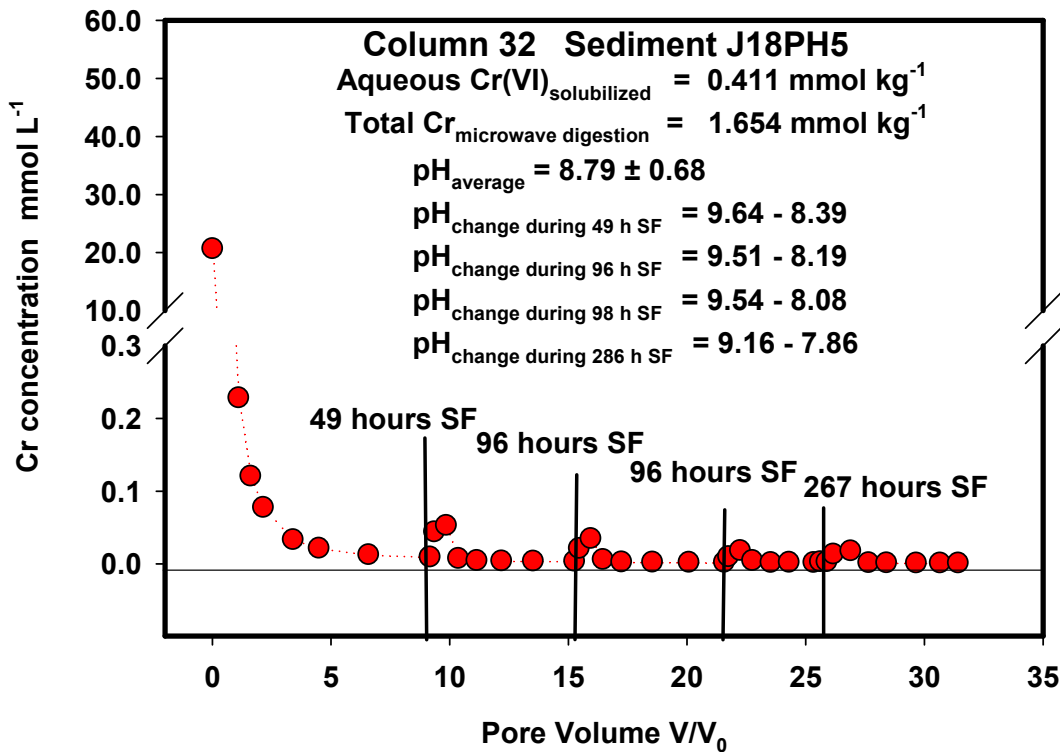


Figure 3.9. Cr(VI) leaching profile of sediment J18PH5. Four stop-flow events with durations of 49, 96, 96, and 267 h were applied during this experiment.

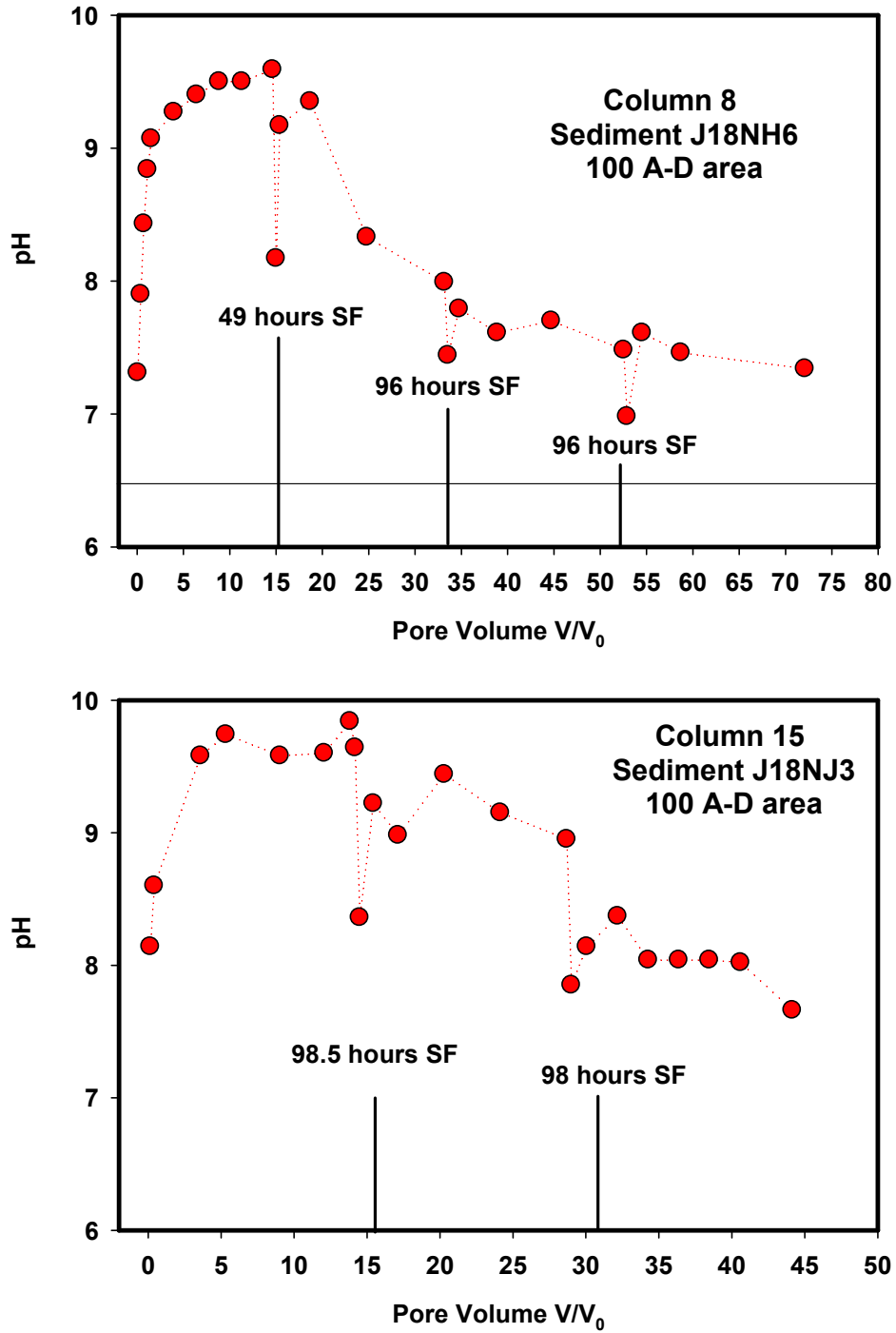


Figure 3.10. Changes in effluent pH during leaching Cr(VI) leaching in experiments conducted with sediments J18NH6, J18NJ3, J18NK0, J18NF7, and J18PH5

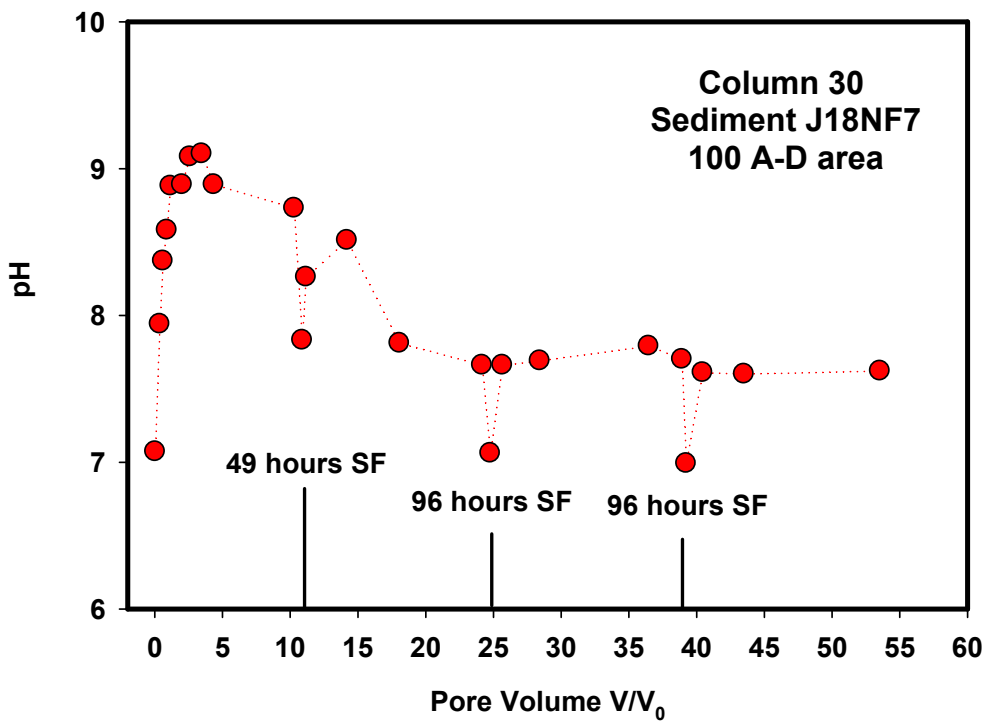
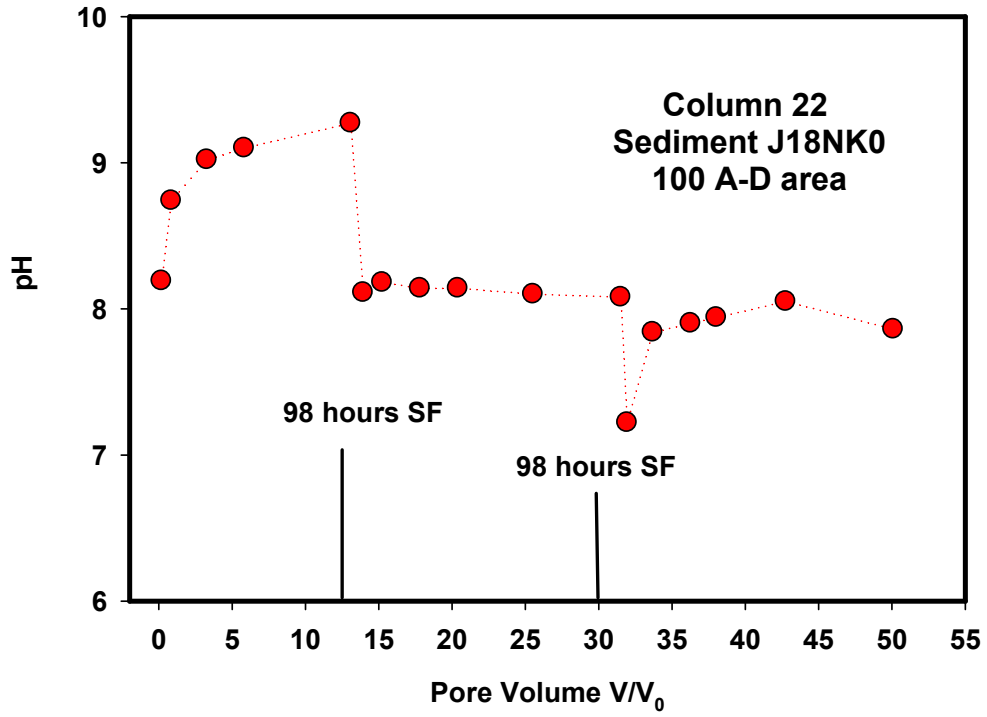


Figure 3.10. (contd)

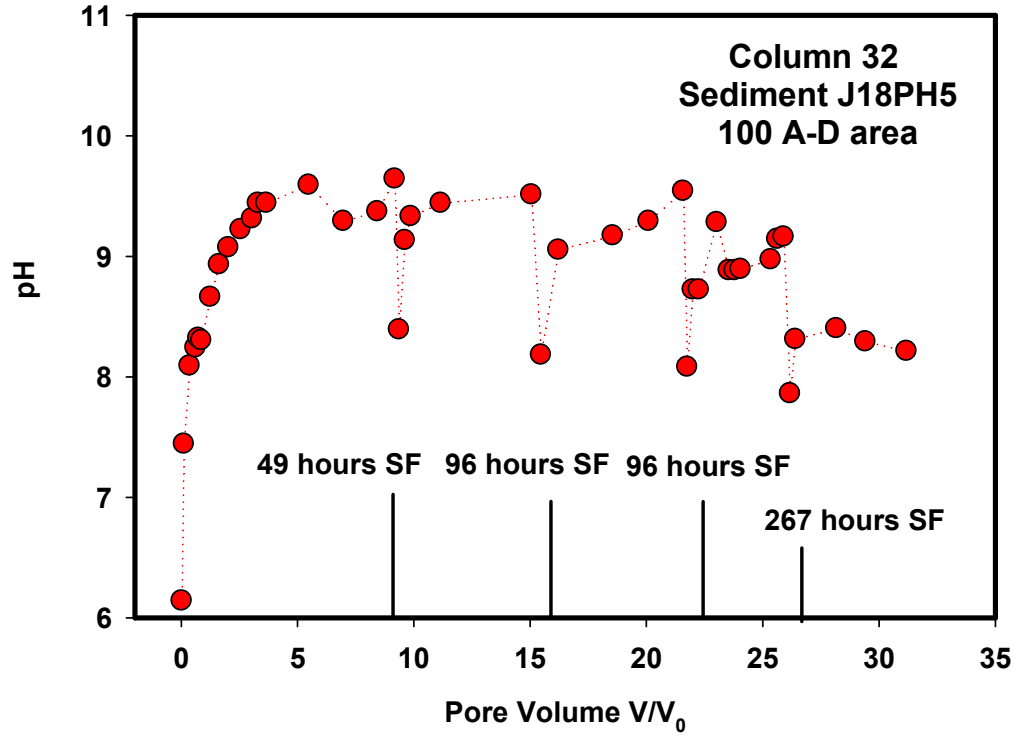


Figure 3.10. (contd)

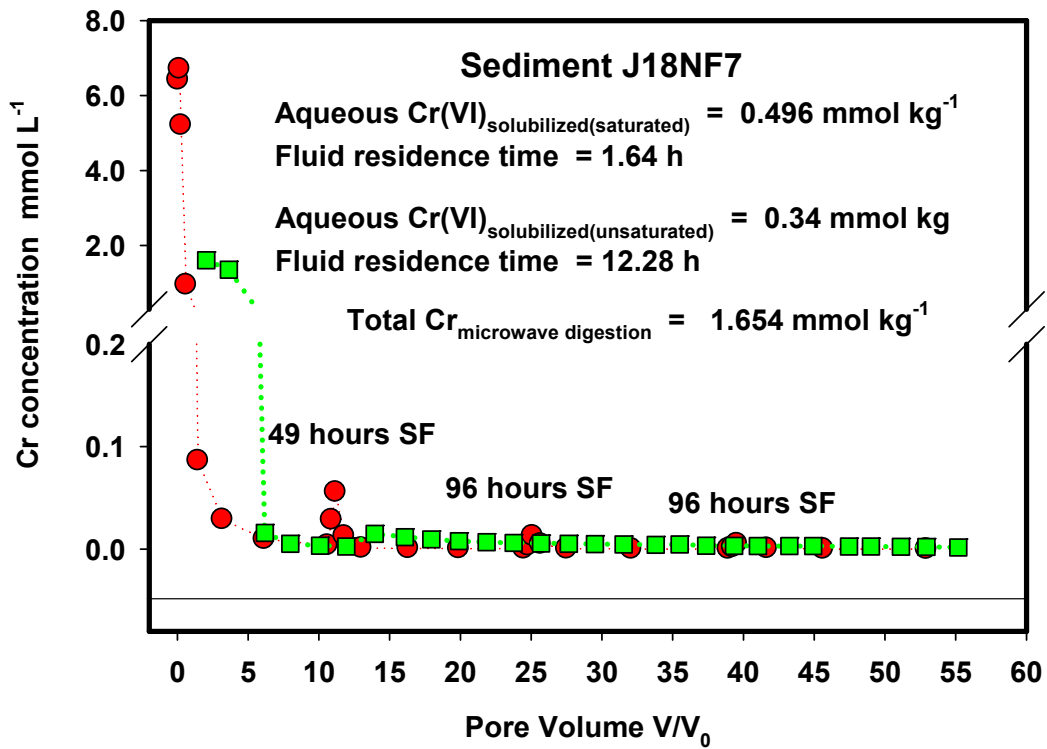


Figure 3.11. Cr(VI) leaching profiles in saturated (red) and unsaturated column experiments conducted with sediment J18NF7

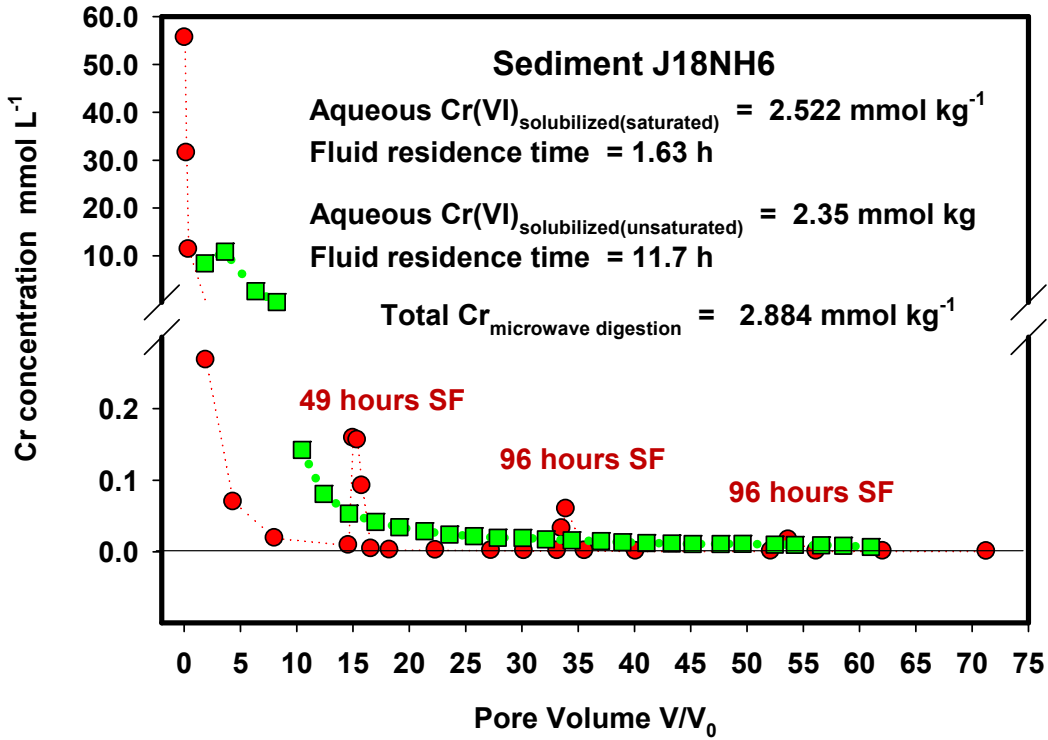


Figure 3.12. Cr(VI) leaching profiles in saturated (red) and unsaturated column experiments conducted with sediment J18NH6

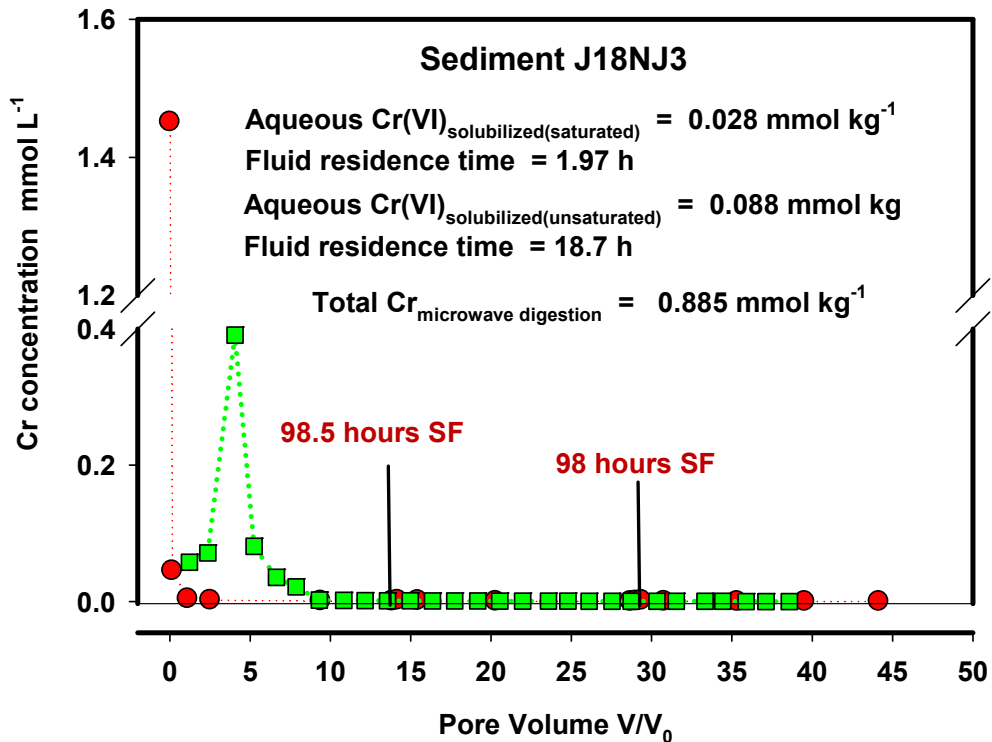
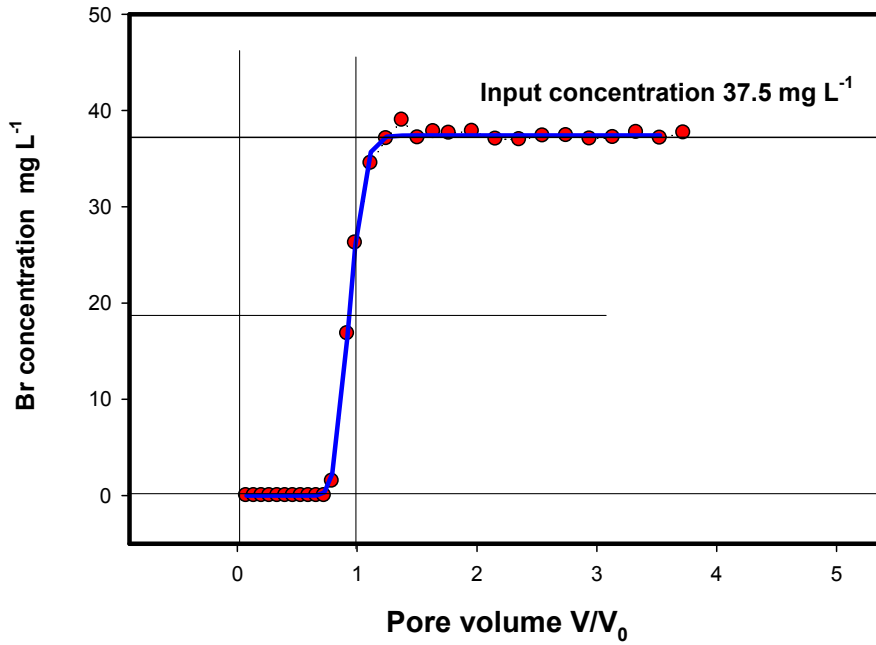


Figure 3.13. Cr(VI) leaching profiles in saturated (red) and unsaturated column experiments conducted with sediment J18NJ3

Br BTC Column 1
Yellow Stained Sediment



Br BTC Column 2
Black Clean Sediment

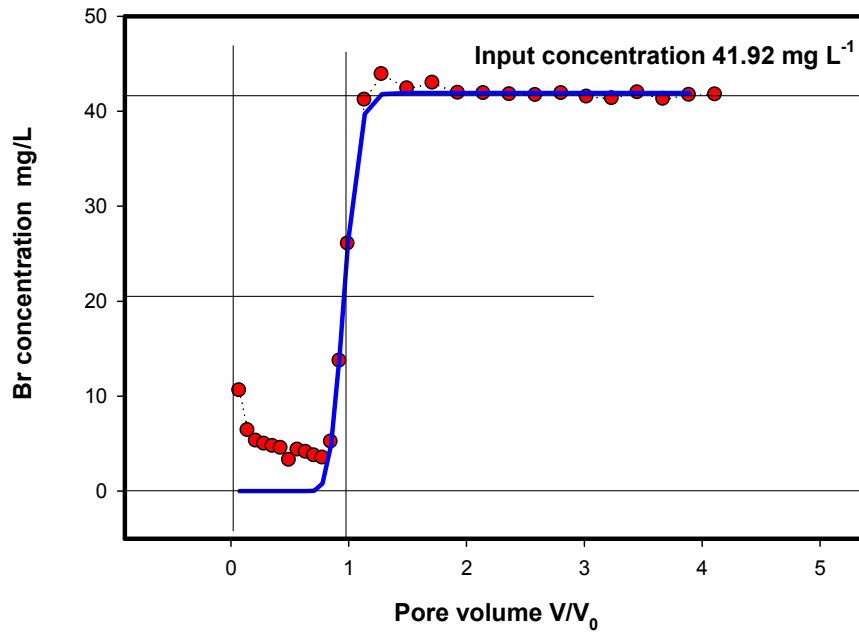


Figure 3.14. Br breakthrough curves obtained in different experiments conducted with sediments YS, BC, and BS. The red circles represent experimental data and the blue line is the fitting line calculated with the CXTFIT computer code.

Br BTC Column 3
Brown Stained Sediment

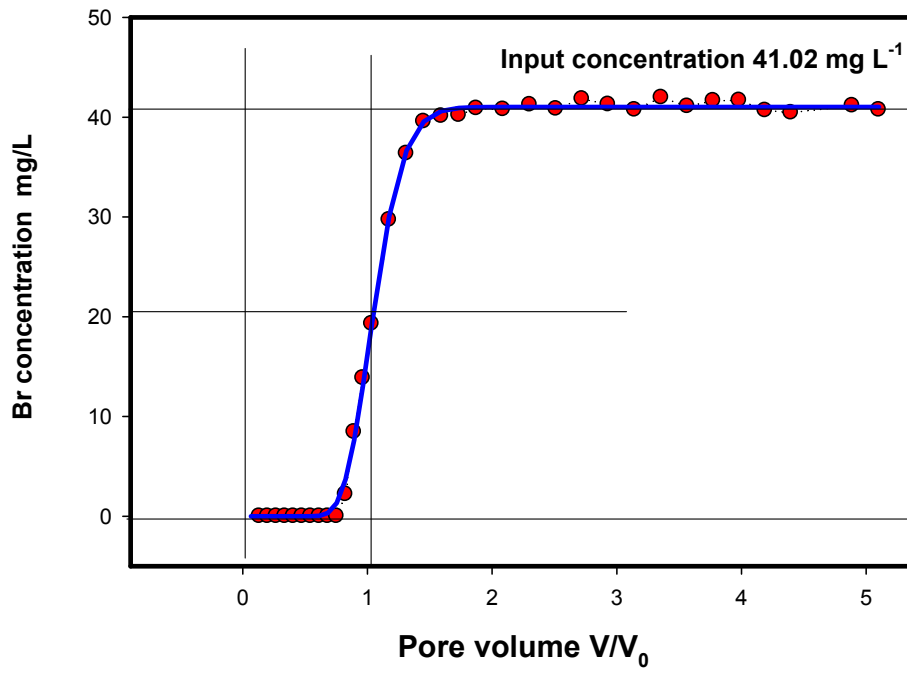
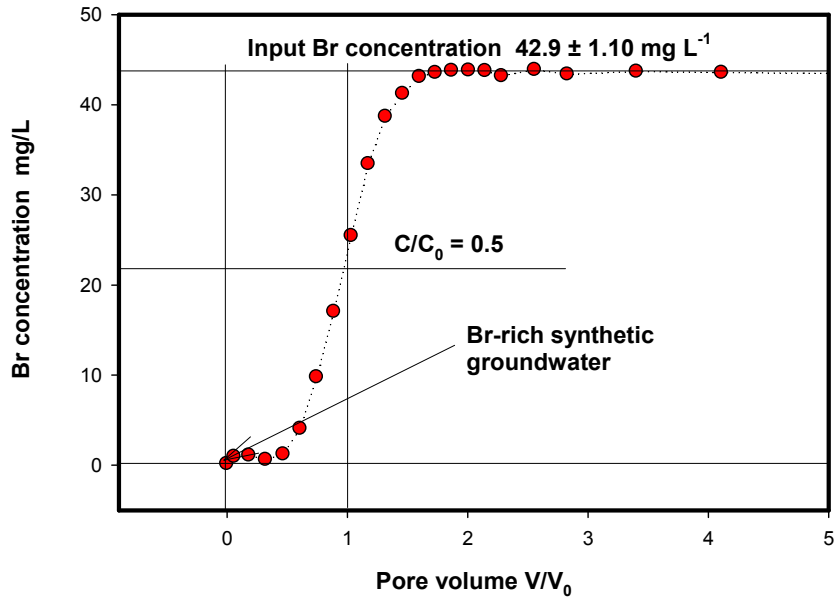


Figure 3.14. (contd)

Br BTC
Column 8: Half interval
Sediment J18NH6



Br BTC
Column 15: Half interval
Sediment J18NJ3

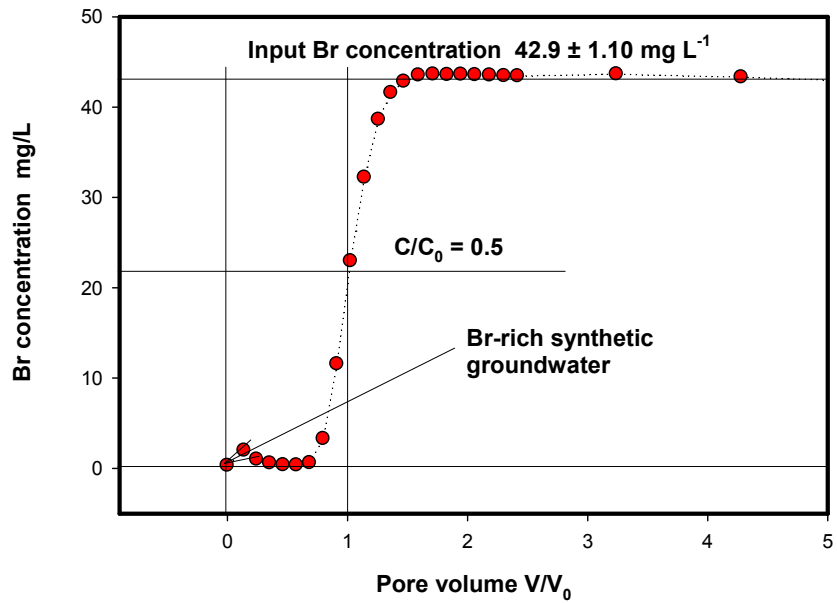
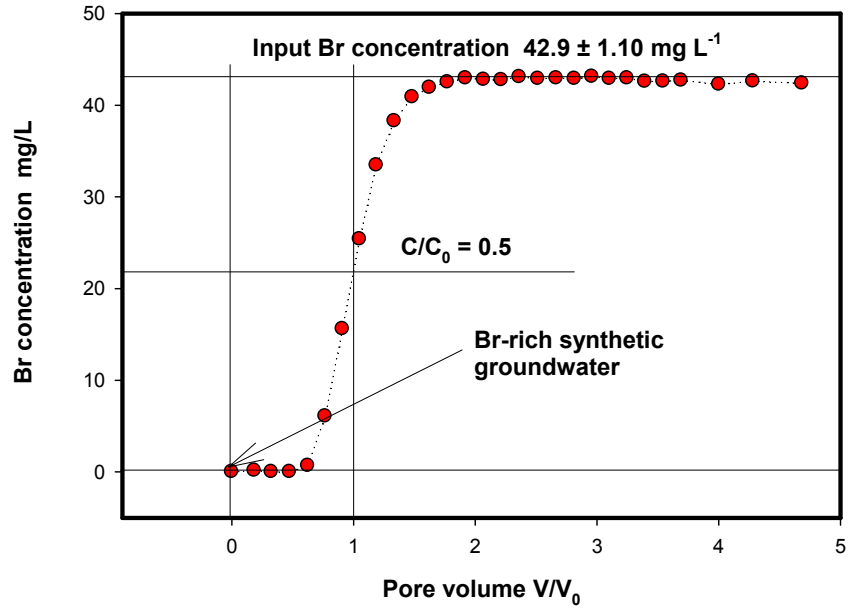


Figure 3.15. Br breakthrough curves obtained in different experiments conducted with sediments J18NH6, J18NJ3, J18NK0, J18NF7, and J18PH5

Br BTC
Column 22: Half interval
Sediment J18K0



Br BTC
Column 30: Half interval
Sediment J18NF7

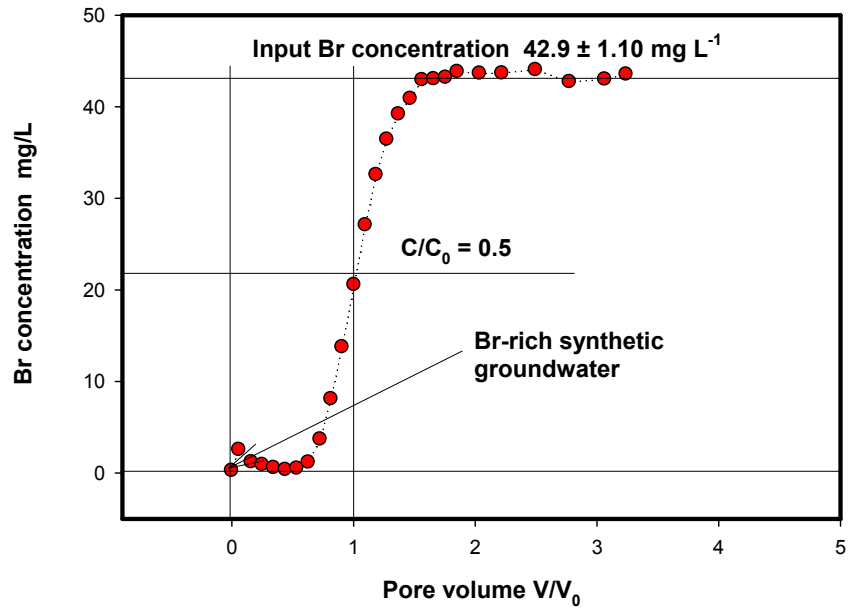


Figure 3.15. (contd)

Br BTC
Column 32: Half interval
Sediment J18PH5

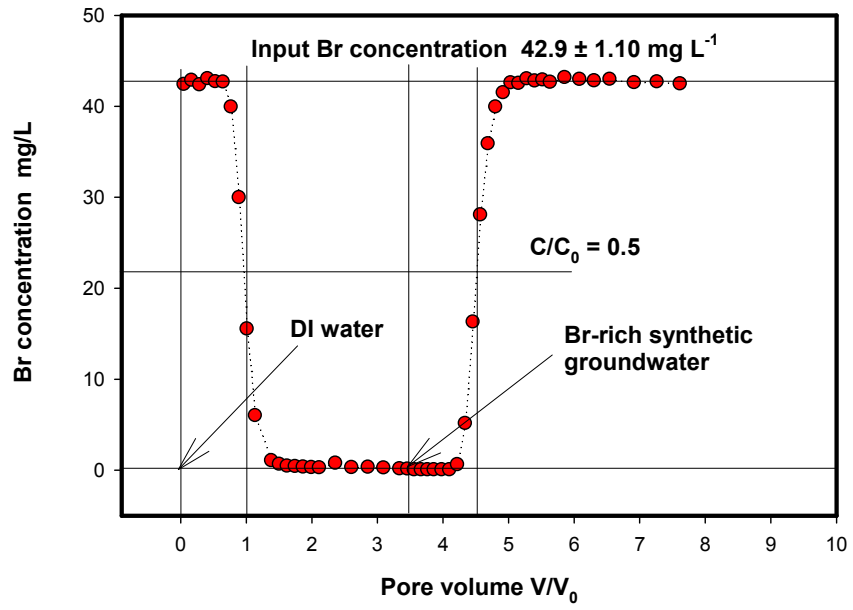


Figure 3.15. (contd)

4.0 Microscopic Investigation of Sediments Chromium Spatial Distribution

4.1 Introduction

The sediment samples were examined with detailed microscopic and spectroscopic techniques to identify areas of high Cr concentration and study the chemical and mineralogical nature of the Cr:sediment interactions and association(s).

The following microscale methods were used in this investigation:

1. Electron microprobe analysis (EMPA)
2. X-ray photoelectron spectroscopy (XPS)
3. Mössbauer spectroscopy.

4.2 Materials and Methods

4.2.1 Electron Microprobe Measurements

For the EMP and measurements, data were collected using a JEOL JXM 8200 electron microprobe. Measurements represent randomly selected areas within each sample. Sample preparation was by commercial preparator, consisting of epoxy imbedding, sectioning, and polishing of sediment samples labeled as shown in the figures.

4.2.2 X-Ray Photoelectron Spectroscopy Measurements

A Scienta ESCA300 that employs a high-flux monochromatic Al K α x-ray beam was used to obtain the XPS data. Operational conditions yielded a Fermi edge width = 0.41 eV for Ag. The binding energy scale was referenced to adventitious C1s at 285.0 eV. Spectra were best fit by nonlinear least squares. Element concentrations were semi-quantified using Scofield photoionization cross sections for the Cr2p_{3/2}, Si2p, Al2p, and Fe2p levels. Significant Ca was present, but likely interference from an Mg auger line with the dominant Ca2p line precluded quantification.

4.2.3 Mössbauer Spectroscopy Measurements

Mössbauer spectroscopy permits identification and quantification of multiple iron oxide phases in a single heterogeneous sample. Mössbauer spectra were collected in the <2 mm fraction of sediments BC and YS using a 50 mCi (initial strength) ⁵⁷Co/Rh source. The velocity transducer MVT-1000 (WissEL) was operated in constant acceleration mode (23 Hz, \pm 12 mm/s). An Ar-Kr proportional counter was used to detect the radiation transmitted through the holder, and the counts were stored in a multichannel scalar as a function of energy (transducer velocity) using a 1024 channel analyzer. Data were folded to 512 channels to give a flat background and a zero-velocity position corresponding to the center shift of a metal Fe foil at room temperature. A closed-cycle cryostat (ARS, Allentown, Pennsylvania) was employed for below room temperature measurements. The Mössbauer data were modeled with the Recoil

software (University of Ottawa, Canada) using a Voigt-based structural fitting routine. The coefficient of variation of the spectral areas of the individual sites generally ranged between 1% and 2% of the fitted values.

4.3 Results and Discussion

4.3.1 Electron Microprobe Measurements

In all 2008 and 2009 sediment samples that were examined, Cr was below detectable limits for EMP (Figures 4.1, 4.2, 4.3, 4.4, 4.5, 4.6, 4.7, and 4.8). In the 2008 sediment samples, it was not possible to locate zones of high Cr concentrations in the randomly selected areas of sediment samples interrogated with the EMP. In the 2009 sediments samples, some high Cr concentrations areas were detected. The authors' focus will be on these areas in the future if there is interest and financial support.

4.3.2 X-Ray Photoelectron Spectroscopy Measurements

4.3.2.1 2008 Sediment Samples

All compositional data for the 2008 sediment samples are given as the ratio of the element of interest to Si (i.e., M/Si) in Table 4.1. Valence determinations for Cr and Fe are given as the mole fractions $\text{Cr(III)}/\text{Cr}_{\text{total}}$ and $\text{Fe(II)}/\text{Fe}_{\text{total}}$ (Table 4.1). Si, Al, Mg, Ca, O, and $\pm\text{Na}$ were detected in surveys of all the samples (Figure 4.9). No Cr was detected on the “black clean” sample; however, Cr was detected on all other samples. For example, the Cr2p regions for the “black clean” and “brown stained” samples are compared in Figure 4.10; although the Cr signal is low, it is clearly present. Both Cr(VI) and Cr(III) were detected (Figure 4.11 and Table 4.1). However, reduction of Cr(VI) to Cr(III) was observed during analysis (this is a common observation) of the “yellow stained” and “yellow stained 2” samples.

Initially, it was attempted to estimate $\text{Cr(III)}/\text{Cr}_{\text{total}}$ ratios by extrapolating a sequence of progressively beam reduced Cr to time zero. However, reduction was erratic and Cr concentrations were so low that analytical error rendered the extrapolated values meaningless. Consequently, only the first analyses for $\text{Cr(III)}/\text{Cr}_{\text{total}}$ are reported in Table 4.1. Note these are maximum values.

Interestingly, $\text{Cr(III)}/\text{Cr}_{\text{total}}$ values were constant between sequential analyses for the “brown stained” samples, despite the presence of detectable Cr(VI). Therefore, it is possible that in this case $\text{Cr(III)}/\text{Cr}_{\text{total}}$ values are correct as given.

Fe was mixed valent, indicating the predominance of Fe(III) but with an appreciable Fe(II) component (Figure 4.12 and Table 4.1). Curve fitting to extract quantitative $\text{Fe(II)}/\text{Fe}_{\text{total}}$ ratios was difficult due to the complicated multiplet structures inherent to the Fe2p line (the Fe3p signal was too weak). Curve fitting all the samples yielded a range in $\text{Fe(II)}/\text{Fe}_{\text{total}} = 0.14 - 0.20$.

Assuming that Si is relatively immobile in this system, it appears the Cr-containing samples are enriched in Fe. This enrichment—like that of Cr, however—may only be limited to the top ~8 nm of the sample (see Section 4.4 for concluding statements). The “brown stained” sample contains the highest Fe/Si ratio. The correlation of Fe and Cr implies a similar temporal origin. The Cr(III)2p binding

energies are suggestive of a Cr(III)-oxyhydroxide, not Cr₂O₃. However, it is not yet possible to rule out the formation of a Fe(III)-Cr(III) oxyhydroxide or possible incorporation into silicates.

It must be emphasized that XPS is a surface-sensitive technique and the information depth is only about 8 nm. Both bulk and higher resolution two-dimensional analyses are required to supplement and aid interpretation of the XPS data. For example, Fe at the near surface of all the samples could be oxidized relative to bulk Fe.

4.3.2.2 2009 Sediment Samples

Cr was not detected in any sediments except sediment J18NH6 (Figure 4.13). Both Cr(VI) and Cr(III) were detected in this sediment. Fe occurred as mixed valence, indicating the predominance of Fe(III) but with an appreciable Fe(II) component.

4.3.3 Mössbauer Spectroscopy Measurements: Preliminary Results

These analyses were conducted only in some 2008 sediment samples. Mössbauer spectroscopy measurements provide information about Fe mineralogy, oxidation state, and coordination environment (tetrahedral or octahedral) in the bulk sediment sample. Measurements were performed in sediment BC at room temperature at 77 K and in sediment YS at 77 K (Figures 4.14 and 4.15).

The preliminary results from sediment BC indicated that most of the Fe (~66% of total Fe) in sediment BC was in the Fe(II) oxidation state and in two different soil minerals or sites (Figure 4.14).

Although preliminary, this finding suggests the abiotic reduction pathway of Cr(VI) to Cr(III) by Fe(II) is a viable pathway of Cr(VI) attenuation in the sediments from this area. Fe(II) may be released into the aqueous phase during dissolution of the Fe(II)-bearing minerals. In addition, sorbed or structural Fe(II) may be also involved in redox reactions with redox-sensitive contaminants such as Cr(VI).

4.4 Summary of the Microscale Characterization Data

1. The objective of this part of the investigation was to use EMP to locate zones of high Cr concentrations and determine Cr:soil mineral associations within the sediments matrix. In addition, a surface-sensitive spectroscopic technique—such as XPS—was used to determine the valence state of surface Cr and Fe. Mössbauer spectroscopy was also used to gain insights on bulk Fe mineralogy of these sediments.
2. Zones of high Cr concentration were not detected in the samples interrogated with EMP.
3. XPS measurements confirmed that Cr was not present in sediment BC. However, Cr was detected in all other samples, although the Cr signal was low.
4. Both Cr(VI) and Cr(III) were detected in the contaminated sediment samples. Interestingly, Cr(III)/Cr_{total} values were constant between sequential analyses for sediment BS despite the presence of detectable Cr(VI). Therefore, it is possible Cr(III)/Cr_{total} values are correct as given.
5. Fe was mixed valent, indicating the predominance of Fe(III) but with an appreciable Fe(II) component. Although difficult, curve fitting of all the samples yielded a range in Fe(II)/Fe_{total} = 0.14 – 0.20.

6. Results indicate the Cr-containing samples are enriched in Fe. However, this enrichment, like that of Cr, may only be limited to the top ~8 nm of the sample because XPS is a surface-sensitive technique.
7. The correlation of Fe and Cr implies a similar temporal origin.
8. Sediment BS contained the highest Fe/Si ratio.
9. The Cr(III)2p binding energies are suggestive of a Cr(III)-oxyhydroxide and not Cr₂O₃. However, it is not yet possible to rule out the formation of a Fe(III)-Cr(III) oxyhydroxide or other pathways, such as the possible incorporation into silicates.
10. Preliminary Mössbauer spectroscopy measurements indicate that a bulk sediment sample (sediment BC) had an appreciable amount of Fe(II)-bearing minerals.
11. Some zones of relatively high Cr concentration were detected in the 2009 samples interrogated with EMPA. XPS measurements confirmed that Cr was detected in at least one sample, although the Cr signal was low. Both Cr(VI) and Cr(III) were detected in the contaminated sediment samples.

Table 4.1. Elemental analyses and valence states of transition metals (based on XPS measurements)

	Cr/Si	Fe/Si	Al/Si	Cr(III)/Cr_{total}	Fe(II)/Fe_{total}
Black Clean	n.d.	0.074	0.392	n.a.	0.21
Yellow Stain	0.018	0.195	0.261	<0.82	0.14
Yellow Stain 2	0.014	0.164	0.240	<0.81	d.n.c.
Brown Stain	0.017	0.226	0.354	0.86	0.19

n.d = not detected; n.a. = not applicable; and d.n.c = did not converge.

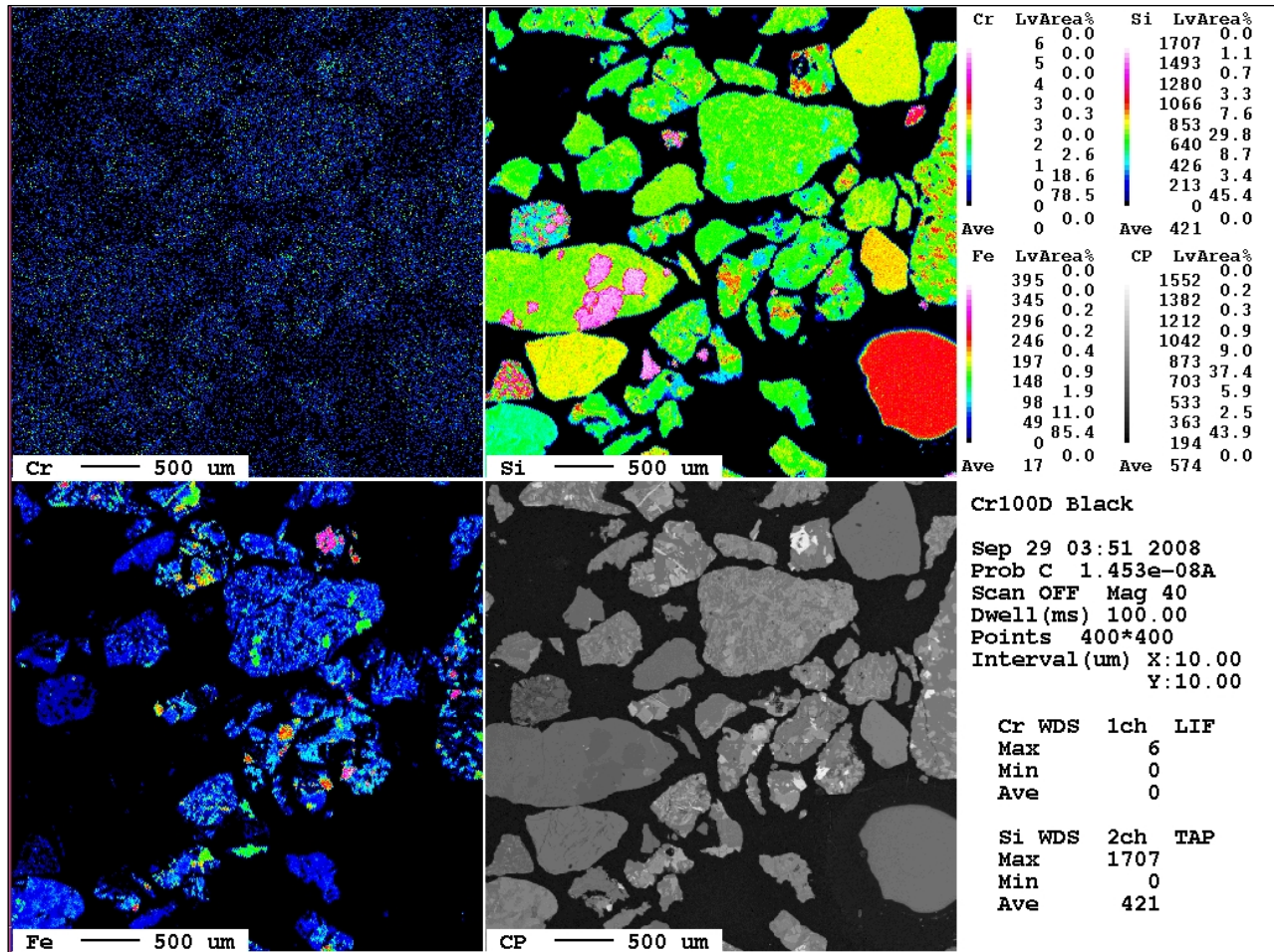


Figure 4.1. Results of the EMP measurements performed in sediment BC (2008)

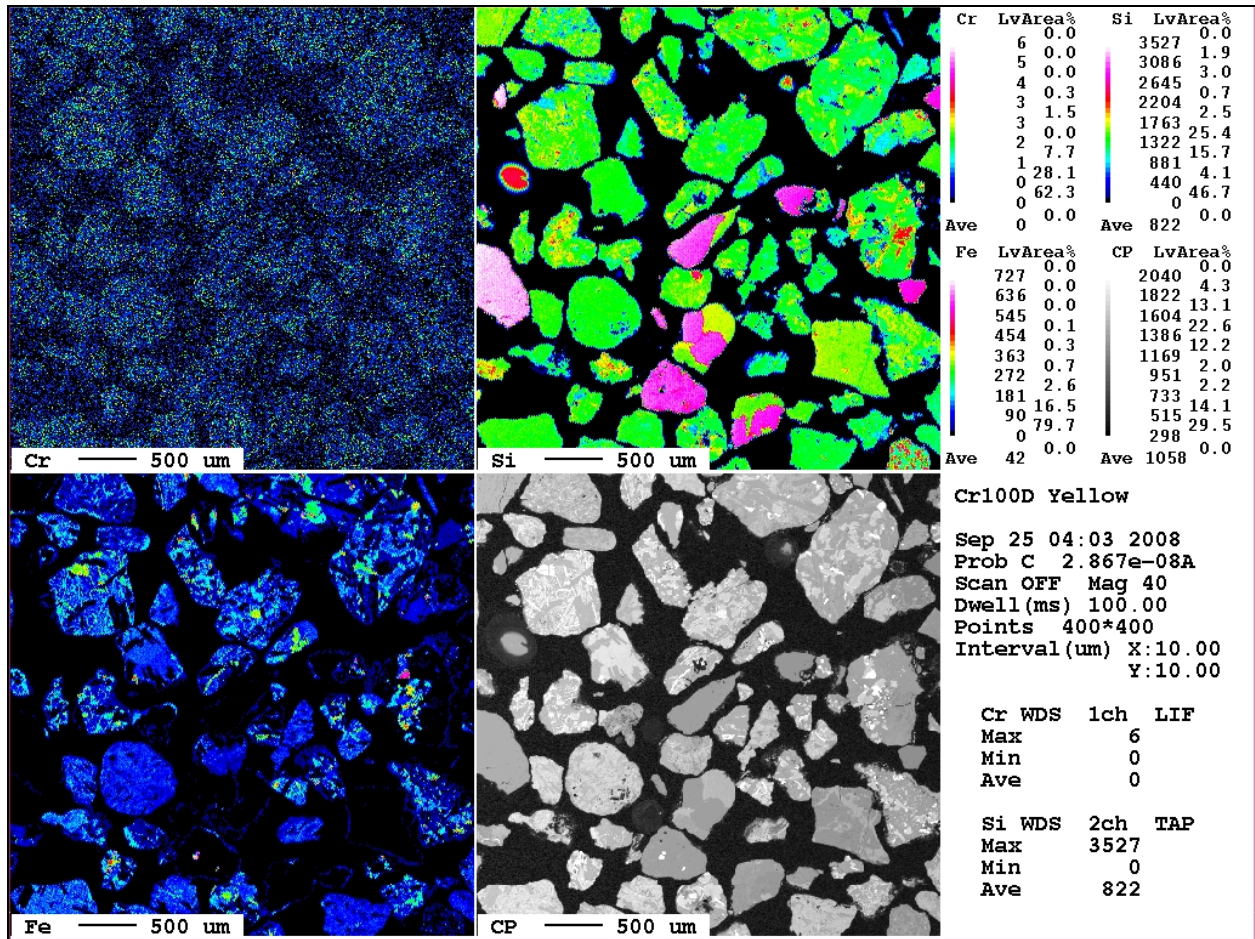


Figure 4.2. Results of the EMP measurements performed in sediment YS (2008)

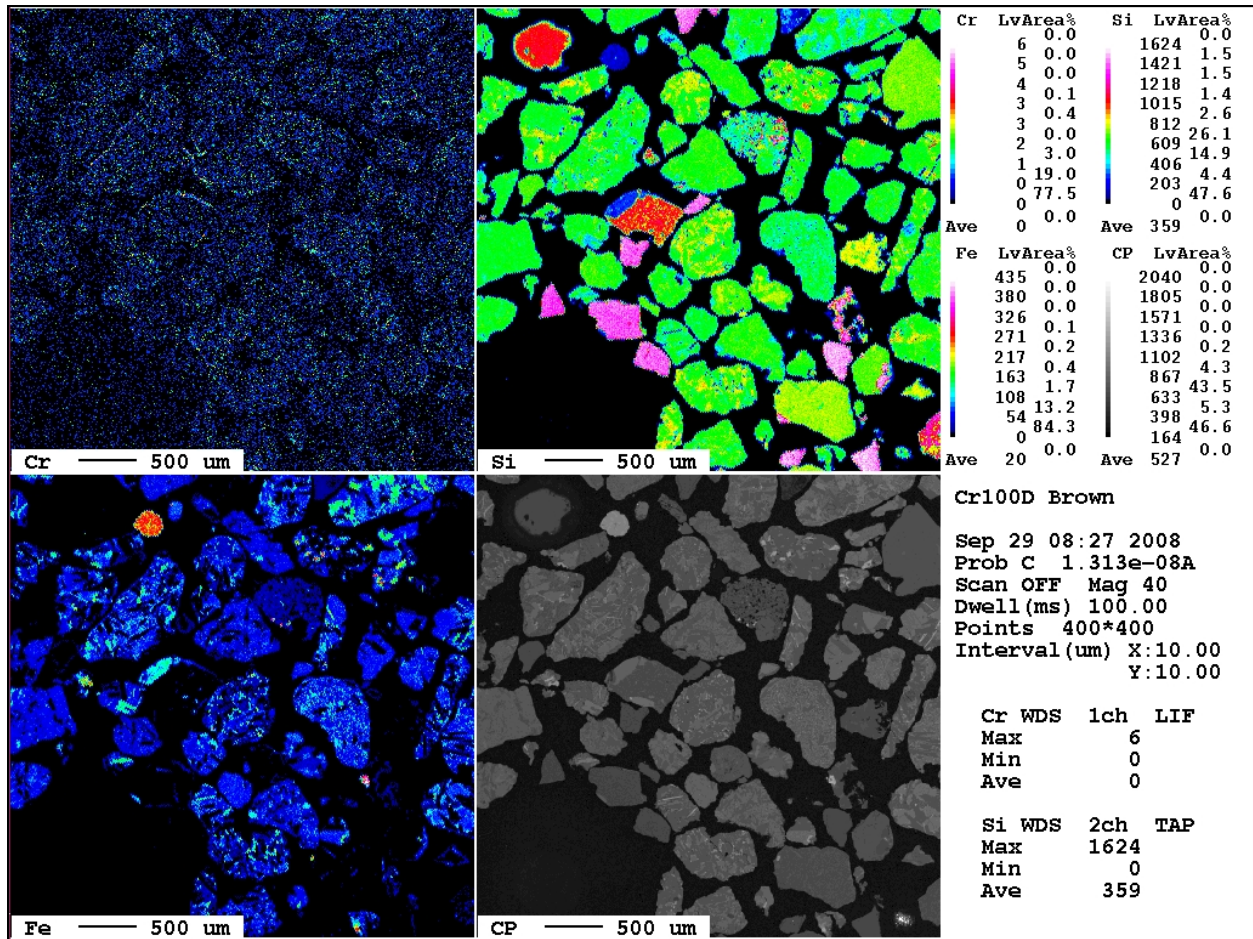


Figure 4.3. Results of the EMP measurements performed in sediment BS (2008)

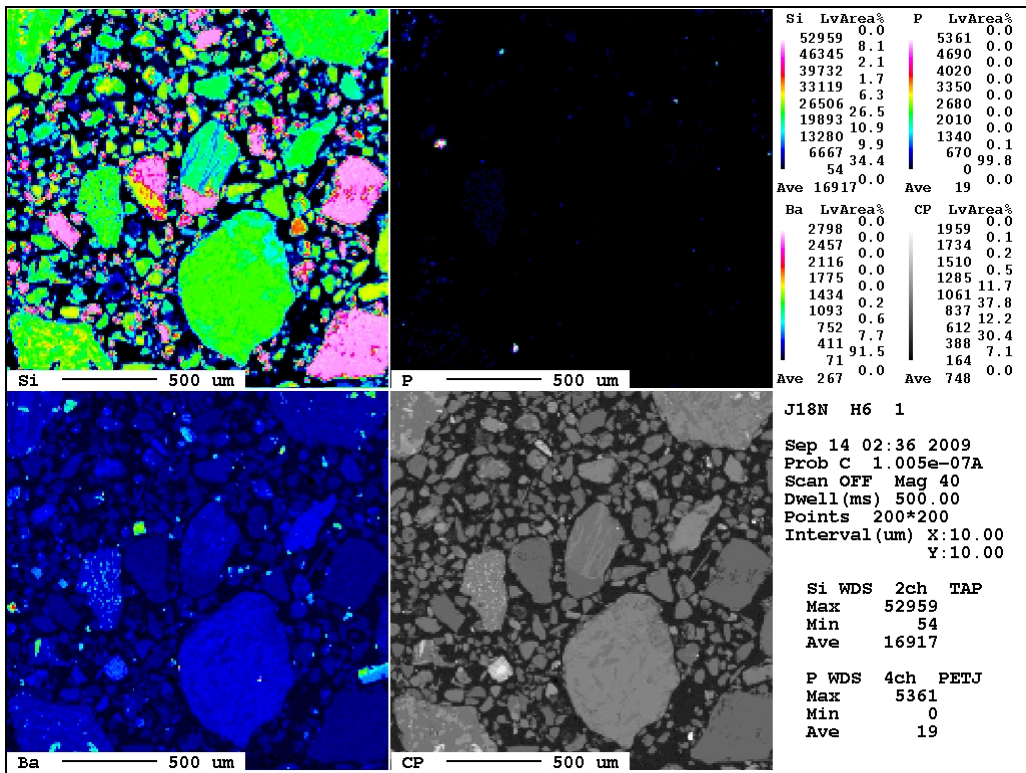
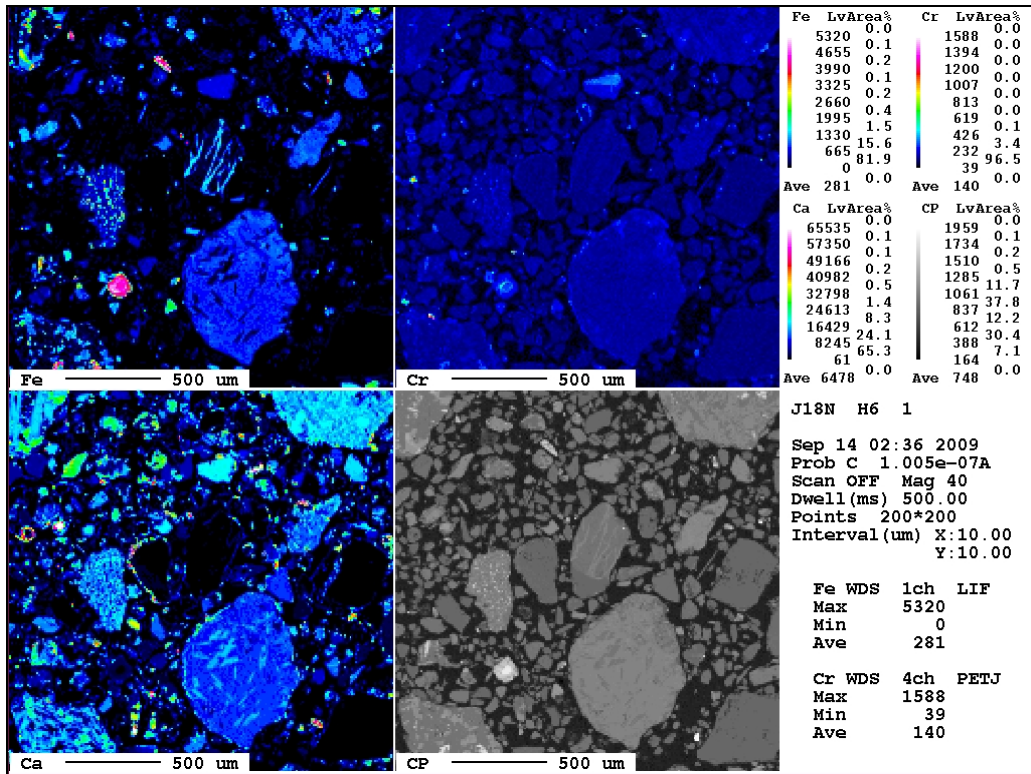


Figure 4.4. Results of the EMPA measurements performed in sediment J18NH6 (2009). Elemental mapping for Fe, Cr, Ca, Si, P, and Ba.

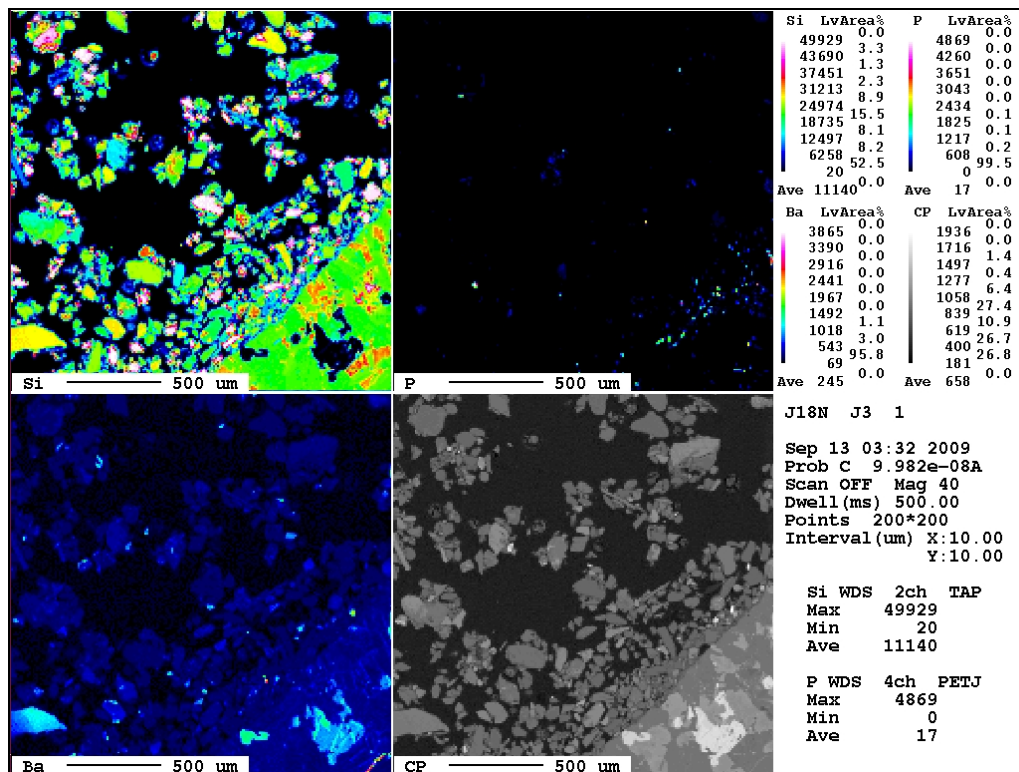
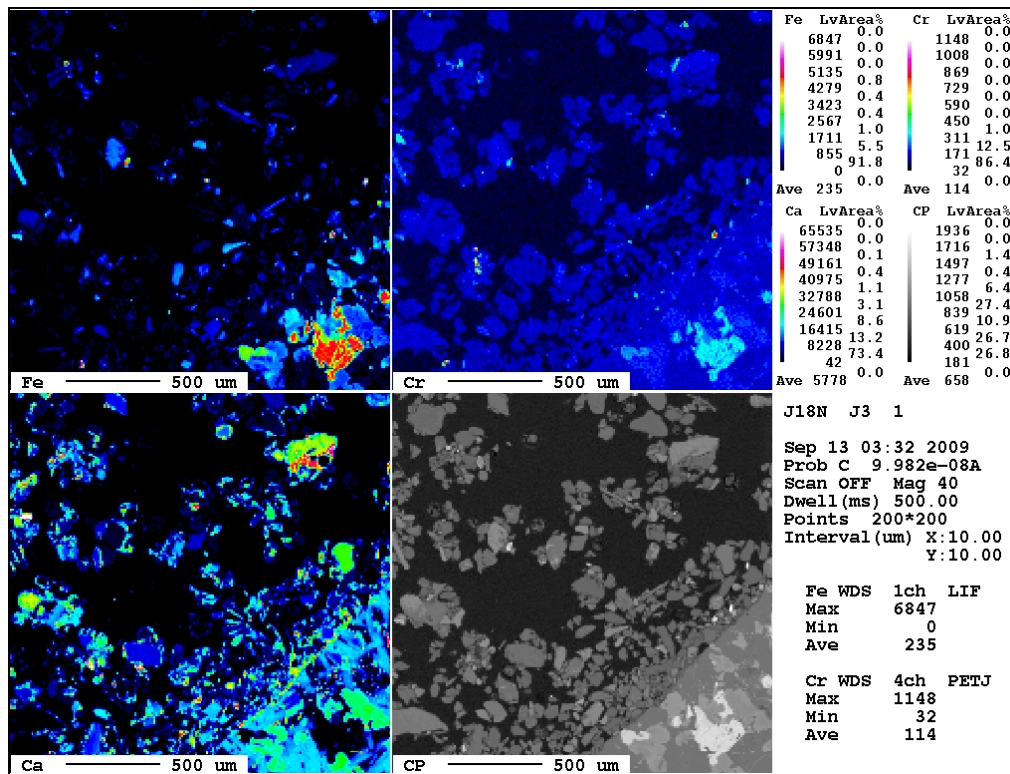


Figure 4.5. Results of the EMPA measurements performed in sediment J18NJ3 (2009). Elemental mapping for Fe, Cr, Ca, Si, P, and Ba.

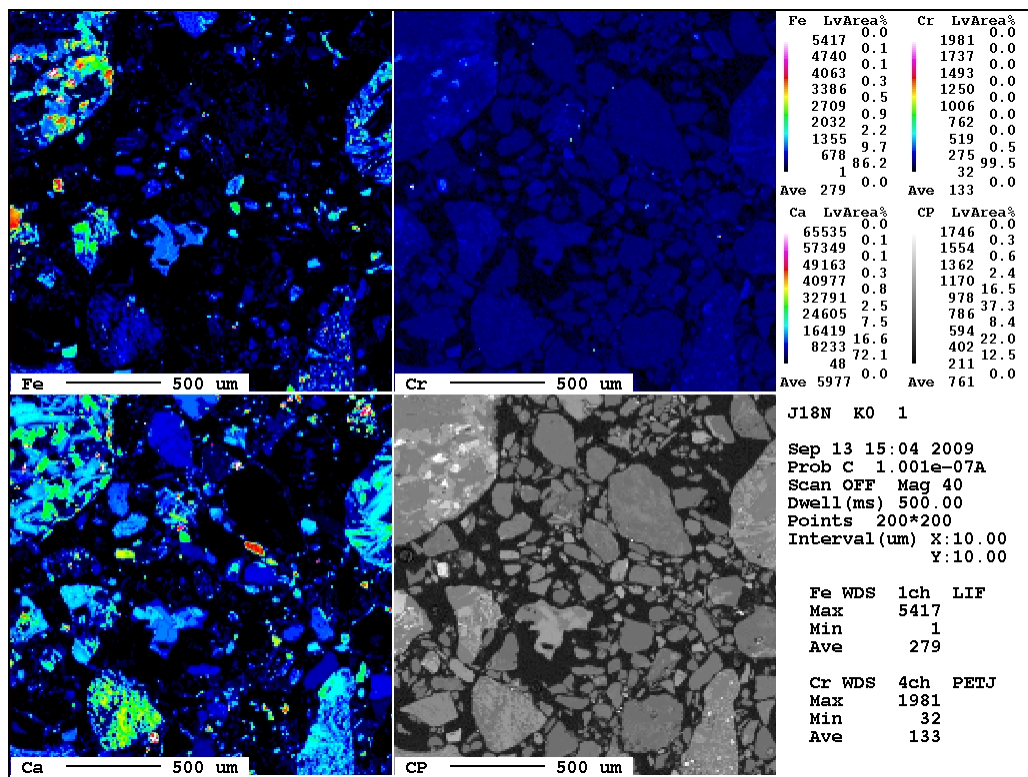
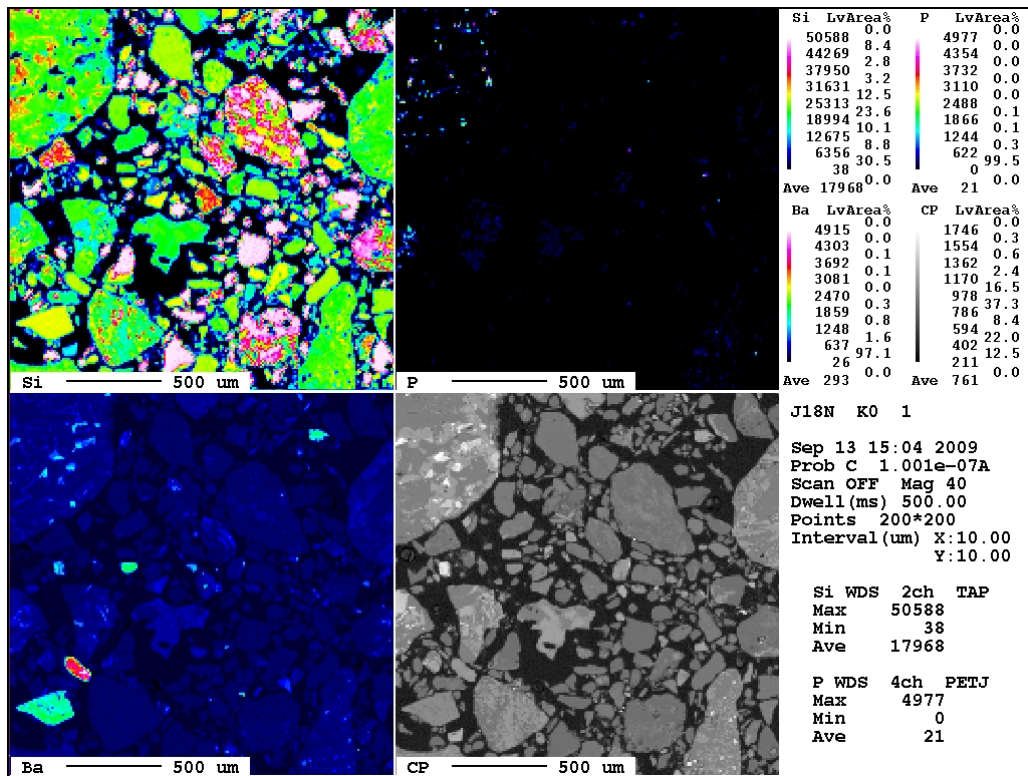


Figure 4.6. Results of the EMP measurements performed in sediment J18NK0 (2009). Elemental mapping for Fe, Cr, Ca, Si, P, and Ba.

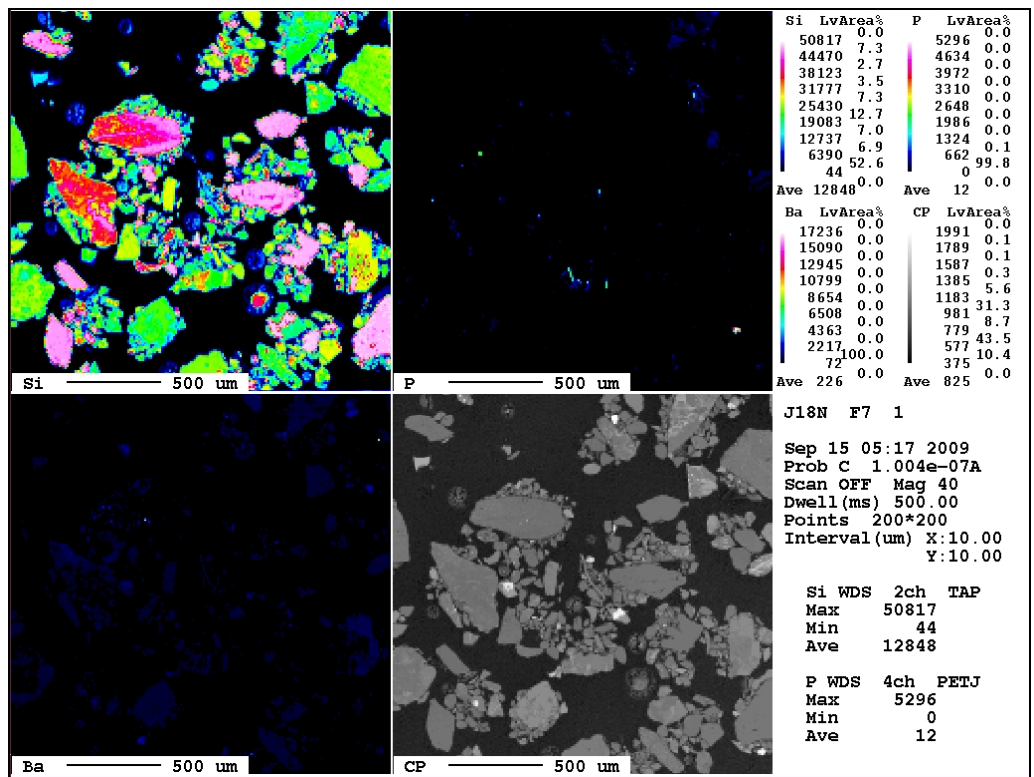
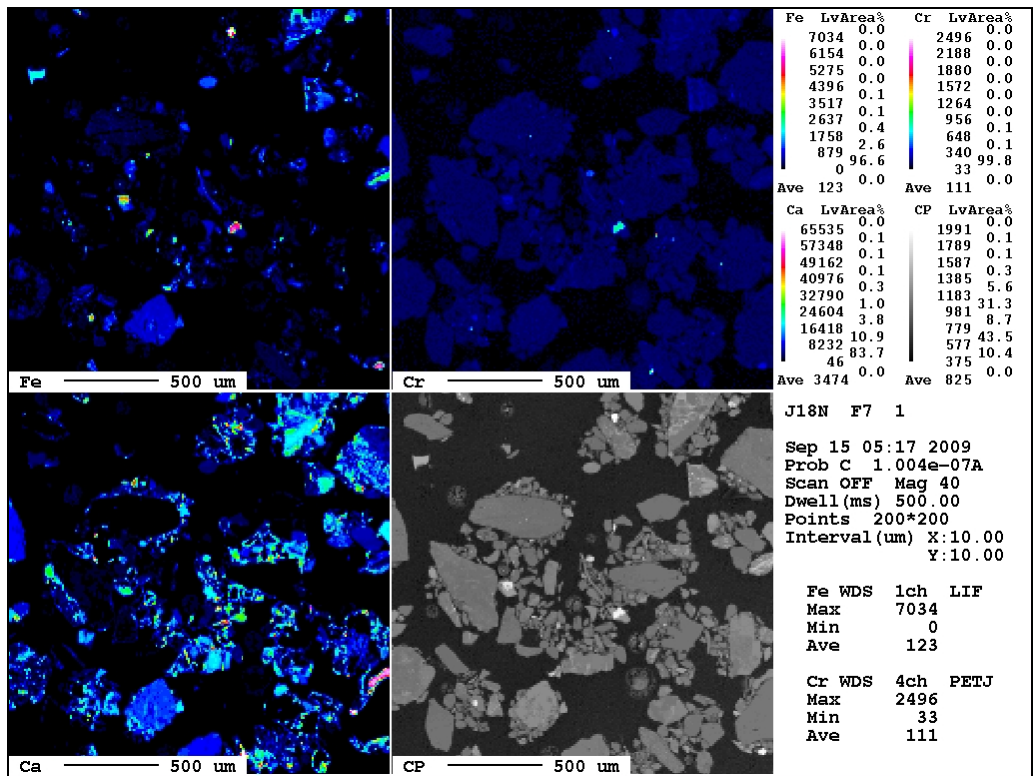


Figure 4.7. Results of the EMP measurements performed in sediment J18NF7 (2009). Elemental mapping for Fe, Cr, Ca, Si, P, and Ba.

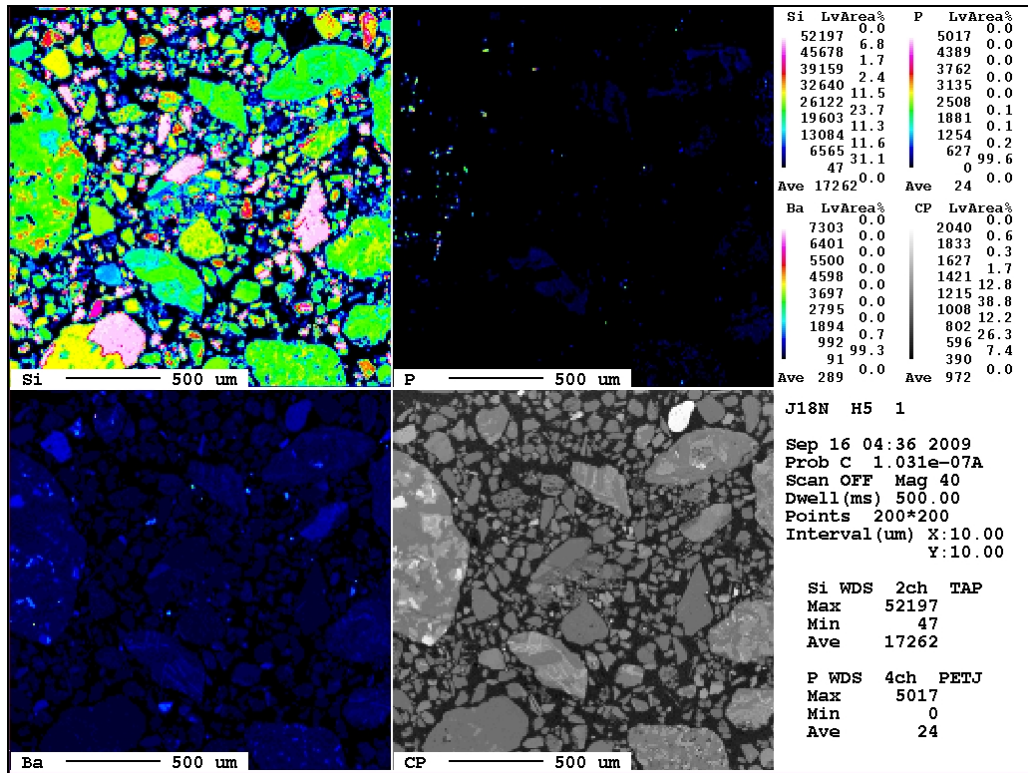
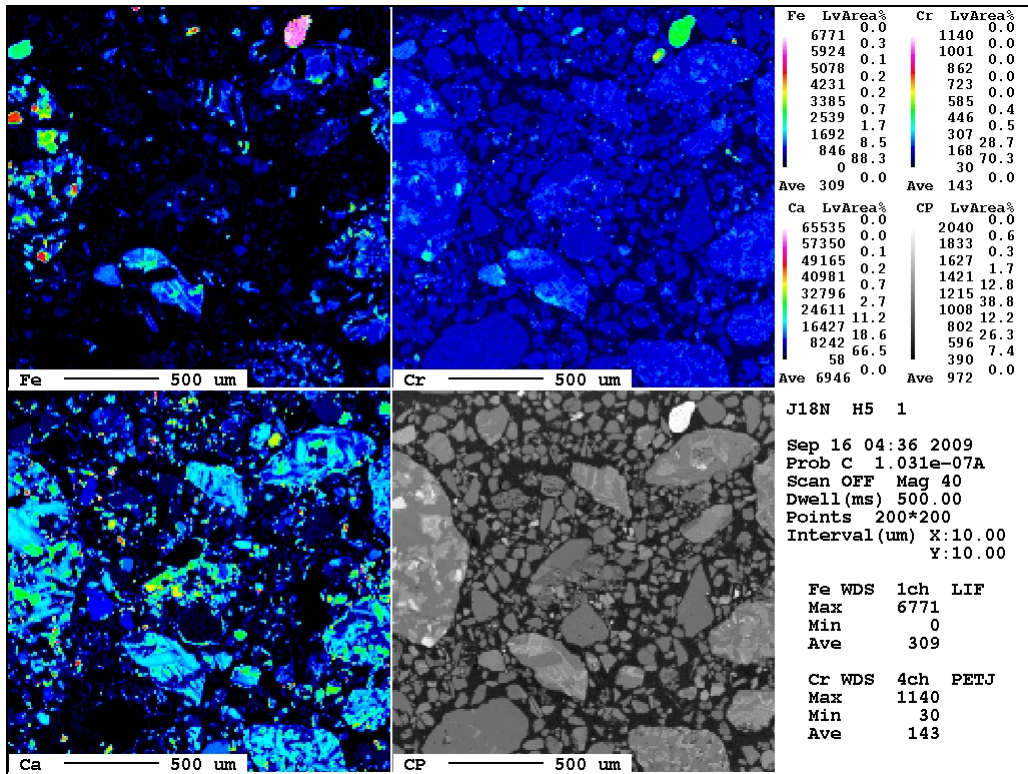


Figure 4.8. Results of the EMP measurements performed in sediment J18PH5 (2009). Elemental mapping for Fe, Cr, Ca, Si, P, and Ba.

XPS survey spectra

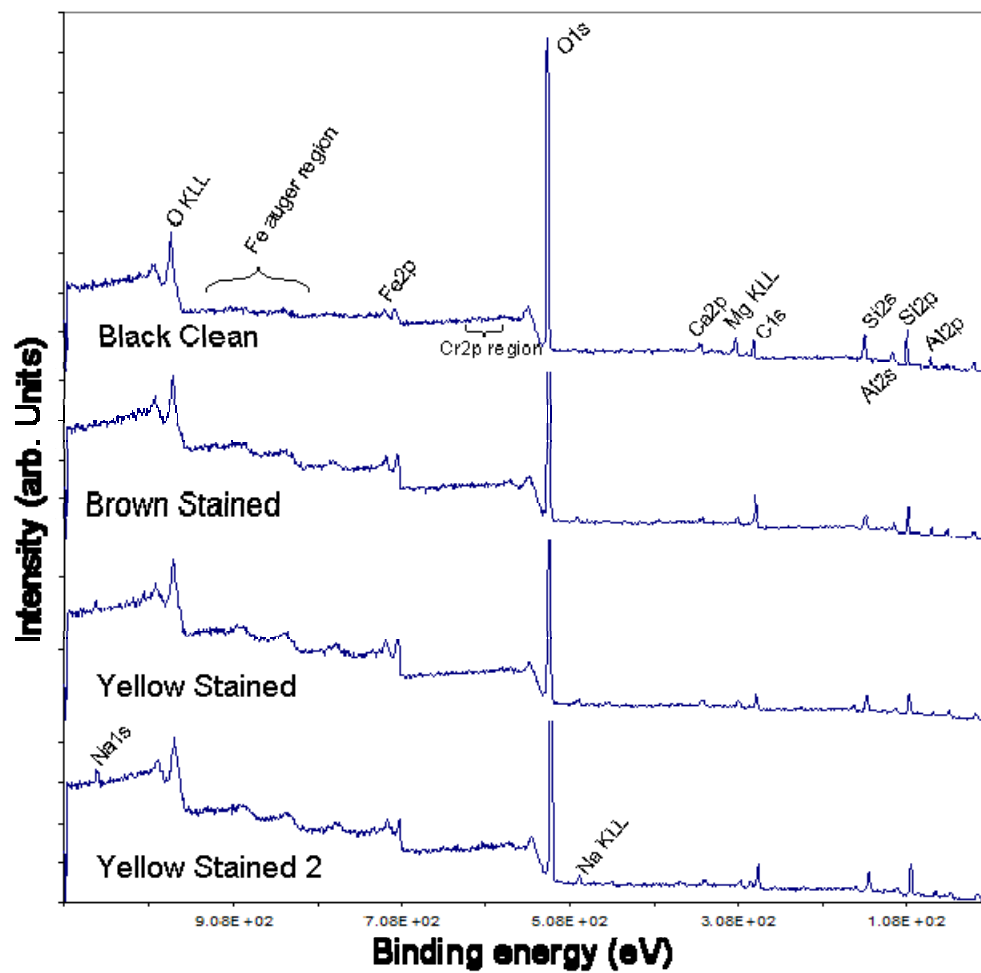


Figure 4.9. XPS survey spectra (2008 sediment samples)

XPS of Cr2p region: Comparison of "Brown stained" and "Black Clean" samples

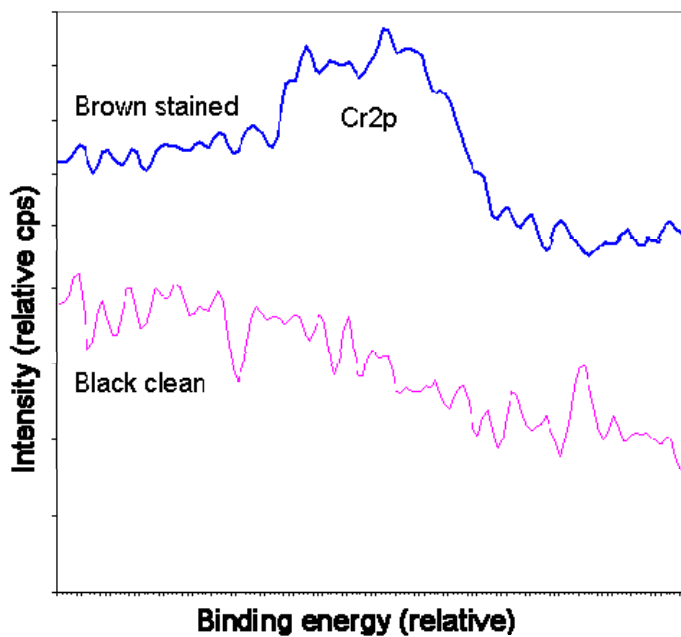


Figure 4.10. XPS of Cr2p region: Comparison of sediments BS and BC (2008)

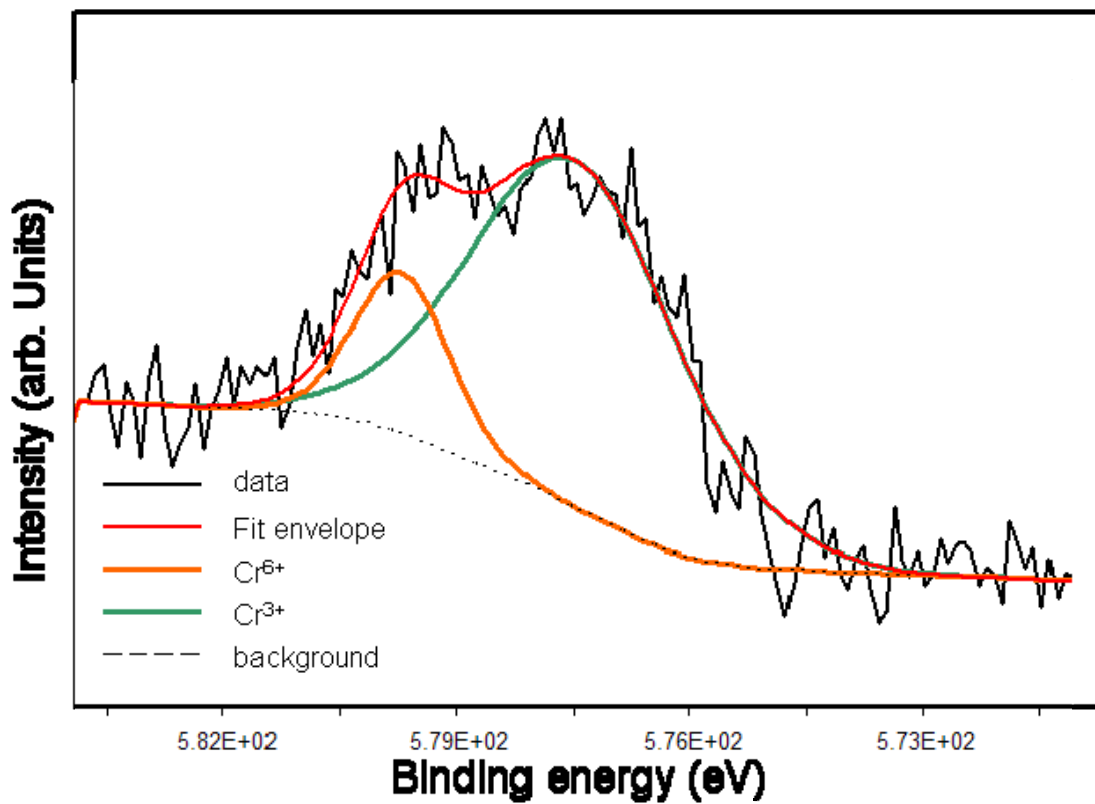


Figure 4.11. XPS of Cr2p3/2 region for sediment YS (2008)

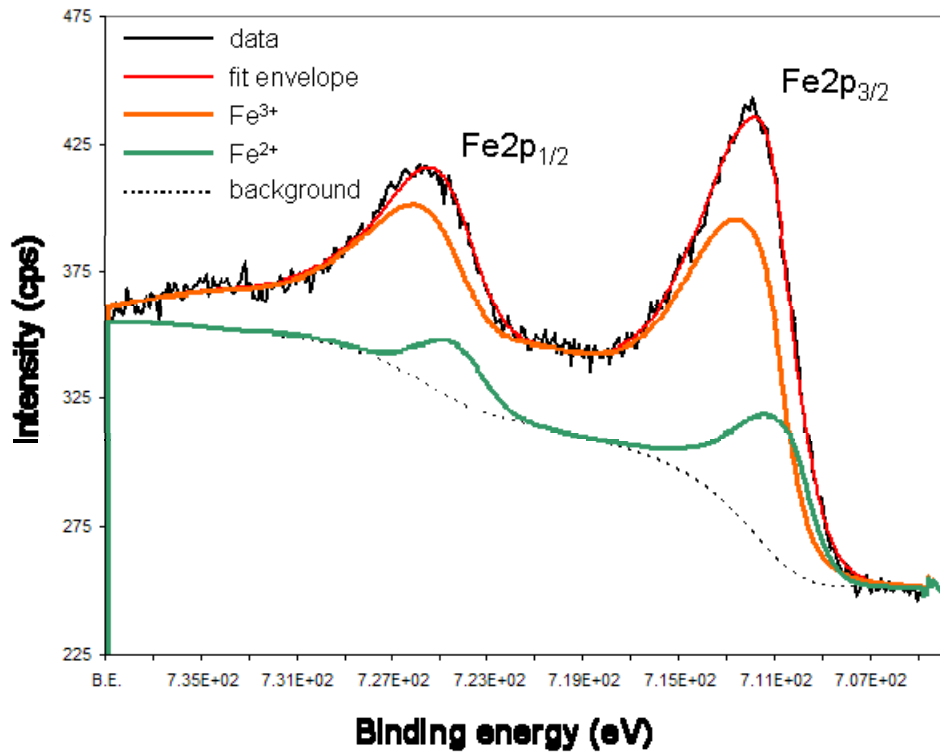


Figure 4.12. XPS of Fe2p region for sediment BS

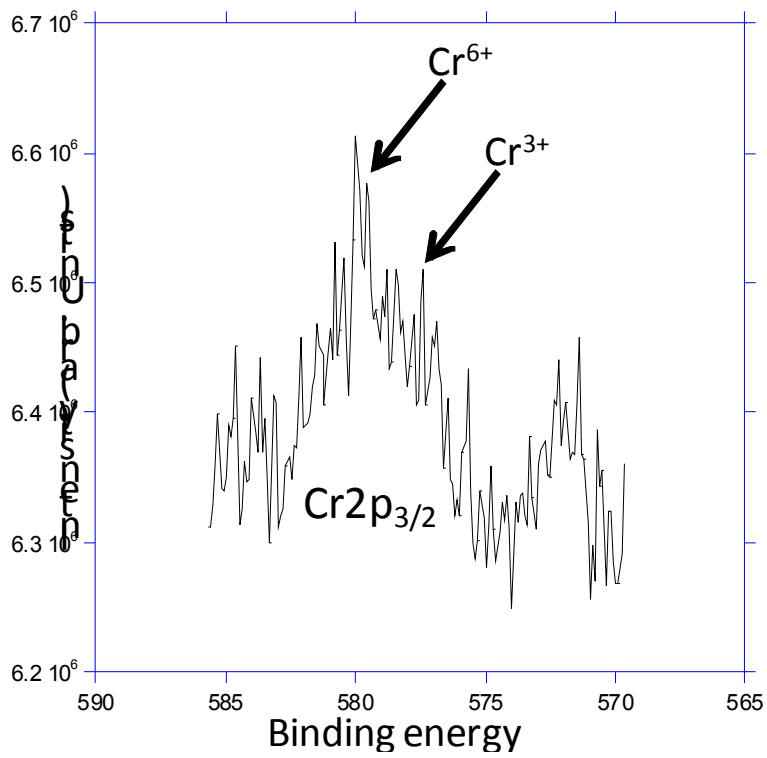


Figure 4.13. XPS survey spectra of sediment J18NH6 (2009)

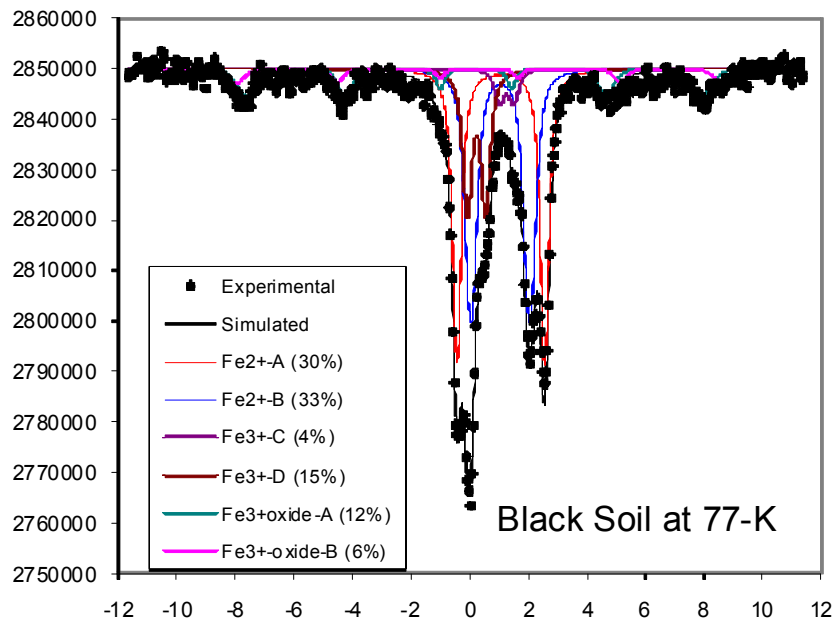
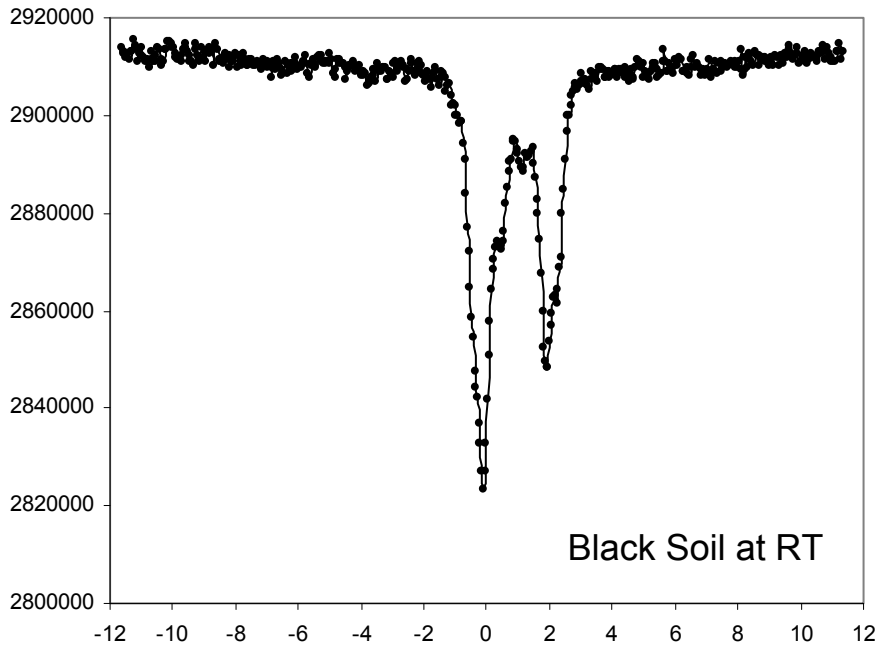


Figure 4.14. Results from the Mössbauer spectroscopy measurements performed in sediment BC (2008) at room temperature and 77 K

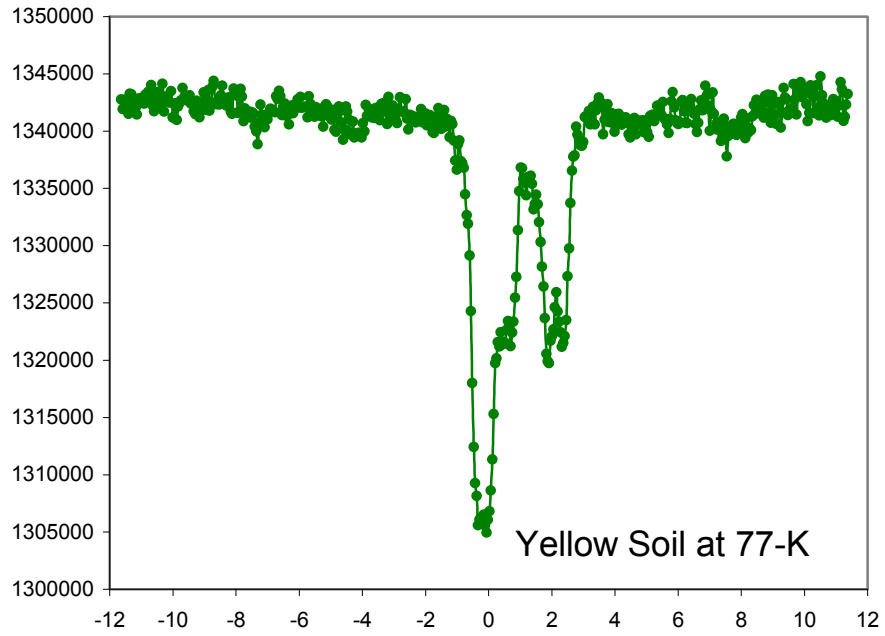


Figure 4.15. Preliminary results of the Mössbauer spectroscopy measurements performed in sediment YS (2008) at 77 K

5.0 Summary of Major Findings

Major conclusions from both the 2008 and 2009 research efforts are summarized in the following:

1. PNNL received four sediment samples collected from the newly discovered area of chromate contamination in the 100-D Area in early 2008. This site received neutralized sulfuric acid waste and also dichromate. The first sample was from a yellow-stained zone (sediment YS) at the bottom of the track-hoe excavation. The second sample was from a rusty brown-stained zone (sediment BS) at the excavation bottom. The third sample was from a yellow-stained zone (sediment YS2) from a shovel excavation that extended approximately 2 ft below the track-hoe pit. A small volume (~100 g) was collected from the third sample. The fourth sample was an unstained sample that is thought to represent the background black “clean” soil (sediment BC).
2. PNNL also received 32 sediment samples (approximately 100 g each) from the 100-D Area. Based on hexavalent and total Cr contents of the sediments, 5 surface sediments—J18NH6, J18NJ3, J18NK0, J18NF7, and J18PH5—were selected to conduct further characterization and leaching studies.
3. The XRD results indicated the sediments had similar mineralogy. However, further detailed work is needed; e.g., semiquantitative and/or quantitative XRD analyses, to determine if there are differences among the sediments in terms of soil mineral types and contents.
4. The particle-size fraction analyses showed 2008 YS and BS samples contained between 73% and 77% of the <2000 μm fraction. The particle-size fraction analyses showed the 2009 sediment J18NH6 contained 6.44 and 15.73 g of <63 μm and <125> 63 size fractions, off a total of 77.91 μm g of <2 mm size-fraction sample. Other sediments had significantly smaller amounts of these small fractions considered the most reactive fractions in the sediments.
5. The surface area analyses indicated 2009 sediments had similar surface areas, which varied from a minimum of $6.623 \pm 0.0416 \text{ m}^2 \text{ g}^{-1}$ in sediment J18NF7, to a maximum of $9.860 \pm 0.0596 \text{ m}^2 \text{ g}^{-1}$ in sediment J18NH3.
6. pH measurements taken in 1:1 solid: solution suspensions demonstrated that 2009 sediment pH was basic (the highest pH = 9.21 was measured in sediment J18NJ3).
7. Water-extractable Cr concentration was small in all 2008 contaminated sediment samples (it varied from 0.06 to $0.36 \mu\text{g g}^{-1}$). In 2009 sediment samples, this parameter varied between $0.105 \mu\text{g g}^{-1}$ in sediment J18NF7 to $2.16 \mu\text{g g}^{-1}$ in sediment J18NH6.
8. Acid and microwave-extractable Cr concentrations were significantly higher in all contaminated 2008 sediment samples. Acid-extractable concentrations varied from 64.4 to $114.9 \mu\text{g g}^{-1}$, while microwave-extractable concentrations were 2–3 times greater than acid-extractable concentrations (they varied from 184.1 to $231.7 \mu\text{g g}^{-1}$). Current cleanup level for WCH surface remediation sites is $2.6 \mu\text{g g}^{-1}$ (or $0.050 \text{ mmol kg}^{-1}$).
9. Acid-extractable Cr concentrations in 2009 sediment samples varied from a minimum of $30.30 \mu\text{g g}^{-1}$ in sediment J18NK0 to a maximum of $74.82 \mu\text{g g}^{-1}$ in sediment J18NH6. Although greater in magnitude, results from 8 M acid extractions were similar to the 0.5 M acid extractions. The 8 M acid-extractable Cr concentration varied from a minimum of $33.5 \mu\text{g g}^{-1}$ in sediment J18NK0, to a maximum of $82.4 \mu\text{g g}^{-1}$ in sediment J18NH6.

10. Microwave digestion analyses of different size-fractions separated from the five 2009 sediment samples demonstrated that smaller-size fractions had more Cr associated with them. The smallest Cr concentration of $3.938 \mu\text{g g}^{-1}$ was found in the 500 – 1000 μm fraction of sediment J18NK0; however, even this concentration is well above the current cleanup level for WCH surface remediation sites, which is $2.6 \mu\text{g g}^{-1}$.
11. Collectively, the results from water, acid extractions and microwave digestion suggest that sediments contained substantial amounts of Cr that were not readily extracted with water at the high solution to solid ratios tested in these experiments.
12. Data from column experiments corroborated the results from wet chemical extractions. With the exception of one 2009 sediment, almost all contaminant Cr mass remained in the sediments; it did not appear in the column effluents, which demonstrated Cr was strongly bounded in the sediments.
13. Experimental data clearly indicated that in at least one 2009 sediment was mobile, but Cr was strongly bounded in other sediments and it was not removed from them during the saturated or unsaturated column experiments conducted with a slightly alkaline artificial groundwater.
14. The average effluent pH during the 2008 column experiments varied from $\text{pH}_{\text{AVERAGE BC}} = 8.15 \pm 0.10$ (sediment BC) to $\text{pH}_{\text{AVERAGE YS}} = 6.91 \pm 0.61$ and $\text{pH}_{\text{AVERAGE BS}} = 6.20 \pm 0.70$ in sediments YS and BS, respectively. This clearly indicated the geochemistry of these sediments was altered by the acidic waste fluids (unaltered sediments from the same area usually have neutral or slightly alkaline pH). The dramatic change in aqueous phase pH during the 450+ h stop-flow events applied in the experiments conducted with sediments YS and BS may be attributed to a time-dependent S release reaction.
15. The average effluent pH measured in the 2009 column experiments was basic and above the usual pH values observed in the sediments from this site. The aqueous phase pH decreased significantly during all stop-flow events of different durations applied during the saturated column experiments. This clearly indicated the sediments' geochemistry was significantly altered as a result of waste fluid: sediment interactions.
16. Analyses of effluent samples indicated that in addition to Cr and S, appreciable amounts of Ca, Mg, and Si were released from sediments YS and BS. Low Ba concentrations were observed in the effluent collected at the beginning of the experiments, suggesting that BaCrO_4 (hashemite) or other less-soluble solid solutions of $\text{BaCrO}_4 - \text{BaSO}_4$, which usually form under high Cr(VI) concentrations, were not controlling Cr(VI) solubility and mobility.
17. Zones of high Cr concentration were not detected in the randomly selected areas of sediment samples during EMP interrogation. More sensitive spectroscopic techniques should be used to detect Cr and determine its solid phase speciation and association with soil minerals.
18. XPS measurements performed in the 2008 and 2009 sediment samples confirmed the following:
 - XPS measurements performed in 2009 confirmed Cr was not present in sediment BC. However, Cr was detected in all other samples (2008 sediment samples YS, YS2, and BS) although the Cr signal was low; Cr(VI) reduction occurred during XPS measurements. However, $\text{Cr(III)}/\text{Cr}_{\text{total}}$ values were constant between sequential analyses for sediment BS despite the presence of detectable Cr(VI). Therefore, it is possible in this case $\text{Cr(III)}/\text{Cr}_{\text{total}}$ values are true representatives or correct as given. Sediment BS contained the highest Fe/Si ratio.

- XPS measurements performed in the 2009 sediment samples confirmed that Cr was detected in at least one sample, although the Cr signal was low.
 - Both Cr(VI) and Cr(III) were detected in the contaminated sediment samples.
 - It must be emphasized that XPS is a surface-sensitive technique and the information depth is only about 8 nm. Both bulk and higher resolution two-dimensional analyses are required to supplement and aid interpretation of the XPS data. For example, Fe at the near surface of all the samples could be oxidized relative to bulk Fe.
 - Fe has mixed valence with the predominance of Fe(III) but with an appreciable Fe(II) component. Although difficult, curve fitting of all the samples yielded a range in $\text{Fe(II)/Fe}_{\text{total}} = 0.14 - 0.20$.
 - It appears Cr-containing samples were enriched in Fe. However, this enrichment, like that of Cr, may only be limited to the top ~8 nm of the sample, because XPS is a surface-sensitive technique. The correlation of Fe and Cr implies a similar temporal origin.
 - The Cr(III)2p binding energies are suggestive of a Cr(III)-oxyhydroxide, not Cr₂O₃. However, it is not yet possible to rule out the formation of a Fe(III)-Cr(III) oxyhydroxide or possible incorporation into silicates.
19. Preliminary Mössbauer spectroscopy measurements indicate the bulk sediment sample (sediment BC) had an appreciable Fe(II) component. A more thorough analyses and interpretation may reveal additional information about Fe(II)/Fe(III) mineralogy and coordination environment in the bulk sediment samples.
 20. Data collected thus far support the hypothesis that most contaminant Cr(VI) was reduced to Cr(III), which subsequently precipitated to form solid phases or solid solutions with limited solubility. Most likely, sorbed, structural, and/or aqueous Fe(II) released as a result of Fe(II)-bearing mineral dissolution may have been involved in redox reactions with aqueous Cr(VI).
 21. The mechanism of Cr attenuation remains unclear. Solid-phase Cr speciation is unknown and further studies are needed on this important subject.
 22. The relative importance of other attenuation pathways is also currently unknown. Cr might be present in the sediments in insoluble solid phases of both its oxidized or reduced forms.

The reduced Cr mobility in the contaminated sediments may have been caused by either the formation of Cr(VI) sparingly soluble solids (such as Ba chromate), or the reduction of Cr(VI) to Cr(III) and subsequent precipitation of Cr(III) phases and/or Cr(III)/Fe(III) solid solutions. Dissolution of soil minerals might have occurred at the time of exposure, and chemical elements such as Ba and Fe(II) might have been released into the aqueous phase. Most likely, Ba and Fe(II) were subsequently involved in chemical and/or redox reactions with aqueous Cr(VI). Both these attenuation pathways may have contributed to contaminant Cr immobilization in these sediments. Further studies are needed to determine the relative importance of these attenuation pathways.

6.0 References

- DOE/RL. 2010. *Hanford Site Groundwater Monitoring and Performance Report for 2009, Volumes 1 & 2*. DOE/RL-2010-11, Rev. 1, U.S. Department of Energy, Richland Operations Office, Richland, Washington.
- Allison JD, DS Brown, and KJ Novo-Gradac. 1991. *MINTEQA2/PRODEFA2, A Geochemical Assessment Model for Environmental Systems: Version 3.0 User's Manual*. U.S. Environmental Protection Agency, Athens, Georgia.
- Allison JD, DS Brown, and KJ Novo-Gradac. 1998. *MINTEQA2/PRODEFA2, A Geochemical Assessment Model for Environmental Systems: User Manual Supplement for Version 4.0*. U.S. Environmental Protection Agency, Athens, Georgia.
- Anselm KA, PE Kreuger, and WS Thompson. 2004. *Results of Hexavalent Chromium Sampling Near 100-D Area Sodium Dichromate Transfer Station Railroad Tracks*. BHI-01747, Rev 0, Bechtel Hanford Inc., Richland, Washington.
- Bartlett RJ and BR James. 1996. "Chromium," p. 683-702. In *Methods of Soil Analysis: Part 3, Chemical Methods*, (ed) DL Sparks, Soil Science Society of America, Inc., American Society of Agronomy, Inc., Madison, Wisconsin.
- Brusseau ML, QH Hu, and R Srivastava. 1997. "Using Flow Interruption to Identify Factors Causing Nonideal Contaminant Transport." *Journal of Contaminant Hydrology* 24:205–219.
- Carpenter RW. 1993. *100-D Area Technical Baseline Report*. WHC-SD-EN-TI-181, Rev. 0, Westinghouse Hanford Company, Richland, Washington.
- Dresel PE, NP Qafoku, JP McKinley, JS Fruchter, CC Ainsworth, C Liu, E Ilton, and JL Phillips. 2008. *Geochemical Characterization of Chromate Contamination in the 100 Area Vadose Zone at the Hanford Site*. PNNL-17674, Pacific Northwest National Laboratory, Richland, Washington.
- EPA. 1996a. *EPA Method 3050B: Acid Digestion of Sediments, Sludges, and Soils*. EPA Method 3050B, Rev. 1, U.S. Environmental Protection Agency, Washington, D.C.
- EPA. 1996b. *EPA Method 3060A: Alkaline Digestion for Hexavalent Chromium*. EPA Method 3060A, Rev. 2, U.S. Environmental Protection Agency, Washington, D.C.
- Foster RF. 1957. *Recommended Limit on Addition of Dichromate to the Columbia River*. HW-49713, General Electric Company, Richland, Washington.
- Ginder-Vogel M, T Borch, MA Mayes, PM Jardine, and S Fendorf. 2005. "Chromate Reduction and Retention Processes within Arid Subsurface Environments." *Environmental Science & Technology* 39:7833–7839.
- Hartman MJ, JA Rediker, and VS Richie. 2009. *Hanford Site Groundwater Monitoring for Fiscal Year 2008*. DOE/RL-2008-66, Rev 0, U. S Department of Energy, Richland, Washington.

Hope SJ and RE Peterson. 1996. *Chromium in River Substrate Pore Water and Adjacent Groundwater: 100-D/DR Area, Hanford Site, Washington*. BHI-00778, Rev. 0, Bechtel Hanford Inc., Richland, Washington.

Jury WA, WR Gardner, and WH Gardner. 1991. *Soil Physics*. John Wiley & Sons, Inc., New York.

Lerch JA. 1998. *100-D Area Chromium Study Summary Report*. BHI-01185, Rev 0, Bechtel Hanford Inc., Richland, Washington.

Mahood RO. 2009. *Fiscal Year 2008 Annual Summary Report for the In Situ Redox Manipulation Operations*. DOE/RL-2009-01, Rev 0., U.S. Department of Energy, Richland, Washington.

Parker JC and MT van Genuchten. 1984. "Determining Transport Parameters from Laboratory and Field Tracer Experiments." *Virginia Agriculture Experiment Station Bulletin* 84.

Petersen SW and SH Hall. 2008. *Investigation of Hexavalent Chromium Source in the Southwest 100-D Area SGW-38757*. Draft A, Fluor Hanford, Richland, Washington.

Petersen SW, KM Thompson, and MJ Tonking. 2009. *Results from Recent Science and Technology Investigations Targeting Chromium in the 100 Area, Hanford Site, Washington, USA*. HNF-43813-FP, Rev. 0, CH2M HILL Plateau Remediation Company, Richland, Washington.

Peterson RE, RF Raidl, and CW Denslow. 1996. *Conceptual Site Models for Groundwater Contamination at 100-BC-5, 100-KR-4, 100-HR-3, and 100-FR 3 Operable Units*. BHI-00917, Rev. 0, Bechtel Hanford Inc., Richland, Washington.

Qafoku NP, CC Ainsworth, and SM Heald. 2007. *Cr(VI) Fate in Mineralogically Altered Sediments by Hyperalkaline Waste Fluids*. *Soil Science* 172:598–613.

Qafoku NP, CC Ainsworth, JE Szecsody, and OS Qafoku. 2003. "Effect of Coupled Dissolution and Redox Reactions on Cr(VI)Aq Attenuation During Transport in the Hanford Sediments Under Hyperalkaline Conditions." *Environmental Science & Technology* 37:3640–3646.

Qafoku NP, CC Ainsworth, JE Szecsody, and OS Qafoku. 2004. "Transport-Controlled Kinetics of Dissolution and Precipitation in the Hanford Sediments Under Hyperalkaline Conditions." *Geochimica et Cosmochimica Acta* 68:2981–2995.

Qafoku NP, PE Dresel, E Ilton, JP McKinley, and CT Resch. 2010. "Chromium(VI) Transport in an Acidic Waste Contaminated Subsurface Medium: The Role of Reduction." *Chemosphere* 81:1492–1500.

Qafoku NP, PE Dresel, JP McKinley, C Liu, SM Heald, CC Ainsworth, JL Phillips, and JS Fruchter. 2009. "Pathways of Aqueous Cr(VI) Attenuation in a Slightly Alkaline Oxidic Subsurface." *Environmental Science & Technology* 43:1071–1077.

Schroeder GC. 1966. *Discharge of Sodium Dichromate Solution. Compliance with Executive Order 11258*. Douglas United Nuclear Inc., Richland, Washington.

Thornton EC. 1992. *Disposal of Hexavalent Chromium in the 100-BC Area - Implications for Environmental Remediation*. WHC-SD-EN-TI-025, Rev. 0, Westinghouse Hanford Company, Richland Washington.

Thornton EC, JE Amonette, JA Olivier, and DL Huang. 1995. *Speciation and Transport Characteristics of Chromium in the 100D/H Areas of the Hanford Site*. WHC-SD-EN-TI-302, Rev. 0, Westinghouse Hanford Company, Richland, Washington.

Thornton EC, TJ Gilmore, KB Olsen, R Schalla, and KJ Cantrell. 2001. *Characterization Activities Conducted at the 183-DR Site in Support of an In Situ Gaseous Reduction Demonstration*. PNNL-13486, Pacific Northwest National Laboratory, Richland, Washington.

Thornton EC, KJ Cantrell, JM Faurote, TJ Gilmore, KB Olsen, and R Schalla. 2000. *Identification of a Hanford Waste Site for Initial Deployment of the In Situ Gaseous Reduction Approach*. PNNL-13107, Pacific Northwest National Laboratory, Richland, Washington.

Toride N, J Leij, and MT van Genuchten. 1999. *The CXTFIT Code for Estimating Transport Parameters from Laboratory or Field Tracer Experiments*. Research Report 137, Agricultural Research Service, U.S. Department of Agriculture, Riverside, California.

Whipple JC. 1953. *Design Planning of a Dichromate System for the 100-K Areas*. HW-26913, Richland Washington.

Distribution

<u>No. of Copies</u>		<u>No. of Copies</u>	
ONSITE		2 Pacific Northwest National Laboratory	
	DOE Richland Operations Office	CF Brown	PDF
	JG Morse	PE Dresel	PDF
		MD Freshley	K9-33
		ES Ilton	PDF
4	CH2M HILL Plateau Remediation Company	RK Kukkadapu	PDF
		JP McKinley	PDF
		N Qafoku (P/PDF)	P7-54
	FH Biebesheimer	CT Resch	PDF
	SW Petersen (2)	W Um	PDF
	JL Smoot		
	Washington Closure Hanford		
	WS Thompson	H4-23	



Pacific Northwest
NATIONAL LABORATORY

*Proudly Operated by **Battelle** Since 1965*

902 Battelle Boulevard
P.O. Box 999
Richland, WA 99352
1-888-375-PNNL (7665)

www.pnl.gov



U.S. DEPARTMENT OF
ENERGY